Bitlis Eren University Journal of Science and Technology

Contact:

Bitlis Eren University Journal of Science and Technology

Bitlis Eren University Journal of Science and Technology

Year: 2023 • Volume: 13 • Issue: 2

Editorial Board

Bitlis Eren University Journal of Science and Technology

Year: 2023 • Volume: 13 • Issue: 2

Bitlis Eren University Journal of Science and Technology (Bitlis Eren Univ J Sci & Technol) is an international, refereed open access electronic journal. Research results, reviews and short communications in the fields of Agriculture, Biology, Chemistry, Engineering Sciences, Mathematics, Medicinal, Molecular and Genetics, Physics, Statistics, and also Engineering Sciences are accepted for review and research article publications. Papers will be published in English. Scientific quality and scientific significance are the primary criteria for publication. Articles with a suitable balance of practice and theory are preferred. Manuscripts previously published in other journals and as book sections will not be accepted.

Bitlis Eren University Journal of Science and Technology indexed in:
- EBSCO
- INDEX COPERNICUS
- CITEFACTOR
- SCILIT
- ACARINDEX
- SOBIAD

Bitlis Eren University Journal of Science and Technology

Articles

RADON CONCENTRATION AND ITS INDICES IN BULAK (MENCILIS) CAVE

Necla ÇAKMAK[1],* iD **, Ulvi KANBUR[1]** iD **, Khalid Hadi Mahdi AAL-SHABEEB[1]** iD **, Ahmet Mustafa ERER[1]** iD

[1] *Karabük University, Department of Physics, Türkiye, neclac@karabuk.edu.tr, ulvikanbur@karabuk.edu.tr, khalidaal-shabeeb@karabuk.edu.tr, mustafaerer@karabuk.edu.tr*
* Corresponding author

KEYWORDS

ARTICLE INFO

ABSTRACT

The Bulak cave is in the village of Bulak near Safranbolu city. It's one of the longest caves in Türkiye, which goes 6 kilometers into the inside, but approximately 400 meters are accessible to visitors. You require a professional guide and special equipment to travel further into the cave with lakes, a waterfall, and rivers which are essential for cavers, tourists, and researchers. However, there are possible several health problems for cave visitors. This study mainly aims to measure the radon concentrations with the nuclear track CR-39 detector in the cave environment. Twenty-two detectors were distributed inside the tourist's area, and another six detectors were in the cave's deeper region. The exposure time was one month on 24 September 2020, in addition to two soil samples collected from the cave used for medical purposes. These detectors are collected after 30 days and then etched with a chemical solution. The radon concentrations were calculated, which ranged between 16.437 (Bq/m^3) and 48.652 (Bq/m^3) using an optical microscope from the track density in detectors. The minimum and maximum values of radiation indices AED (mSv/y), LCR (WLM), PAEC (mWL), D_{soft} (nGy/h), D_{lung} (nGy/h) and H_{eff} (nSv/h) are presented, and all results for the radon and radiation indices are within the global limit. Radon concentrations for two soil samples were 26.956 (Bq/m^3) and 59.172 (Bq/m^3), and all the results were within the acceptable limits recommended by ICRP and UNSCEAR. The XRF examination was performed, which indicated the presence of Fe, Cu, Zn, As, and Mn minerals with high concentrations of 101607, 552, 1337, 237, and 1601 ppm, respectively, which are all more than the world permissible limits. The XRD analyses for the soil sample indicated the presence of clay and non-clay minerals such as Feldspar, Quartz, Gypsum, Calcite, Palygorskite, Kaolinite, and Montmorillonite.

1 INTRODUCTION

Radon (Rn-222) and its daughters (Po-218, Po-214, and Bi-214) radiate in the air as alpha particle that contributes more than 50% of public natural exposure [1]. An electrically charged nucleus (Po-218) sticks to atoms of dust or to dust and water droplets in the atmosphere and materials on the surface of the earth. So, the air in which radon is present contains dust particles loaded with the decomposition products of radon with high radioactivity. Radon gas residues stick to all surfaces in nature, including air and soil [2], and there are two ways that radon and its disintegration products can enter the human body, especially the respiratory and digestive systems. The latter does not represent a danger, because the presence of food in the stomach, even if its thickness is within a millimetre, can stop most of the alpha particles resulting from the disintegration of radon and its offspring. In the case of inhalation of radon offspring suspended in the air, if they enter the respiratory system they stick to the wall of the lungs [3]. The radiation may lead to DNA damage directly by displacing electrons from the DNA molecule or by changing the composition of other molecules in the cell. They may interact with the DNA and lead to cell damage or change the growth of the cell and the occurrence of a genetic mutation [3,4]. As stated in the committee's fourth report composed to study the biological effect of ionizing radiation, about 3-14% of cancer injuries result from radon gas [5]. Many studies have classified radon as a human carcinogen, which was done in Europe, North America, and China [6-8]. Caves are natural sites between rocks that extend in such a way as to allow human entry. It is found in most mountainous regions, and it was formed over thousands of years and has a unique landscape. It has great importance as a site for recreational, tourism, and scientific activities, especially in Türkiye [9-15]. The radon concentrations of Mencilis (Bulak) cave have been determined by using passive nuclear track detectors [16]. Radon measurements in houses in the provinces of Bingöl and Muş (Türkiye) and their neighbouring villages have been carried out by means of CR-39 nuclear track detectors [17]. Radon concentration has been examined in surface water samples taken from Van Lake in spring and autumn by using CR-39 solid nuclear track detectors and RadoSYS radon measurement system [18]. The radon concentration levels in the spring and summer seasons in two rooms (the kitchen and the living

room) of a building in the city centre of Manisa have been determined by means of CR-39 nuclear track detectors [19]. Radon concentrations can be measured by two methods, the active method (by means of electronic devices) and the passive method (by means of solid-state nuclear track detectors, SSNTDs). In the second method, it is common to use CR-39, known as (Columbia Resin-39), which is a poly allyl diglycol carbonate (PADC). It has a cross-linked lattice structure. It is partially crystalline. Amorphous with ~20% crystallinity (and contains carbon bonds in its monomer, and these bonds can be easily broken as they are relatively weak when exposed to radiation or ionizing particles [20].

In this study, radon concentrations in the air and soil of the Bulak cave were measured with CR-39 nuclear track detectors. At the same time, mineral analysis was performed in the selected soil sample. This work will contribute to the many studies investigating the influence of indoor air quality in caves and other interior environments [21-23]. The paper is organized as follows: Section 1 presents shortly literature and general information about the paper. Section 2 describes the experimental part used in the calculation, and Section 3 presents the study's findings. Finally, concluding remarks are presented in Section 4.

2 EXPERIMENTAL PART

The map in Figure 1 shows the location of Bulak (Mencilis) Cave, which has the coordinates of the entrance to the cave: 41 16′28.60N, 32 37′28.58E and elevation 753.2 m [24]. This cave which forms a large ecosystem is still alive today. The Jurassic Cretaceous period was 65-200 million years ago and occurred in limestone. The entrance level of the Bulak Cave is 291 m above the water source entrance, where the underground stream is exposed. The cave's temperature is 12-14°C, and the humidity is relatively high (60-70%) [25]. The Mencilis Cave in the village of Bulak near Safranbolu is a tourist attraction. It is the fourth-largest cave in Türkiye with a length of 5250 meters [24], and its natural beauty attracts the attention of domestic and foreign tourists. The first 350 m of the cave has been opened to tourism since 2003 [24]. The cave consists of three interconnected floors. It has an underground river at the main entrance on the ground floor, and there is a siphon directly in front of the entrance. The floor above it is 200 m northeast of the main entrance fossil

layer. The total length of the fossil floor is 1200 m, and it contains beautiful stalactites, stalagmites, columns, and walls.
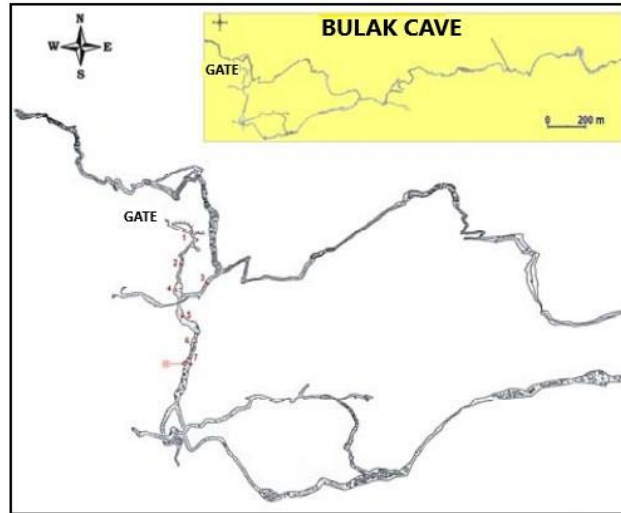
Figure 1. Location map of Bulak cave. (Taken from ref. [16] with permission of the authors.)

At the bottom of the cave, a water source contributes to Safranbolu's drinking water. The flow rate of the underground river on the lower floor varies between 0.55 – 2.20 m^3/s depending on the rainy seasons. The underground river has formed lakes of different sizes, reaching 5 meters in depth. An image of the interior view of the cave is given in Figure 2. Considering all the floors of the cave, it forms a large ecosystem with its living and non-living assets [25].

Figure 2. Interior view of Bulak cave.

Twenty-two detectors were distributed within the cave at 20 meters intervals from each other in the walking area of the tourists. These detectors were kept in a sponge as shown in Figure 3 and placed in a wide and deep area (group B consisting of 6 detectors) inside the cave as well as in the area under the walking path reserved for tourists. The detectors were collected after a period of one month, and the detectors were transferred after the exposure process to a chemical etching process using a sodium hydroxide solution with a normality of 6.25 at a temperature of 60°C for 6 hours. The detectors transferred to the process of calculating the tracks using a Nikon type-168 optical microscope.
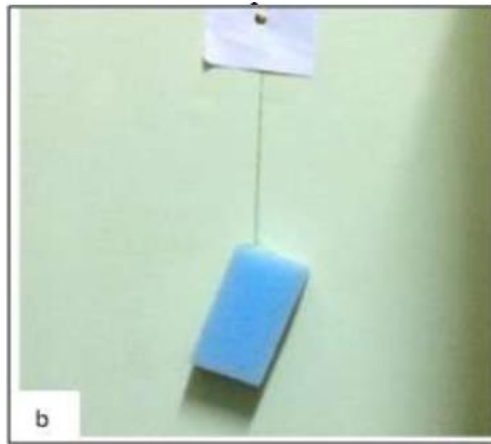
Figure 3. *The nuclear track CR-39 detectors inside the sponge.*

The radon concentration (C_{Rn}) is calculated after comparing it with the standard source in Figure 4 by using the following equations [26].

$$C_{Rn} = (\rho/t)(E_s/\rho_s) \tag{1}$$

where ρ is the track density given by $\rho = N_{avg}/A$, where N_{avg} is the number of tracks, A is the area of the view of the microscope, t is the exposure time (days), E_s is the radon exposure of standard source (Bq.day.m^{-3}), and ρ_s is the track density (number of tracks per mm^2) of the standard source. Equation (1) can be rewritten as

$$C_{Rn} = \rho k/t \tag{2}$$

where k is the calibration factor. It gives the linear relationship between E_s and ρ_s. The value of k is dependent on the radius and the effective height of the measuring can. The radiation indices are calculated, like the annual effective dose (mSv/y) by using the following equation [27]

$$D\left(\frac{\text{mSv}}{\text{y}}\right) = C\,E\,h\,t\,f \tag{3}$$

where E is the equilibrium factor (0.4), h is the occupancy factor (0.8), t is the conversion factor for year 8760 (h/y), f is the dose factor of conversion (9×10^{-6} mSv/Bq.h.m^{-3}) [26].

For millions of lung cancer patients every year, the lung cancer compact panel (LCCP) value is calculated using the following equation [26]

$$LCCP = D \times 18 \times 10^{-6} \tag{4}$$

Also, the concentration of potential alpha energy (WL) is obtained by equation [24]:

$$PAE(\text{WL}) = E\frac{C_{\text{Rn}}}{3700} \tag{5}$$

The dose rate related to soft tissues of inhaled radon that partly dissolved with a factor of (0.4) is given by the following relationship [29]:

$$\dot{D}_{\text{soft tissues}}(\text{nGyh}^{-1}) = 0.005\chi_{\text{Rn, air}}(\text{Bqm}^{-3}) \tag{6}$$

Assuming that the air volume in the lungs is (3.2×10^{-3} m^3) for the reference man, the dose rate for the lungs and the effective equivalent dose rate are defined by [29].

$$\dot{D}_{\text{lung}}(nGyh^{-1}) = 0.004\chi_{\text{Rn, air}}(Bqm^{-3}) \tag{7}$$

and

$$\dot{H}_{\text{eff}}(nSvh^{-1}) = 0.18\chi_{\text{Rn, air}}(Bqm^{-3}) \tag{8}$$

where the quality factor for alpha-radiation equals 20, and the weighting factor for the lungs and other tissues are 0.12 and 0.88, respectively.

3 RESULTS AND DISCUSSION

The radon concentrations and radiation indices for Bulak cave and soil sample taken from the cave and the mineral concentrations in this soil sample were measured using the nuclear track CR-39 detectors and presented in Tables 1-3.

Table 1. Radon concentrations and radiation indices for Bulak cave. The global limit values are 100-200 (Bq/m³) [35], 3-10 (mSv/y) [35], 170-230 [35], 53.33 (mWL) [26], and 1.15 (mSv/yr) [36] for the radon concentration (Bq/m³), the AED (mSv/y), the LCR (WLM) per 10⁶ persons, the PAEC (mWL), and H_{eff} (nSv/h), respectively.

SN	Track density (ρ) (track/mm²)	Radon concentration (Bq/m³)	AED (mSv/y)	LCR (WLM) per 10⁶ persons	PAEC (mWL)	D_{soft} (nGy/h)	D_{lung} (nGy/h)	H_{eff} (nSv/h)
1B	996	65.483	1.644	29.592	7.963	0.328	2.619	11.786
2B	952	62.590	1.572	28.296	7.655	0.316	2.518	11.330
3B	950	62.459	1.568	28.224	7.596	0.313	2.498	11.242
4B	735	48.323	1.213	21.834	5.877	0.242	1.933	8.697
5B	886	58.251	1.463	26.334	7.084	0.292	2.330	10.484
6B	760	49.967	1.255	22.590	6.076	0.250	1.998	8.993
1	300	19.724	0.498	7.200	2.399	0.099	0.789	3.550
2	270	17.751	0.448	8.064	2.159	0.089	0.710	3.195
3	260	17.094	0.431	7.758	2.079	0.085	0.684	3.077
4	370	24.326	0.614	11.052	2.959	0.122	0.973	4.379
5	610	40.105	1.012	18.216	4.878	0.201	1.604	7.219
6	630	41.420	1.045	18.810	5.038	0.207	1.657	7.456
7	570	37.475	0.945	17.010	4.558	0.187	1.499	6.746
8	530	34.845	0.879	15.822	4.238	0.174	1.394	6.272
9	640	42.078	1.062	19.116	5.118	0.210	1.683	7.574
10	600	39.448	0.995	17.910	4.798	0.197	1.578	7.101
11	250	16.437	0.415	7.470	1.999	0.082	0.657	2.959
12	580	38.133	0.962	17.316	4.638	0.191	1.525	6.864
13	410	26.956	0.680	12.240	3.278	0.135	1.078	4.852
14	350	23.011	0.581	10.458	2.799	0.115	0.920	4.142
15	370	24.326	0.614	11.052	2.959	0.122	0.973	4.379
16	640	42.078	1.062	19.116	5.118	0.210	1.683	7.574
17	740	48.652	1.227	22.086	5.917	0.243	1.946	8.757
19	400	26.298	0.663	11.934	3.198	0.131	1.052	4.734
20	410	26.956	0.680	12.240	3.278	0.135	1.078	4.852
21	420	27.613	0.697	12.456	0.003358	0.138	1.105	4.970
22	410	26.956	0.680	12.240	0.003278	0.135	1.078	4.852

As can be seen from Table 1, it can be noted that the highest value of radon concentration is in sample-17 (48.652 Bq/m^3) and the lowest value in sample-11 (16.437 Bq/m^3). In group B, the highest value of radon concentration is (65.483 Bq/m^3) in sample-1B and the lowest value is (48.323 Bq/m^3) in sample-4B which represents a region deeper than the first region and through the observation of radon concentrations.

It has been measured that they are different because the cave areas are sometimes open and wide, and others are narrow. This also affects the results of radon concentration in two soil samples. According to the procedure in reference [30], the measured results for the black and red samples are 58.298 Bq/m^3 and 127.972 Bq/m^3, as shown in Table 2. These soil samples contain some minerals that contribute to increasing the concentration of uranium in them. Since they are rich in minerals, they can be used in the treatment of certain skin diseases.

Table 2. Radon concentrations and radiation indices for soil sample of Bulak cave.

	Sample		
	Red	Black	Global Limit
Radon concentration (Bq/m^3)	127.972	58.298	(100-200 Bq/m^3) [35]
Radium equivalent content (Bq/kg)	3.361	1.531	(370 Bq/kg) [36]
Area exhalation rate (Bq/m^2.h)	0.160	0.073	(2.5 Bq/m^2.h) [26]
Mass exhalation rate (Bq/kg.h)	0.012	0.012	–

The minimum values of radiation indices AED (mSv/y), LCR (WLM), PAEC (mWL), D_{soft} (nGy/h), D_{lung} (nGy/h) and H_{eff} (nSv/h) are 0.415, 7.470, 1.499, 0.082, 0.657, and 2.959. The maximum values of these radiation indices are 1.227, 22.086, 5.917, 0.243, 1.946, and 8.757. All results for the radon and radiation indices are within the global limit [26, 35-37].

There are approximately 40.000 caves in Türkiye, most of which are protected to preserve geological formations. Only 1% of them are for tourism purposes because they are dangerous to human health due to the quality of the air and the concentration of radon in it. There are limited studies on the nature of the atmosphere inside the caves in Türkiye [15-24]. The mineral concentrations obtained from the XRF examination of the soil samples are given in Table 3. We find that all concentrations of minerals are higher than the acceptable limit given by some science institutions.

Table 3. Mineral concentrations in a soil sample of Bulak cave.

Minerals	Sample		
	Red	Black (ITU) [31]	Permissible Limits (ppm) [32-34]
Fe	132400	8800	3800
Cu	550	489	30
Zn	1393	0.044	50
As	260	-	10
Mn	1905	-	300
Pb	-	-	10
Cr	-	2	70
Co	-	-	8
Cd	-	-	0.06
Ni	-	-	40
Hg	-	-	-

The relationship between E_s and ρ_s is shown in Figure 4. The value of *k* is equal to 0.169 Track. m^3/Bq.Day.mm^2.
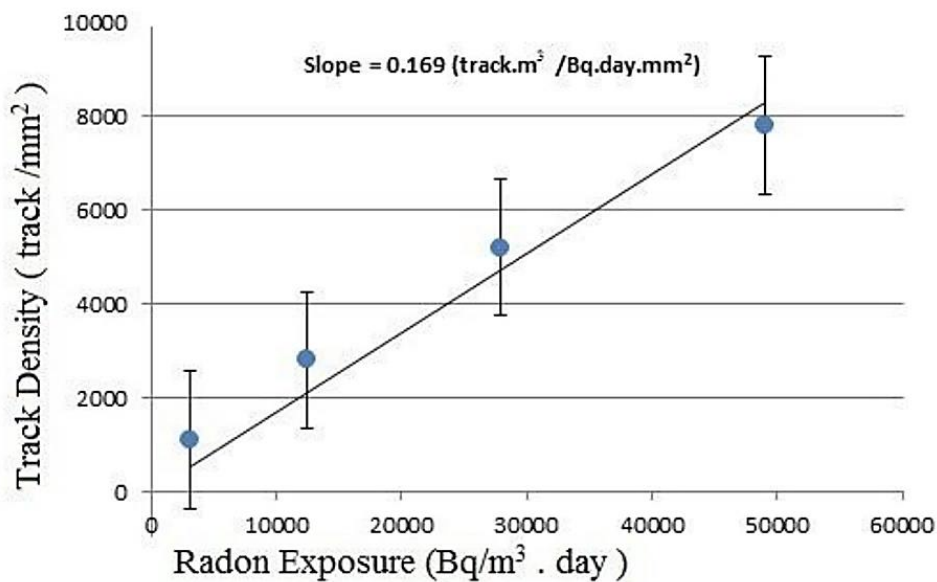
Figure 4. The linear relationship between E_s and ρ_s.

The clay and the non-clay minerals such as Kaolinite, Feldspar, Montmorillonite, Calcite, Palygorskite, Gypsum, and Quartz in the soil sample (the red one) detected with the XRD analyses are presented in Appendix 1 (a-g).

4   CONCLUSIONS

There are different types of soil due to the narrow and wide areas inside the cave, so we conclude that the variation of radon concentrations according to the different regions is normal. The reason for all this is probably the geological composition of the rocks of this cave. The XRF and XRD analyses show that the soil samples taken from the cave are rich with minerals. The mineral concentrations are above acceptable limits set by some scientific institutions. Radon concentrations and radiation indices obtained in this study are within the global limit by UNSCEAR (2000), ICRP (2009), ICRP (2010), and OECD (1979). To reduce radon concentration and improve air quality by reducing carbon dioxide, we recommend at least the construction of ventilation corridors in the area reserved for tourism.

This study will be useful for the next measurements of the concentration of radon in the cave. It is important to make regular radon measurements at least every five years to reduce the risk of exposure to radon gas and the possibility of cancer from this gas. Most of the studies around the world agree that radon risk increases by ~10% with the increase in radon concentration of 100 Bq/m^3 [3]. The present work is a support to the study conducted by [38] on the quality of air and carbon dioxide concentrations inside the cave.

Conflict of interest

There is no conflict of interest among the authors.

Authors contributions

Necla ÇAKMAK and Ulvi KANBUR participated in design and coordination of the study; helped to draft the manuscript; performed the statistical analysis. Khalid Hadi Mahdi AAL-SHABEEB and Ahmet Mustafa ERER participated in the experimental studies. All authors read and approved the final manuscript.

REFERENCES

[1] A. Abd-Elmoniem, "Assessment of indoor Radon doses received by the students and staff in schools in some towns in Sudan," *International Journal of Science and Research*, vol. 4, no. 1, pp. 2319–7064, 2013.

[2] H. G. Ishnayyin, *Finding an empirical relationship for the measurements of radon emitted from building materials inside residential homes*. Iraq, 2015.

[3] H. Zeeb and F. Shannoun, *WHO handbook on indoor radon: A public health perspective. World Health Organization*. Geneva, Switzerland, 2009.

[4] *EPA assessment of risks from Radon in homes, office of radiation and indoor air*. Washington, DC 20460, 2003.

[5] "European Environment and Health Information System (ENHIS)," *European Environment and Health Information System*, 2009.

[6] M. Belson, B. Kingsley, and A. Holmes, "Risk factors for acute leukaemia in children: A review," *Environmental Health Perspectives*, vol. 115, pp. 138–145, 2007.

[7] O. Raaschou-Nielsen *et al.*, "Domestic radon and childhood cancer in Denmark," *Epidemiology*, vol. 19, no. 4, pp. 536–543, 2008.

[8] A. F. Olshan, "Commentary Are 'further studies' really needed? If so, which ones?," *Epidemiology*, vol. 19, no. 4, pp. 545-546, 2008.

[9] Y. Ulusan and O. Batman, "Alternatif turizm çeşitlerinin Konya turizmine etkisi üzerine bir araştırma," *Selçuk Üniversitesi Sosyal Bilimler Enstitüsü Dergisi*, vol. 23, pp. 244–260, 2010.

[10] Ş. Yazgan and E. Kadanalı, "Ağrı ilinin kırsal turizm potansiyelinin değerlendirilmesi," *Karamanoğlu Mehmetbey Üniversitesi Sosyal ve Ekonomik Araştırmalar Dergisi*, vol. 14, pp. 5–10, 2012.

[11] M. Cetin, H. Sevik, and K. Isınkaralar, "Changes in the particulate matter and CO2 concentrations based on the time and weather conditions: The case of Kastamonu," *Oxidation Communications*, vol. 40, pp. 477–485, 2017.

[12] Ö. Arpacı, B. Zengin, and O. Batman, "Karaman'ın mağara turizmi potansiyeli ve turizm açısından kullanılabilirliği," *Karamanoğlu Mehmetbey Üniversitesi Sosyal ve Ekonomik Araştırmalar Dergisi*, vol. 14, no. 23, pp. 59–64, 2012.

[13] A. Aydogdu and H. Sevik, *Indoor air quality: The samples of Ilgarini and Mantar Caves. I. Eurasia International Tourism Congress: Current Issues, Trends, and Indicators*. Konya, Turkey, 2015.

[14] M. Cetin and H. Sevik, "Evaluating the recreation potential of Ilgaz Mountain National Park in Turkey," *Environ. Monit. Assess.*, vol. 188, no. 1, p. 52, 2016.

[15] M. Cetin and H. Sevik, "Assessing potential areas of ecotourism through a case study in ilgaz mountain National Park," in *Tourism - From Empirical Research Towards Practical Application*, InTech, 2016.

[16] B. Haner, A. Yilmaz, M. E. Kürkçüoğlu, and A. Karadem, "Mencilis (Bulak) mağarasında Radon seviyesi ölçümleri. Süleyman Demirel Üniversitesi," *Fen Bilimleri Enstitüsü Dergisi*, vol. 14, no. 3, pp. 218-224, 2010.

[17] P. Koc, N. Ekinci, E. Cinan, and E. Kavaz, "Determination of radon concentration by using CR-39 plastic track detectors in dwellings of bingöl and mus provinces of turkey," *Asian J. Chem.*, vol. 30, no. 1, pp. 226–230, 2018.

[18] H. Kayakökü and M. Dogru, "Radon concentration measurements in surface water samples from Van Lake, Turkey using CR-39 detectors," *Bitlis Eren Univ. J. Sci. Technol.*, vol. 10, no. 1, pp. 35–42, 2020.

[19] K. S. Çam and Y. Parlak, "Indoor radon concentrations and annual effective dose rates for spring and summer seasons by using CR-39 nuclear track detectors in dwellings in Manisa," *Turkey. Arabian Journal of Geosciences*, vol. 15, 2022.

[20] R. M. Cassou and E. V. Benton, "Properties and applications of CR-39 polymeric nuclear track detector," *Nucl. Track Detect.*, vol. 2, no. 3, pp. 173–179, 1978.

[21] U. Cevik, A. Kara, N. Celik, M. Karabidak, and A. Celik, "Radon survey and exposure assessment in Karaca and Çal caves, turkey," *Water Air Soil Pollut.*, vol. 214, no. 1–4, pp. 461–469, 2011.

[22] H. Aytekin, R. Baldik, N. Celebi, B. Ataksor, M. Tasdelen, and G. Kopuz, "Radon measurements in the caves of Zonguldak, Turkey," *Radiation Protection Dosimetry*, vol. 118, no. 1, pp. 117–121, 2006.

[23] R. Baldik, H. Aytekin, N. Celebi, B. Ataksor, and M. Taşdelen, "Radon concentration measurements in the Amasra coal mine, Turkey," *Radiat. Prot. Dosimetry*, vol. 118, no. 1, pp. 122–125, 2006.

[24] B. Haner, A. Yılmaz, M. E. Kürkçüoğlu, and A. Karadem, "Radon level measurements in Mencilis (Bulak) Cave. Süleyman Demirel Üniversitesi," *Fen Bilimleri Enstitüsü Dergisi*, vol. 14, no. 3, pp. 218-224, 2010.

[25] Mengi, H., 2005. Türkiye'nin Doğal Mağaraları. T.C. Kültür ve Turizm Bakanlığı Yayınları, 320 s.

[26] "UNSCEAR United Nations Scientific Committee on the Effects of Atomic Radiation, 2000," *Sources and Effects of Ionizing Radiation*, vol. 1, 2000.

[27] A. A. Mowlavi, M. R. Fornasier, A. Binesh, and M. de Denaro, "Indoor radon measurement and effective dose assessment of 150 apartments in Mashhad, Iran," *Environ. Monit. Assess.*, vol. 184, no. 2, pp. 1085–1088, 2012.

[28] A. A. Battawy, *Internal and external radiation exposure evaluation amongst selected workers and locations in Iraq*. Malaysia, 2013.

[29] "Protection against Radon-222 at home and at work: A report of a task group of the international commission on radiological protection," *Ann ICRP*, vol. 23, no. 2, pp. 1–45, 1994.

[30] K. H. Mahdi, A. M. Erer, U. Kanbur, S. Ağduk, S. Oguz, and N. Çakmak, "Measurement of outdoor Radon Concentrations in Soil Samples collected from Karabuk University in Turkey by using CR-39 Detector," *J. Phys. Conf. Ser.*, vol. 1879, no. 3, p. 032115, 2021.

[31] "Geochemistry Research Laboratory, Analysis Sheet," *Analysis Sheet*, 2018.

[32] Lindsay. W.L.. 1979. Chemical equilibria of soils. John Wiley and Sons. pp.449. W. L. Lindsay. *Chemical Equilibria in Soils*, New York, USA: John Wiley and Sons, 1979, pp.449.

[33] Y. N. Vodyanitskii, "Chromium and arsenic in contaminated soils (Review of publications)," *Eurasian Soil Sci.*, vol. 42, no. 5, pp. 507–515, 2009.

[34] S. Brouder, B. Hofmann, E. Kladivko, R. Turco, and A. Bongen, *Interpreting nitrate concentration in tile drainage water*. 2003.

[35] International Commission on Radiological Protection Statement on Radon (ICRP), 2009. Ref. 00/902/09. International Commission on Radiological Protection Statement on Radon (ICRP), Ref. 00/902/09, 2009. [Online]. Available:
https://www.icrp.org/docs/ICRP_Statement_on_Radon(November_2009).pdf

[36] M. Tirmarche *et al.*, "ICRP Publication 115. Lung cancer risk from radon and progeny and statement on radon," *Ann. ICRP*, vol. 40, no. 1, pp. 1–64, 2010. M. Tirmarche *et al.*, "Lung cancer risk from radon and progeny and statement on radon," ICRP Publication 115 *Ann. ICRP*, vol. 40, no. 1, pp. 1-64, 2010.

[37] "Organization for Economic Cooperation and Development (OECD)," *Organization for Economic Cooperation and Development*, 1979.

[38] M. Cetin, H. Sevik, and A. Saat, "Indoor air quality: The samples of Safranbolu Bulak Mencilis cave," *Fresenius Environmental Bulletin*, pp. 5965–5970, 2017.

APPENDIX

(e) Mass data CKM/Data1
$(Mg_{2.074} Al_{1.026}) (Si_4 O_{10.48})_2 (OH)_2 (H_2O)_{10.68}$

(f) Mass data CKM/Data1
$Ca (S O_4) (H_2 O)_2$
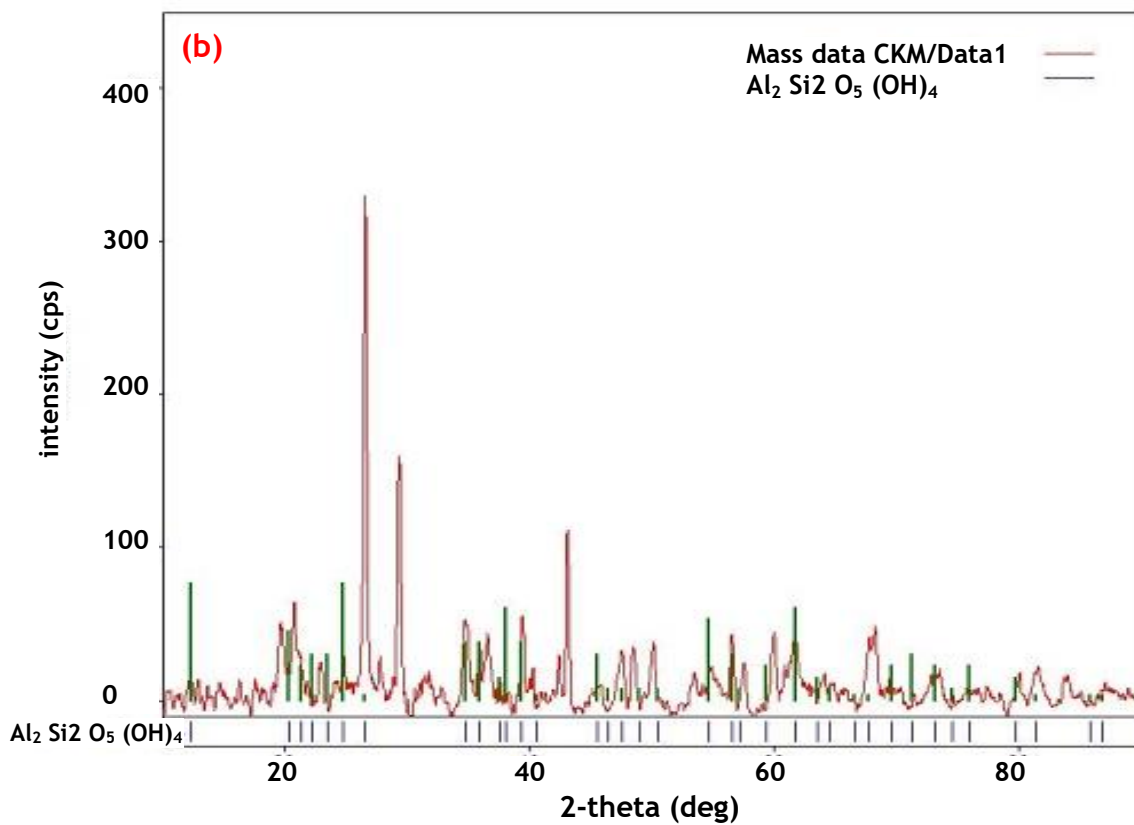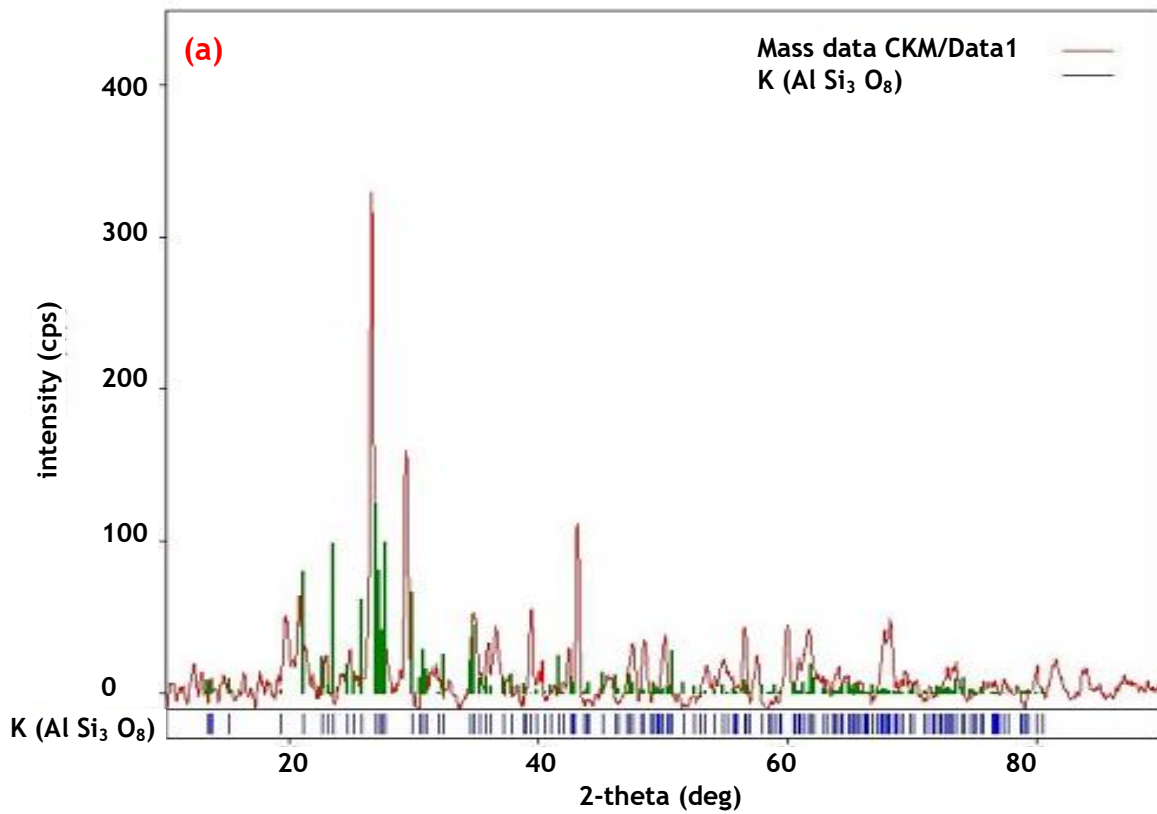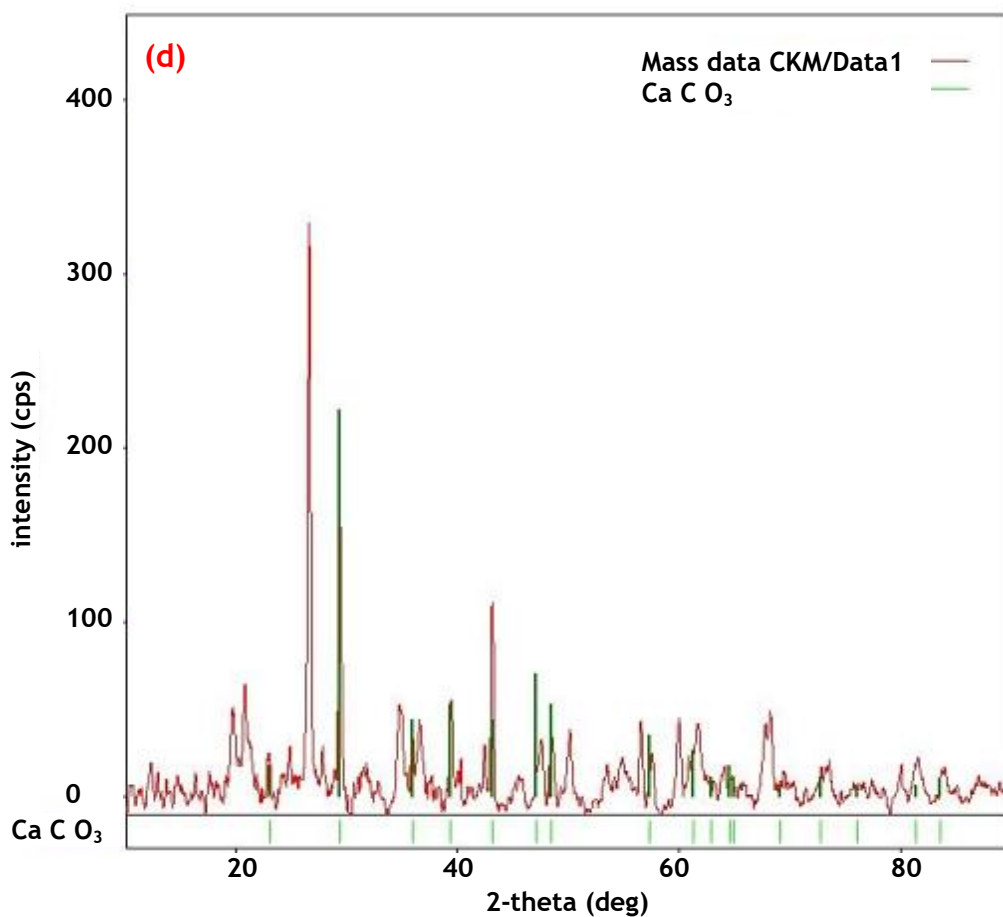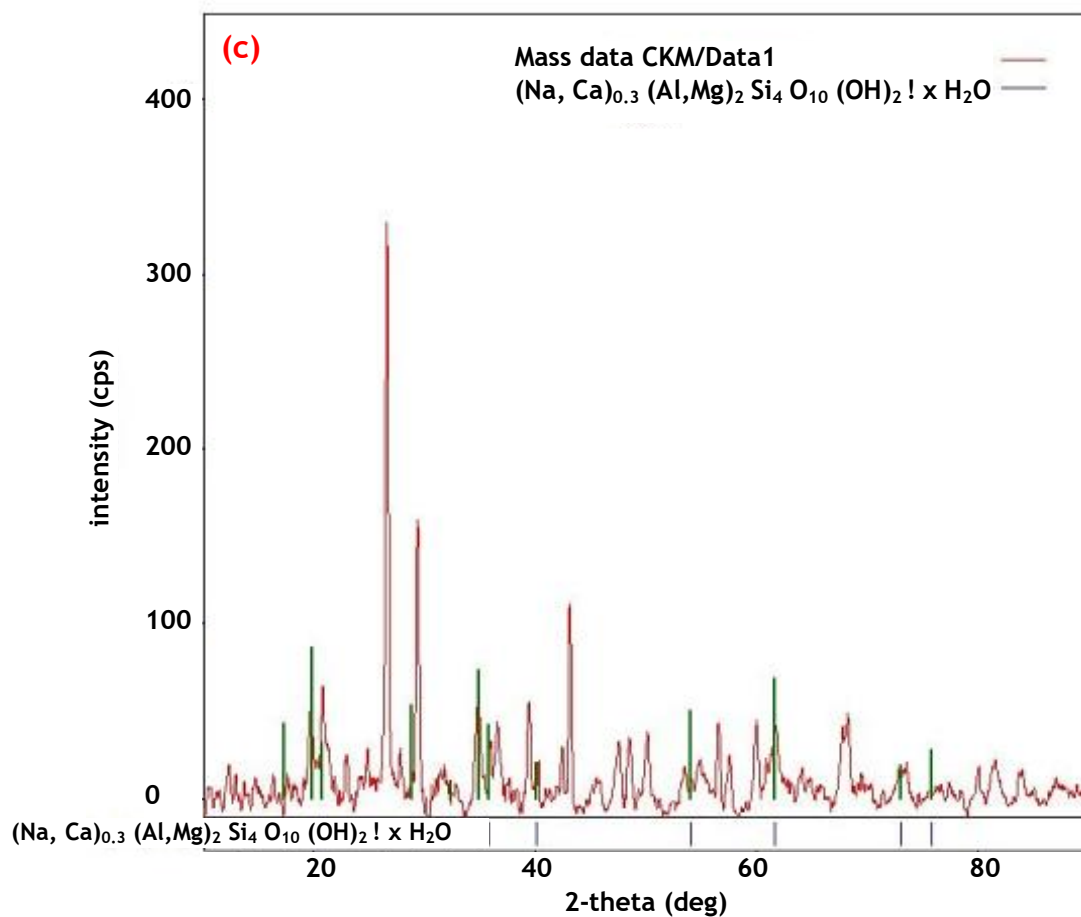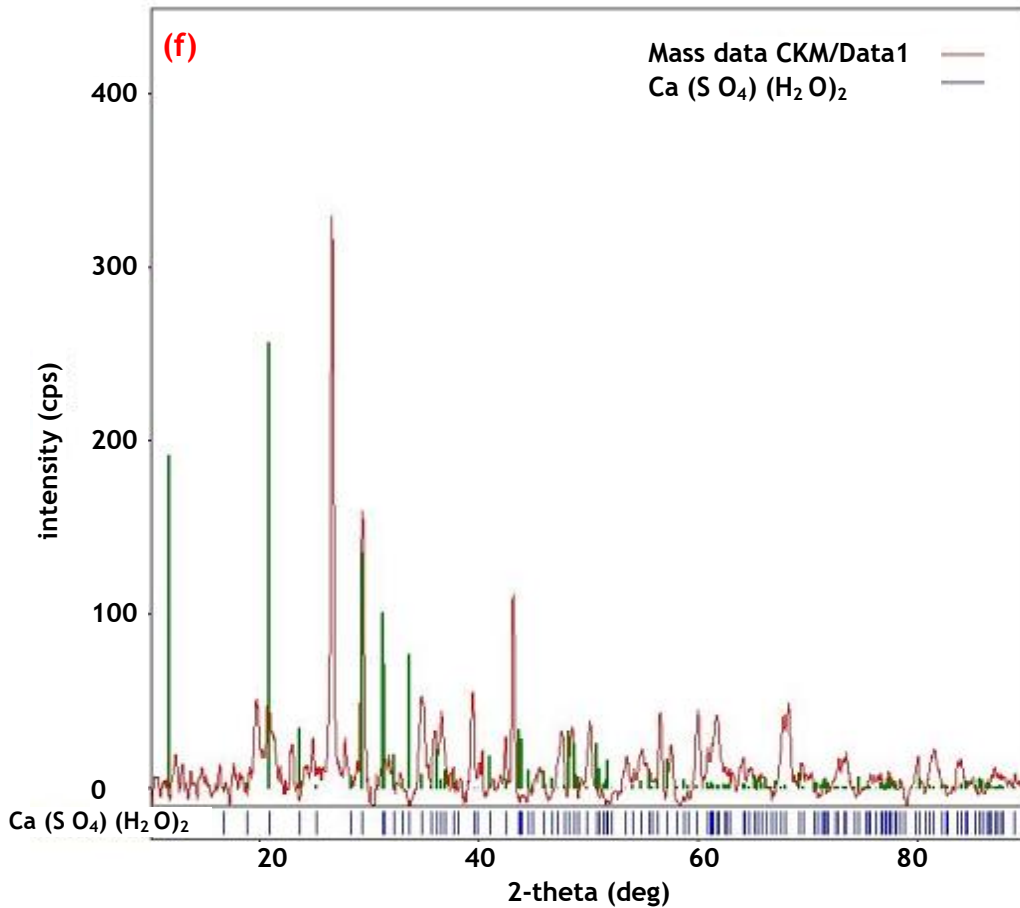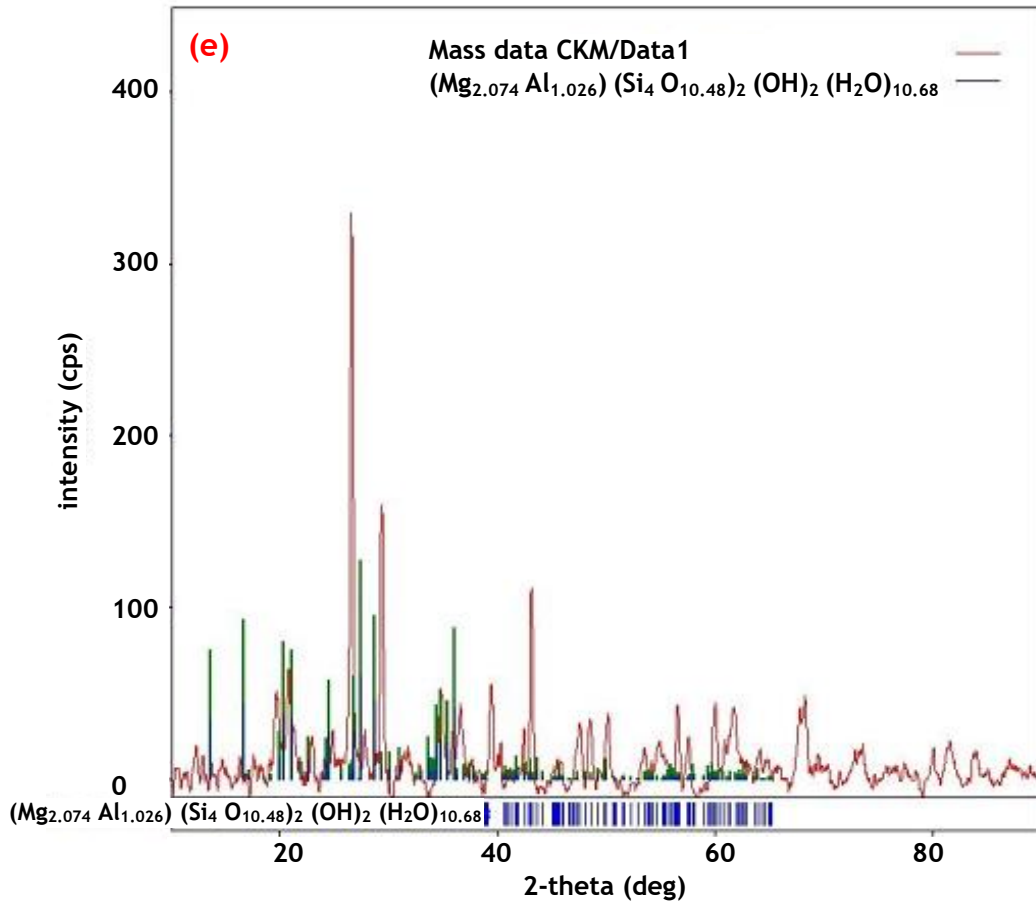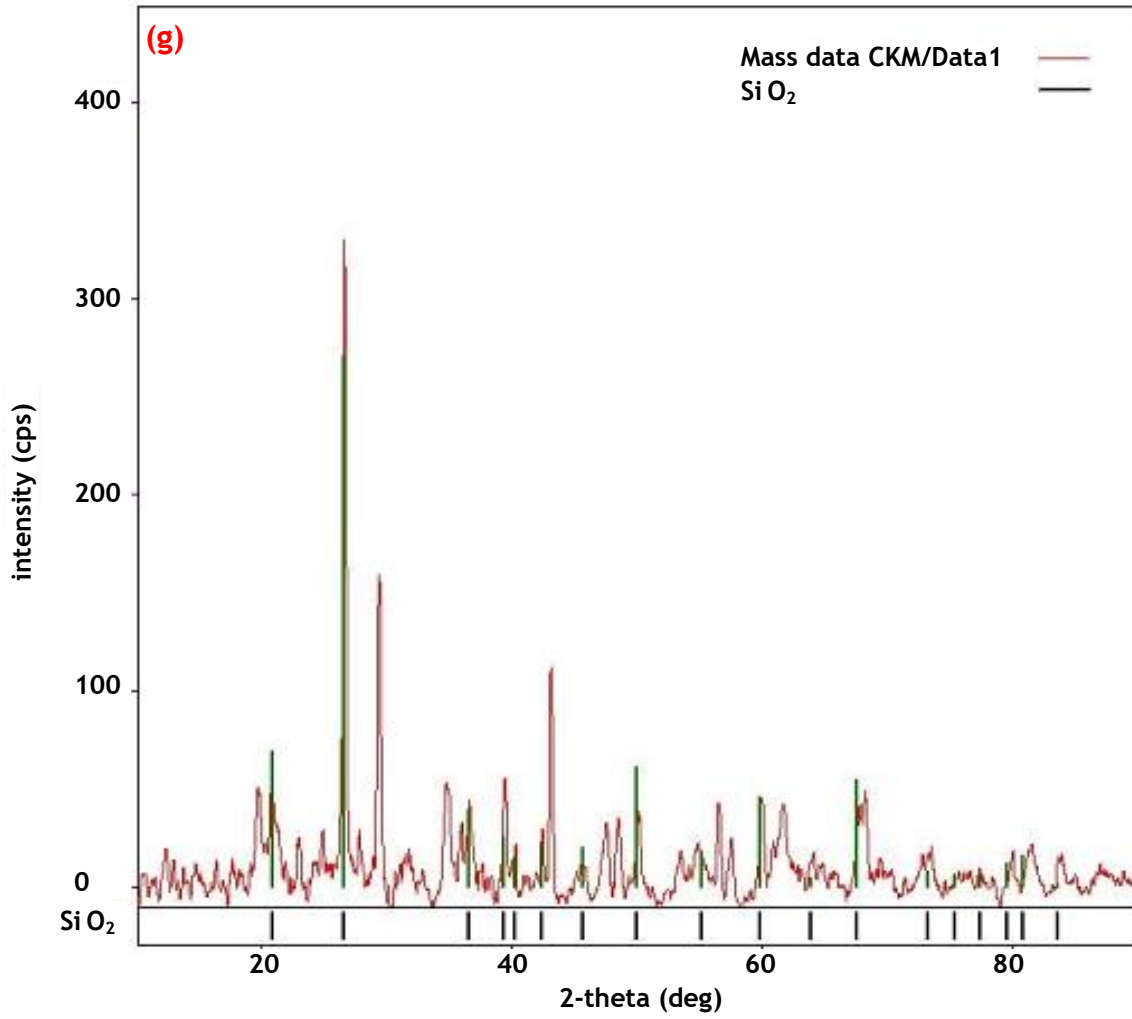
***Appendix 1**. The XRD analyses for the soil sample (the red one), and represent **(a)** Kaolinite, **(b)** Feldspar, **(c)** Montmorillonite, **(d)** Calcite, **(e)** Palygorskite, **(f)** Gypsum, and **(g)** Quartz minerals.*

ISSUES AND CHALLENGES IN THE PHILIPPINE CONSTRUCTION INDUSTRY: AN OPPORTUNITY FOR BIM ADOPTION

Erold Pasajol DIMACULANGAN[1] iD

[1] *Batangas State University, Department of Civil Engineering, Philippines,*
dimaculanganerold@gmail.com

ABSTRACT

The construction industry is widely regarded as the driving force behind global economic growth. The Philippines recorded a GDP increase of 11.8% in the second quarter of 2021. The construction industry is one of the main contributors, with a growth rate of 25.7%. However, the industry faces numerous challenges and issues, the most well-known of which involve the iron triangle of project management, attributed mainly to poor technology adoption, resulting in massive declines in productivity.

Building Information Modeling (BIM) is a popular technology with proven benefits, as demonstrated by countries that have mandated its use. However, BIM is said to be in its infancy in the Philippines. Construction professionals have a low level of awareness, and BIM is primarily used by firms that are outsourcing their services for international projects.

This study aims to identify construction industry issues and their degree of occurrence in Philippine construction. The study also seeks to determine the current state of BIM and identify the current BIM applications to resolve these issues. The study utilized a mixed-methods approach involving a literature review and a structured survey. Data analysis includes Cronbach's alpha for reliability testing, descriptive statistics, the Relative Importance Index (RII), and Kendall's W test.

1   INTRODUCTION

The construction sector is widely regarded as the driving force behind economic growth around the world. This is apparent in both developed and developing countries [1]. In the Philippines, the Department of Trade and Industry (DTI) reported that a GDP growth rate of 11.8% was recorded as of the second quarter of 2021. The construction industry is one of the main contributors, with a growth rate of 25.7% and an average employment of 4.337 million workers [2].

However, the construction industry is often portrayed as a backward industry that fails to adopt innovation, causing a massive decline in productivity as compared to other industries [3]. The industry is confronted with numerous challenges and issues, the most well-known of which are issues involving the iron triangle of project management (time, cost, scope, and quality). Several projects face time and cost overruns, reworks and poor quality, construction claims, waste generation, and other issues. These problems and issues are primarily the result of the construction industry's fragmentation [4]. A study claimed that the conventional way of doing construction failed to address the increasing trend of poor construction performance [5]. In a report conducted by McKinsey Global Institute (MGI) in 2017, the conventional method of construction had lost an estimated $1.63 trillion as of 2015 due to the industry's productivity gap. Over the last two decades, global labor productivity growth in construction has averaged only 1% per year. The construction industry is highly fragmented. As a result, there is poor project management, insufficient design processes, and a lack of investment in skill development and innovation [6].

MGI identified seven ways to tackle the root causes of poor productivity growth. The infusion of technology to improve the performance of the construction industry is one way to optimize the construction process and productivity growth [6]. Many studies have established that the lack of framework, policies, and programs is the main concern of construction companies when adopting technology and innovations [7]-[9]. To address the increasing trend of low productivity and the severity of construction problems, the issues of fragmentation and poor technology adoption must be resolved. In recent years, technology and innovation have presented multiple ways to improve the construction industry's performance. Some

of these includes Augmented Reality/Virtual Reality, Robotics, 3D Printing, Digital Twin, Sensor Data, Building Information Modelling and many others [10].

Building Information Modelling (BIM) is a technology that is gaining popularity due to the proven benefits and return on investment demonstrated by countries that have adopted and mandated its use in construction [11]. The concept of BIM is said to be at a developmental stage in the Philippines. The application of BIM principles in the Philippine construction industry has not been widely adopted in terms of implementation, owing primarily to the high cost of BIM software [12]. The government sector has a low level of awareness of the BIM process. The majority of early BIM adopters were working on large-scale projects that required BIM submittals. Furthermore, BIM is not yet included as a part of undergraduate coursework for engineering and architecture students [13].

This study aims to identify issues and obstacles in the construction industry, as well as the frequency with which these issues are encountered by Filipino construction professionals. The study also aims to determine the current state of BIM in the Philippines and identify current BIM applications in the nation. Finally, the opportunity offered by BIM to address concerns and challenges in the construction industry will be identified.

2 ISSUES AND CHALLENGES IN CONSTRUCTION

Construction industry challenges and issues exist all over the world, whether in developed or developing countries. These impediments and challenges, on the other hand, are more visible in developing countries such as the Philippines, along with a general state of socioeconomic stress, chronic resource shortages, institutional inadequacies, and an overall inability to deal with major concerns. Furthermore, there is evidence that the scope and severity of the problems have grown in recent years [14].

Numerous studies have been discussed on various issues that the construction industry faces and the problems that emerge upon construction project implementation. Table 1 presents a summary of construction issues from various studies where BIM technology has the potential to positively impact and create more opportunities for the industry.

Table 1. *Issues frequently encountered in a construction project.*

Construction Issues	Literature
Variation/change orders	[15], [16], [17], [18]
Design changes	[19], [20], [21], [22]
Time overruns/project delays	[23], [24], [25], [26]
Cost overruns	[27], [28], [29], [30]
Lack of collaboration	[31], [32], [33], [34]
Poor communication	[35], [36], [37]
Reworks	[38], [39], [40]
Quality	[38], [41], [42]
Safety	[42], [43], [44]
Handover/turnover	[45], [46], [47]
Construction wastes	[16], [48], [49]

3   BUILDING INFORMATION MODELLING (BIM)

BIM is a system or approach for managing important building design and project data digitally throughout the life cycle of a building. It is a collection of regulations, software, processes, and technology that are all linked together [50]. BIM uses an intelligent model and a cloud platform to create a digital representation of an asset throughout its existence, from planning and design to construction and operations [51].

BIM-based methodologies can be utilized at any step of a building or infrastructure project, including design, construction, and operation [52]. BIM provides numerous opportunities for all stakeholders to improve the built output and industrial sustainability for the benefit of all. Table 2 outlines the applications of BIM throughout the construction lifecycle, from pre-construction to post-construction, as reported in various literature.

BIM has a wide range of uses and applications [50]. Visualizations may be created using 3D rendering [54], drawings and shop drawings [57] can be extracted, and building codes can be examined using object parameter analysis [52], [53]. Renovations, maintenance, and operation may all be made easier [85], [86], and cost estimation can be done by analyzing the quantity of materials [60], [63].

Construction sequencing can also be used to make scheduling more efficient [61], [62]. Aside from that, the model may be used to run a variety of various analyses and simulations in order to improve the overall performance of any project [87], [88].

Table 2*. Applications of BIM in the construction industry.*

Applications of BIM	Literature
Visual presentation	[52], [53], [54], [55]
Design and analysis	[20], [52], [53], [56]
Drawing and detailing	[52], [53], [57], [58]
Project scheduling and controlling	[59], [60], [61], [62]
Cost estimation	[50], [60], [63], [64]
Quantity surveying	[60], [65], [66], [67]
Tendering	[52], [53], [68, [69]
Site utilization and lay-out	[70], [71], [72], [73]
Constructability analysis	[50], [74], [75], [76]
Collaboration	[53], [77], [78]
Safety management	[79], [80], [81], [82]
Facility management	[83], [84], [85], [86]

4 KNOWLEDGE GAPS

To identify knowledge opportunities, an investigation of related studies in the Philippines itself is crucial. In the Philippines, there is little research focused on BIM technology. Prior to 2013, almost no research on BIM in developing nations existed, and the current studies are limited to the three countries of China, India, and Malaysia [89]. More research is needed on BIM awareness, definitions, and developments, as well as how these difficulties should be addressed.

The most recent study related to BIM application in the Philippines was conducted by Silva et al. in 2021, which focused on creating an interdisciplinary framework integrating BIM and Lean Construction principles concerning the triple constraints of project management using Structural Equation Modelling (SEM) [90].

The study is focused on determining the impacts and prospects of BIM and Lean integration but does not provide a specific assessment of BIM or construction issues.

Rodriguez et al. conducted a study in 2019 on BIM adoption in the Philippines. The study was focused on determining the acceptance level of BIM in the AEC industry and evaluating the prospects and challenges of BIM as applied to lean construction principles [12]. This research used a structured survey questionnaire with questions aimed at describing the current state of BIM in relation to key prospects and problems in lean construction in the Philippines. This study is limited to BIM status assessment and does not evaluate the issues in construction.

Ongpeng conducted another study in 2018 which he used BIM as a simulation tool to compare the time and expenses of two formwork methodologies: traditional and steel deck. A Process Control Model (PCF) approach was used to measure quality costs between methods [91]. This study demonstrated how BIM simulation may assist managers in deciding which construction methodology to use in order to balance project cost and schedule. This study is purely a case study about practical BIM application in decision-making and does not provide an assessment of construction issues.

Based on a thorough review of the literature, it was established that no particular research has been conducted into the Philippine construction industry in order to assess the construction issues and identify the opportunities for resolving these issues through BIM technology. To close this knowledge gap, this study aims to evaluate all of these gaps, provide an assessment of the frequency of construction issues, identify BIM opportunities to resolve these issues, and assess the current BIM status in the Philippines.

This research will focus on covering knowledge areas such as construction issues, applications of BIM, and current BIM status in the Philippine construction industry.

5 RESEARCH METHODOLOGY

This study was conducted using a mixed-methods approach incorporating both qualitative and quantitative methodologies. The research data will be collected in two phases. The first phase is a qualitative approach that involves a review of related

literature to determine the issues and challenges in the construction industry and the applications of BIM. Phase 2 is a quantitative approach that includes the distribution of a survey questionnaire to construction professionals in the Philippines.

5.1   Literature Review

The review of related literature resulted in the identification of 11 issues frequently encountered in the construction industry and 12 commonly cited applications of BIM in the construction process.

The 11 issues include: variation or change orders, design changes, time overruns or project delays, cost overruns, lack of collaboration, poor communication, reworks, quality, safety, handover or turnover, and construction waste.

The 12 BIM applications include: visual presentation, design and analysis, drawing and detailing, project scheduling and controlling, cost estimation, quantity surveying, tendering, site utilization and layout, constructability analysis, collaboration, safety management, and facility management.

These findings will be used in constructing the survey questionnaire to be used in the data collection.

5.2   Survey Questionnaire

The study utilized a structured survey to elicit responses among construction professionals and establish the degree of agreement and frequency for each variable. A 6-point Likert scale was used to eliminate neutral responses and solicit a more valid response as compared to odd-numbered Likert scales [92].

The survey consists of three parts, which include: (1) demographic profile; (2) construction issues; and (3) BIM awareness and current applications.

5.2.1 Demographic profile of respondents

The first part aims to collect the demographic profile of the respondents, including their educational attainment, profession, years of experience in construction, sector involved, construction stakeholder group, type of construction

involved, position level in their current company or organization, project location, project cost and company size.

5.2.2 Issues in the construction industry

This part involves collecting responses on the degree of frequency with which each respondent encountered the listed issues in the construction. The list of construction issues was based on the literature review. Each issue will be rated by the responder based on a 6-point Likert scale: 6 for Always, 5 for Very frequently, 4 for Occasionally, 3 for Rarely, 2 for Very rarely, and 1 for Never.

5.2.3 Current BIM status and its applications

The last part involves collecting data from respondents on the current status of BIM in the Philippines in terms of awareness and applications. The first two questions aim to identify the knowledge of the respondents about BIM and whether they are BIM users or not. For the non-BIM users, the questions were about the current technology or process that they use in preparing designs, plans, estimates, and project schedules. For BIM users, the questions were about the BIM software that they use and the applications of BIM in their current project(s). Finally, all respondents were asked about their perception of the future of BIM in the country.

5.2.4 Sampling method

The sampling method used is purposive sampling, which specifically targets construction professionals in the Philippines. Professional organizations provided an approximate number of registered professionals, numbering 233,300, as shown in Table 3.

Table 3. *Approximate number of registered construction professionals in the Philippines as of 2021.*

Profession	Number	Source
Civil Engineer	100,000	[97]
Architects	42,000	[98]
Mechanical Engineer	65,000	[99]
Electrical Engineer	23,000	[100]
Sanitary Engineer	3,300	[101]
Total	233,300	

The minimum required sample was calculated using Slovin's method as shown:

$$n = \frac{N}{1 + Ne^2} \tag{1}$$

where n is the sample size, N is the population and "e" is the margin of error taken as 9% or 0.09. The calculated minimum sample size is 124.

5.2.5 Pilot testing

The initial survey draft was sent to 12 construction experts for pilot testing. The experts hold supervisory and management level positions. The profiles of the experts are presented in Table 4.

Table 4. Profile of experts for pilot testing.

Expert	Job title	Years of Experience
1	Department Head	5
2	Senior Civil Engineer	17
3	Senior Architect	23
4	Director	24
5	Project Manager	20
6	Lead Architect	9
7	Portfolio Planning Engineer	5
8	BIM Manager	7
9	Lead BIM Engineer	12
10	Operations Manager	20
11	Associate Professor IV	24
12	Senior Lead Piping Engineer	23

The experts were from various organizations, such as academia, city engineering offices, consulting and design firms, AAA contractors, and construction management firms. Aside from minor revisions such as the inclusion of project location, the general consensus suggests the validity of the instrument to gather the relevant data required.

5.3 Data Analysis

This study used descriptive statistics and the Relative Importance Index (RII) to assess the level of importance of each construction issue. A reliability test was also performed to determine whether or not a respondent would give the same score

on a variable if it were given to the same respondent again and again. The data will be analysed using Microsoft Excel and SPSS software.

5.3.1 Reliability test

This test was conducted using Cronbach's alpha (α), which is a measure of internal consistency and determines if all variables are moving in the same direction and have a statistically significant relationship [93]. Cronbach's alpha (α) can be calculated using the formula shown:

$$\propto = \frac{K}{K-1}\left(1 - \frac{\sum s_y{}^2}{s_x{}^2}\right)$$
(2)

where K is the number of items/questions, $\sum s2y$ is the sum of variance for each item/question and s2x is the variance of the observed total test scores.

5.3.2 Relative importance index (RII)

The Relative Importance Index (RII) approach is widely used to examine survey data resulting from the use of response scales in construction management research surveys. RII is calculated in several ways across construction management research. The frequently cited formula [94] and the simplest form of RII are calculated as:

$$RII = \frac{\sum W}{AN}$$
(3)

where W is the sum of scores awarded a variable from N respondent sample, A is the largest integer on the response scale (Likert) and N is the total number of samples.

5.3.3 Kendall's W – coefficient of concordance

It measures how well "k" sets of rankings agree with one another. It is a linear relationship between the mean rank correlation coefficients for all ranking pairs [95]. Kendall's W is determined as follows:

$$W = \frac{12S}{n^2 k(k-1)}$$
(4)

where S is the squared deviation, n is the number of observers/raters and k is the number of objects to be ranked. Chi-square (x^2) is also calculated using SPSS. If the number of items to be ranked exceeds 7, chi-square analysis should be used instead of Kendall's W. The chi-square for Kendall's W can be calculated as:

$$\chi^2 = k(N-1)W \qquad\qquad (5)$$

where k is the number of respondents, n is the number of items to be ranked and W is the Kendall's coefficient. If the calculated x^2 exceeds the critical value, there is significant agreement among "n" observers in the ranking of "k" objects.

6 RESULTS AND DISCUSSIONS

The initial minimum required sample calculated using Slovin's method is 124 respondents. After the distribution of the survey questionnaire online, a total of 134 valid responses were collected.

6.1 Demographic Profile

The first part of the survey aims to identify the demographic profile of the respondents.

The first question asks for the respondents' highest educational attainment. The results are presented in Figure 1.
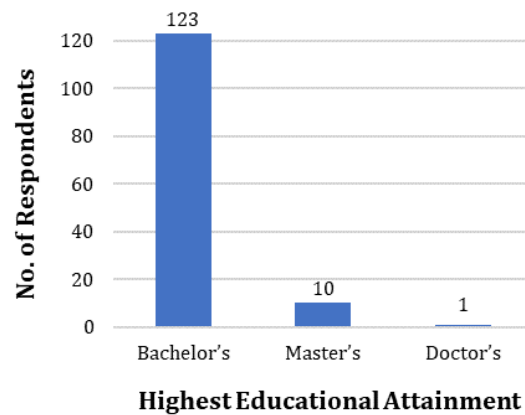
Figure 1. *Respondents' educational profile.*

Based on the survey, most respondents have relevant bachelor's degrees (123) and some of them have master's degrees (10), but only one has a doctorate.

The next question asks for the respondents' profession related to the construction industry. The results are presented in Figure 2.
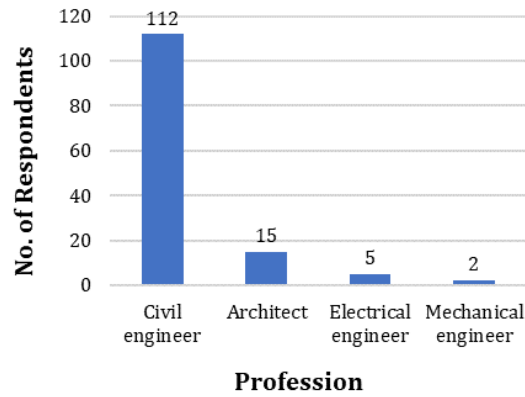
Figure 2. *Respondents' professional profile.*

From Figure 2, the majority of the respondents are civil engineers (112), followed by architects (16), electrical engineers (5), and mechanical engineers (2).

The next question aims to identify the level of construction-related experience of the respondents. The results are presented in Figure 3.
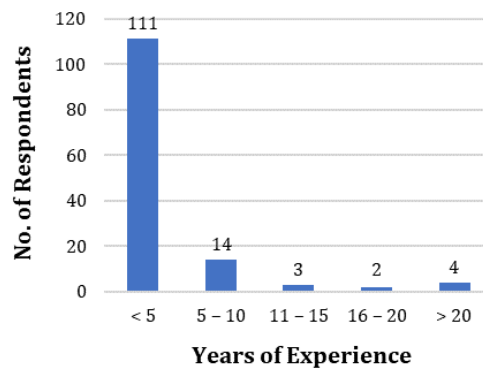
Figure 3. *Respondents' experience profile.*

From the survey, the majority of respondents are young professionals with less than five years of experience (111); fourteen have 5–10 years of experience; three have 11–15 years of experience; two have 16–20 years of experience; and four have more than 20 years of experience.

The next question is about the current sector affiliation of each respondent. The results are presented in Figure 4.
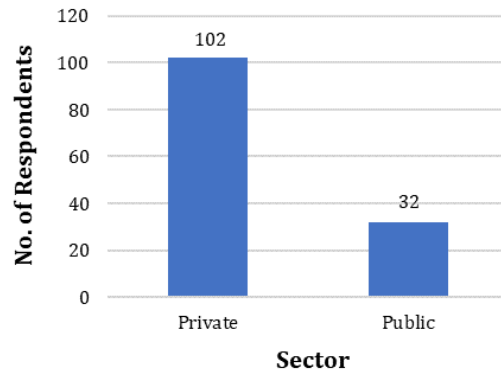
Figure 4. *Respondents' sector profile.*

From the survey, the majority of respondents are from the private sector (102) while only 32 are from the public sector.

The next question is about the stakeholder group of each respondent. The results are presented in Figure 5.
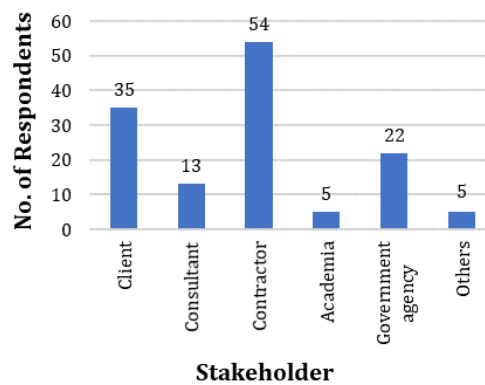
Figure 5. *Respondents' stakeholder profile.*

From the survey, the majority of respondents are from the contractor's group (54), followed by the client's group (35), the government agency (22), the consultant's group (13), academia (5), and other groups (5).

The next question is about the level of position in the company of each respondent. The results are presented in Figure 6.
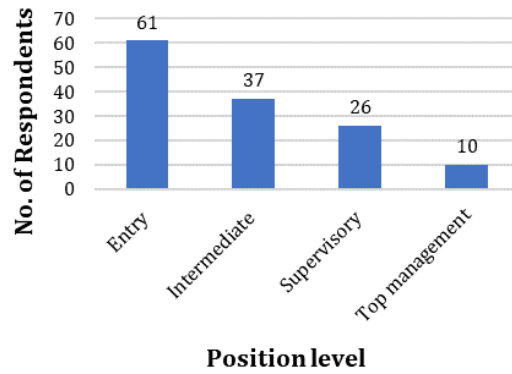
Figure 6. Respondents' company position profile.

From the survey, the majority of respondents hold an entry-level position (61), 37 hold an intermediate-level position, 26 hold a supervisory-level position, and 10 hold a top management-level position.

The next question is about the project costs handled by the respondents' companies. The results are presented in Figure 7.
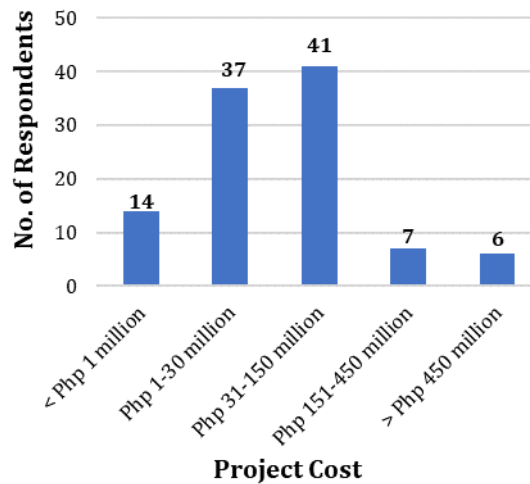
Figure 7. Respondents' project cost profile.

From the survey, the majority of respondents' companies handle projects costing 31–150 million pesos (41), followed by projects costing 1–30 million pesos (37), then projects costing less than 1 million pesos, then projects costing 15–150 million pesos (7), and lastly projects costing more than 450 million pesos (6).

The next question is about the geographical location of each project handled by the respondents' companies. The results are presented in Figure 8.
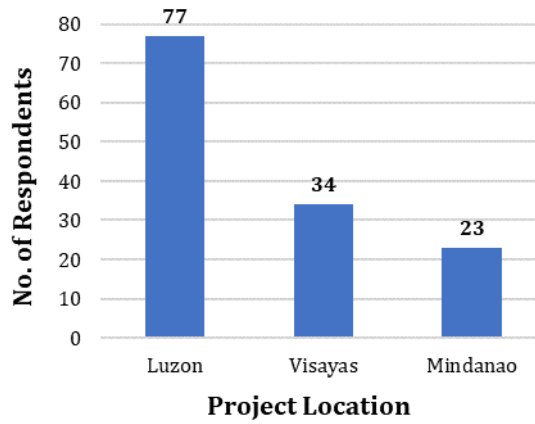
Figure 8. Respondents' project location profile.

From the survey, the majority of respondents' projects are located in the Luzon area (77), followed by the Visayas area (34), and lastly, the Mindanao area (23). This suggests that the concentration of construction activities is still within the area of Luzon, where the two highly industrialized regions are located: the National Capital Region and the Calabarzon region.

The next question aims to identify the company size of each respondent to determine the extent of their workforce. The results are presented in Figure 9.
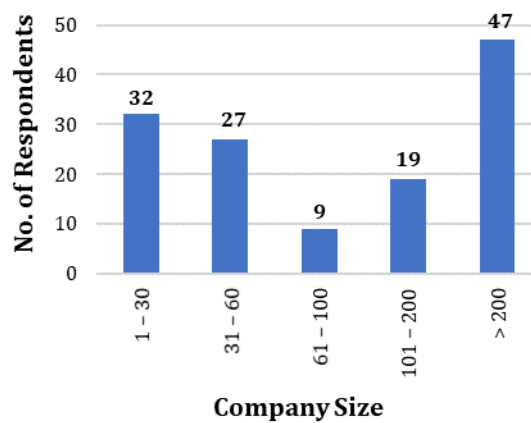
Figure 9. Respondents' company size profile.

From the survey, the majority of respondents belong to large companies with more than 200 employees (47), followed by companies with 1–30 employees (32), then followed by companies with 31–60 employees (27), followed by companies with 101–200 employees (19), and lastly by companies with 61–100 employees (9).

The last question is about the type of construction project that each respondent handles. This question asks about all types of projects in which the respondents are involved. The results are presented in Figure 10.
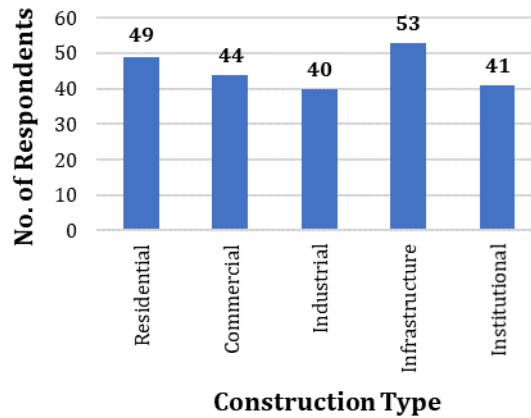
Figure 10. Respondents' construction type profile.

From the survey, the majority of respondents are handling infrastructure type projects such as roads, bridges, and flood controls (53), followed by residential type (49), then commercial type (44), then institutional type such as schools and hospitals (41) and lastly, industrial type (40).

6.2   Construction Issues

A total of 11 issues frequently encountered in construction have been identified. The respondents were asked to rate each issue based on its degree of severity or occurrence in their construction projects and experiences.

The results of the survey were tested first for reliability using Cronbach's alpha. The test results showed that the sum of the variance for each barrier (Σs_y^2) is 18.39 and the variance of the observed total rating (s_x^2) is 174.32. The calculated Cronbach's alpha for the 11 items is $\alpha = 0.984$, which signifies "Excellent" internal consistency and reliability [96].

The results of the survey are presented in Table 5.

Table 5. *Rankings of construction issues from the survey.*

Construction Issues	$\bar{x}$	σ	RII	Rank	Importance Level
Change order	4.806	1.28	0.801	2	High
Time delays	4.866	1.28	0.811	1	High
Cost overruns	4.597	1.32	0.766	6	Medium High
Lack of collaboration	4.418	1.31	0.736	10	Medium High
Poor communication	4.343	1.28	0.724	11	Medium High
Design changes	4.716	1.33	0.786	4	Medium High
Reworks	4.522	1.31	0.754	8	Medium High
Safety management	4.709	1.33	0.785	5	Medium High
QA/QC	4.761	1.22	0.794	3	Medium High
Handover issues	4.552	1.32	0.759	7	Medium High
Construction waste	4.470	1.30	0.745	9	Medium High

Note: $\bar{x}$ = mean and σ = standard deviation

Based on the results of the RII rankings shown in Table 5, the top five issues that are frequently encountered in construction are time delays, variation or change orders, quality issues, design changes, and safety. The most frequent issue encountered in construction is time delays, with an RII of 0.811. This is consistent with the findings of Sweis in 2013, wherein it is mentioned that time overruns are a common occurrence and are almost always associated with construction projects [26]. Consequently, if there are change orders, additional duration will automatically follow, and based on the survey, change orders have an RII of 0.801. Keane et al. stated that consultant-related variations due to changes in the design are the norm in the construction industry [17]. Quality issues ranked third with an RII of 0.794. In a study by Wawak et al., it was stated that only 14% of construction projects are successful, 67% are challenged, and up to 19% fail in terms of delivering quality projects and customer satisfaction [41]. Design changes ranked fourth with an RII of 0.786. Design changes generally contribute to change orders that ultimately lead to additional costs and project durations [21]. Safety-related issues are the fifth most common, with a RII of 0.785, which is consistent with the study of Zaid Alkilani et al., which found that safety problems in the construction industry are becoming more widespread than previously recorded [44]. Ogwueleka mentioned that because of its

unique nature, the construction industry is regarded as the most dangerous [42]. As a result, these top five issues are the major issues that the respondents frequently experienced during project implementation.

Based on the data, issues such as cost overruns and reworks are ranked 6th and 8th, respectively. Literature proves that the other issues stated were substantially caused by the major issues such as poor communication, design changes, and poor quality, resulting in additional costs, duration, waste, and issues during project handover. Overall, all 11 issues have RII values above 0.60, which generally indicates that all these issues have medium-high to high importance level and need to be addressed to improve the construction industry [94].

To validate the rankings of the construction issues, the Kendall's W test was performed using the SPSS. The null hypothesis (Ho) states that "*There is no significant agreement among respondents within a group in the ranking of construction issues.*" Since the number of items to be ranked is 11, which is greater than 7, the chi-square statistic is used instead of Kendall's W to decide for the null hypothesis. The calculated $\lambda 2$ for the respondents is 121.803, and the critical $\lambda 2$ for n = 11 is 19.675. The calculated asymptotic significance for the group is 0.000, which is less than 0.05. Hence, the null hypothesis should be rejected. According to the result of the statistical test, there is sufficient evidence to conclude that the respondent's groups of rankings for construction issues are interdependent, with a high degree of agreement within each group.

6.3   Current BIM Status and Its Applications

The data from the third part of the survey shows that 35.82% of the respondents are not aware of BIM, 58% are aware but do not have substantial knowledge of BIM, and only 20.90% are knowledgeable and are currently practicing BIM. Overall, 79.10% of the respondents are not BIM users, and 20.90% are BIM users.

For non-BIM users, all respondents stated that instead of BIM, they are currently using computer-aided drawing and design (CADD) to produce drawings and designs for construction. The respondents also stated that currently, spreadsheets and manual calculations are being utilized in preparing material quantity take-offs, cost estimates, and project schedules.

For BIM users, data shows that 64.29% of the respondents use Autodesk Revit, 21.43% use Tekla, 17.86% use ArchiCAD, 35.71% use Bentley, 39.29% use Navisworks, and 10.71% use other software such as Edgewise and Vectorworks. A total of 12 construction-related applications for BIM were presented to the BIM users, and the result of the survey is presented in Table 6.

Table 6. Current BIM applications status.

BIM Application	Frequency	Percentage (%)	Rank
Visual presentation	11	39.29	6
Design and analysis	26	92.86	1
Drawing and detailing	22	78.57	2
Projects scheduling and controlling	13	46.43	4
Cost estimation	12	42.86	5
Quantity surveying	10	35.71	7
Tendering	5	17.86	9
Site utilization and lay-out	16	57.14	3
Constructability analysis	7	25.00	8
Collaboration	13	46.43	4
Safety management	5	17.86	9
Facility management	2	7.14	10

The data shows that the top five applications of BIM among BIM users are design and analysis (92.86%), drawing and detailing (78.57%), site utilization and layout (57.14%), collaboration and project scheduling (46.43%), and cost estimation (42.86%). The least common applications of BIM are for tendering and safety management (17.86%) and facility management (7.14%). These show that the current BIM applications among BIM users provide substantial evidence that BIM can improve and resolve the top issues in the construction industry, such as design changes, change orders, and quality issues.

Finally, all respondents were asked about their perceptions of the future of BIM in the Philippines. The majority of the respondents (61.19%) feel that there will be increasing use of BIM, 26.87% feel that there will be a mandatory requirement for the use of BIM, and 11.94% feel that there will be no usage of BIM.

7 CONCLUSIONS

The technological advancement provides multiple opportunities and advantages for construction to further improve its productivity and efficiency and contribute to more sustainable construction. The aim of this study is to identify the common issues and challenges in construction and determine the degree of frequency of each issue among Filipino construction professionals. Furthermore, the study also aims to determine the current status of BIM in the country and identify the current applications of BIM in construction.

The literature review identified 11 common issues and challenges, which include change orders, time and cost overruns, lack of collaboration and poor communication, quality issues and reworks, design changes, safety issues, and construction waste. 12 BIM applications were also identified, which include design and analysis, drawing and detailing, project scheduling, cost estimations, quantity surveying, safety and facility management, collaboration, visual presentation, constructability analysis, site utilization, and tendering.

The study shows that the top five issues that Filipino construction professionals encountered and found most significant in terms of RII were time delays (0.707), change orders (0.694), quality issues (0.660), design changes (0.636), and safety issues (0.627). Overall, all 11 issues proved to be significant among respondents with RII values above 0.50, which indicates a medium-to-highly significant level. Survey data revealed that the current awareness level about BIM is not that high, with 35.82% of the respondents having no awareness and only 20.90% having significant knowledge and skills about BIM. The study shows that the majority of the industry does not implement BIM in their current construction processes and is currently still using traditional methods such as CADD-based drawing and spreadsheets. BIM users generally use Autodesk Revit to perform BIM-related applications, but other software is also being utilized, such as ArchiCAD and Bentley. Currently, data shows that the top five applications of BIM among users include: (1) design and analysis; (2) drawing and detailing; (3) site utilization and layout; (4) project scheduling and collaboration; and (5) cost estimation. Data shows that currently, the Philippine construction industry is starting to realize the opportunities

of using BIM to further enhance and improve construction. The majority of the respondents feel that the direction of BIM is towards the adoption of BIM technology.

This study contributes to the promotion of using BIM in Philippine construction and provides insight on the opportunities and advantages that the technology can provide. The findings of this study can help in developing strategies to further increase the awareness of the industry about BIM and provide actions to disseminate BIM education and knowledge among construction stakeholders. Furthermore, a more in-depth study is suggested to explore the topic of BIM adoption strategies in Philippine construction.

Statement of Research and Publication Ethics

The study is complied with research and publication ethics.

REFERENCES

[1] O. Balaban, "The negative effects of construction boom on urban planning and environment in Turkey: Unraveling the role of the public sector," *Habitat International*, vol. 36, no. 1, pp. 26-35, 2012.

[2] Department of Trade and Industry (DTI), "Construction industry contributes 16.6% to GDP amidst pandemic," dti.gov.ph. [Philippines]; [accessed January 21, 2022]. Available: https://www.dti.gov.ph/news/construction-industry-contributes-to-gdp/

[3] J. B. H. Yap, C. G. Y. Lam, M. Skitmore, and N. Talebian, "Barriers to the adoption of new safety technologies in construction: A developing country context," *Journal of Civil Engineering and Management*, vol. 28, no. 2, pp. 120-133, 2022.

[4] J. Challender and R. Whitaker, *The Client Role in Successful Construction Projects*. Routledge, 2019.

[5] S. Gao and S. P. Low, *Lean Construction Management: The Toyota Way*. Springer, 2014.

[6] F. Barbosa, J. Woetzel, and J. Mischke, *Reinventing construction: A route of higher productivity*. McKinsey Global Institute, 2017.

[7] M. Regona, T. Yigitcanlar, B. Xia, and R. Y. M. Li, "Opportunities and adoption challenges of AI in the construction industry: a PRISMA review," *Journal of Open Innovation: Technology, Market, and Complexity*, vol. 8, no. 1, 2022.

[8] H. M. F. Shehzad, R. B. Ibrahim, A. F. Yusof, and K. A. M. Khaidzir, "Building information modeling: factors affecting the adoption in the AEC industry," in 2019 6th International Conference on Research and Innovation in Information Systems (ICRIIS), IEEE, 2019, pp. 1-6.

[9] S. Mamter, A. R. A. Aziz, and J. Zulkepli, "Root causes occurrence of low BIM adoption in Malaysia: System dynamics modelling approach," in AIP Conference Proceedings, vol. 1903, no. 1, AIP Publishing, 2017.

[10] G. Ellis, "8 Innovations that Will Change Construction As We Know It," Digital Builder. Retrieved March 9, 2022, from https://constructionblog.autodesk.com/construction-innovations/

[11] H. M. Bernstein, S. A. Jones, M. A. Russo, D. Laquidara-Carr, W. Taylor, J. Ramos, and Y. Terumasa, *The business value of BIM for construction in major global markets*. Bedford: McGraw Hill Construction, 2014.

[12] L. V. Rodriguez, O. R. Bagcal, M. A. Baccay, and B. M. Barbier, "Adoption of Building Information Modeling (BIM) in the Philippines' AEC Industry: Prospects, Issues, and Challenges," *Journal of Construction Engineering, Technology and Management*.

[13] V. Villasenor, F. Villasenor, and D. Gonzalez, *Educating Green Building Stakeholders About the Benefits of BIM - The Philippines Experience*. Manila: Joint APEC-ASEAN Workshop - How Building Information Modeling Standards Can Improve Building Performance, 2012.

[14] J. M. Hussin, I. A. Rahman, and A. H. Memon, "The way forward in sustainable construction: issues and challenges," *International Journal of Advances in Applied Sciences*, vol. 2, no. 1, pp. 15-24, 2013.

[15] V. T. Nguyen and S. T. Do, "Assessing the relationship chain among causes of variation orders, project performance, and stakeholder performance in construction projects," *International Journal of Construction Management*, vol. 23, no. 9, pp. 1592-1602, 2023.

[16] A. Porwal, M. Parsamehr, D. Szostopal, R. Ruparathna, and K. Hewage, "The integration of building information modeling (BIM) and system dynamic modeling to minimize construction waste generation from change orders," *International Journal of Construction Management*, vol. 23, no. 1, pp. 156-166, 2023.

[17] P. Keane, B. Sertyesilisik, and A. D. Ross, "Variations and change orders on construction projects," *Journal of Legal Affairs and Dispute Resolution in Engineering and Construction*, vol. 2, no. 2, pp. 89-96, 2010.

[18] W. Khalifa and I. Mahamid, "Causes of Change Orders in Construction Projects," *Engineering, Technology & Applied Science Research*, vol. 9, no. 6, 2019.

[19] J. R. Lin and Y. C. Zhou, "Semantic classification and hash code accelerated detection of design changes in BIM models," *Automation in Construction*, vol. 115, 103212, 2020.

[20] M. Juszczyk, A. Tomana, and M. Bartoszek, "Current issues of BIM-based design change management, analysis and visualization," *Procedia Engineering*, vol. 164, pp. 518-525, 2016.

[21] R. M. Choudhry, H. F. Gabriel, M. K. Khan, and S. Azhar, "Causes of discrepancies between design and construction in the Pakistan construction industry," *Journal of Construction in Developing Countries*, vol. 22, no. 2, pp. 1-18, 2017.

[22] S. Han, S. Lee, and F. Pena-Mora, "Identification and quantification of non-value-adding effort from errors and changes in design and construction projects," *Journal of Construction Engineering and Management*, vol. 138, no. 1, pp. 98-109, 2012.

[23] A. Kavuma, J. Ock, and H. Jang, "Factors influencing time and cost overruns on freeform construction projects," *KSCE Journal of Civil Engineering*, vol. 23, pp. 1442-1450, 2019.

[24] D. Honnappa and S. S. Padala, "BIM-based framework to quantify delays and cost overruns due to changes in construction projects," *Asian Journal of Civil Engineering*, vol. 23, no. 5, pp. 707-725, 2022.

[25] M. Gunduz and M. AbuHassan, "Causes of construction delays in Qatar construction projects," *International Journal of Civil, Environmental, Structural, Construction and Architectural Engineering*, vol. 10, no. 4, pp. 516–521, 2015.

[26] G. J. Sweis, "Factors affecting time overruns in public construction projects: The case of Jordan," *International Journal of Business and Management*, vol. 8, no. 23, pp. 120, 2013.

[27] O. A. Hussain, R. C. Moehler, S. D. Walsh, and D. D. Ahiaga-Dagbui, "Minimizing Cost Overrun in Rail Projects through 5D-BIM: A Systematic Literature Review," *Infrastructures*, vol. 8, no. 5, pp. 93, 2023.

[28] O. Sánchez, K. Castañeda, R. F. Herrera, and E. Pellicer, "Benefits of Building Information Modeling in Road Projects for Cost Overrun Factors Mitigation," in *Construction Research Congress 2022*, pp. 472-482.

[29] A. Shibani and K. Arumugam, "Avoiding cost overruns in construction projects in India," *Management Studies*, vol. 3, no. 7-8, pp. 192-202, 2015.

[30] S. Vaardini, S. Karthiyayini, and P. Ezhilmathi, "Study on cost overruns in construction projects: a review," *International Journal of Applied Engineering Research*, vol. 11, no. 3, pp. 356-363, 2016.

[31] S. Deep, T. Gajendran, and M. Jefferies, "A systematic review of 'enablers of collaboration' among the participants in construction projects," *International Journal of Construction Management*, vol. 21, no. 9, pp. 919-931.

[32] M. Oraee, M. R. Hosseini, D. J. Edwards, H. Li, E. Papadonikolaki, and D. Cao, "Collaboration barriers in BIM-based construction networks: A conceptual model," *International Journal of Project Management*, vol. 37, no. 6, pp. 839-854, 2019.

[33] H. Faris, M. Gaterell, and D. Hutchinson, "Investigating underlying factors of collaboration for construction projects in emerging economies using exploratory factor analysis," *International Journal of Construction Management*, vol. 22, no. 3, pp. 514-526, 2022.

[34] J. S. J. Koolwijk, C. J. Van Oel, J. W. F. Wamelink, and R. Vrijhoef, "Collaboration and integration in project-based supply chains in the construction industry," *Journal of Management in Engineering*, vol. 34, no. 3, pp. 1–13, 2018.

[35] Y. Gamil and I. Abd Rahman, "Studying the relationship between causes and effects of poor communication in construction projects using PLS-SEM approach," *Journal of Facilities Management*, vol. 21, no. 1, pp. 102-148, 2023.

[36] A. Suleiman, H. Almasaeid, N. Hussain, and J. Abahre, "Addressing the Causes and Effects of Poor Communication in the Jordanian Construction Industry: A Study on Improving Project Performance," *Civil and Environmental Engineering*.

[37] S. Kamalirad, S. Kermanshachi, J. Shane, and S. Anderson, "Assessment of construction projects' impact on internal communication of primary stakeholders in complex projects," in Proceedings for the 6th CSCE International Construction Specialty Conference, 2017, pp. 074-01.

[38] A. L. Olanrewaju and A. H. J. Lee, "Investigation of the poor-quality practices on building construction sites in Malaysia," *Organization, Technology and Management in Construction: An International Journal*, vol. 14, no. 1, pp. 2583-2600, 2022.

[39] D. L. D. M. Nascimento, E. D. Sotelino, T. P. S. Lara, and R. G. G. Caiado, "Constructability in industrial plants construction: a BIM-lean approach using the digital Obeya room framework," *Journal of Civil Engineering and Management*, vol. 23, no. 8, pp. 1100–1108, 2017.

[40] G. Ye, Z. Jin, B. Xia, and M. Skitmore, "Analyzing causes for reworks in construction projects in China," *Journal of Management in Engineering*, vol. 31, no. 6, 04014097, 2015.

[41] S. Wawak, Ž. Ljevo, and M. Vukomanović, "Understanding the key quality factors in construction projects—A systematic literature review," *Sustainability*, vol. 12, no. 24, 10376, 2020.

[42] A. C. Ogwueleka, "A review of safety and quality issues in the construction industry," *Journal of Construction Engineering and Project Management*, vol. 3, no. 3, pp. 42–48, 2013.

[43] A. Marefat, H. Toosi, and R. Mahmoudi Hasankhanlo, "A BIM approach for construction safety: applications, barriers and solutions," *Engineering, Construction and Architectural Management*, vol. 26, no. 9, pp. 1855-1877, 2019.

[44] S. Zaid Alkilani, J. Jupp, and A. Sawhney, "Issues of construction health and safety in developing countries: a case of Jordan," *Australasian Journal of Construction Economics and Building*, vol. 13, no. 3, pp. 141-156, 2013.

[45] C. S. Schultz, K. Jørgensen, S. Bonke, and G. M. G. Rasmussen, "Building defects in Danish construction: project characteristics influencing the occurrence of defects at handover," *Architectural Engineering and Design Management*, vol. 11, no. 6, pp. 423-439, 2015

[46] L. Zhu, M. Shan, and Z. Xu, "Critical review of building handover-related research in construction and facility management journals," *Engineering, Construction and Architectural Management*, vol. 28, no. 1, pp. 154-173, 2021.

[47] N. Forcada, M. Macarulla, M. Gangolells, and M. Casals, "Handover defects: comparison of construction and post-handover housing defects," *Building Research & Information*, vol. 44, no. 3, pp. 279-288, 2016.

[48] B. Salgın, A. Akgün, N. Coşgun, and K. Agyekum, "Construction waste reduction through BIM-based site management approach," *International Journal of Engineering Technologies*, vol. 3, no. 3, pp. 135-142, 2017.

[49] M. Osmani and P. Villoria-Sáez, "Current and emerging construction waste management status, trends and approaches," in Waste, Academic Press, 2019, pp. 365-380.

[50] R. Sacks, C. Eastman, G. Lee, and P. Teicholz, *BIM Handbook: A Guide to Building Information Modeling for Owners, Designers, Engineers, Contractors, and Facility Managers*, John Wiley & Sons, 2018.

[51] Autodesk, "What is BIM?" Autodesk.com. [accessed January 21, 2022]. Available: https://www.autodesk.com/industry/aec/bim

[52] A. Borrmann, M. König, C. Koch, and J. Beetz, *Building Information Modeling: Why? What? How?*, Springer International Publishing, 2018.

[53] M. Casini, *Construction 4.0: Advanced Technology, Tools and Materials for the Digital Transformation of the Construction Industry*, Woodhead Publishing, 2021.

[54] B. Ali et al., "BIM aided information and visualization repository for managing construction delay claims," *Journal of Information Technology in Construction*, vol. 26, pp. 1023–1040, 2021.

[55] N. Khan et al., "Visual language-aided construction fire safety planning approach in building information modeling," *Applied Sciences*, vol. 10, no. 5, 1704, 2020.

[56] A. Girardet and C. Boton, "A parametric BIM approach to foster bridge project design and analysis," *Automation in Construction*, vol. 126, 103679, 2021.

[57] A. Z. Sampaio and A. M. Gomes, "BIM interoperability analyses in structure design," *CivilEng*, vol. 2, no. 1, pp. 174-192, 2021.

[58] C. M. Clevenger and R. Khan, "Impact of BIM-enabled design-to-fabrication on building delivery," *Practice Periodical on Structural Design and Construction*, vol. 19, no. 1, pp. 122-128, 2014.

[59] A. S. Aredah, M. A. Baraka, and M. ElKhafif, "Project scheduling techniques within a building information modeling (BIM) environment: A survey study," *IEEE Engineering Management Review*, vol. 47, no. 2, pp. 133-143, 2019.

[60] S. D. Patil, "Application of BIM for scheduling and costing of building project," *International Journal for Research in Applied Science & Engineering Technology*, vol. 6, no. 6, pp. 1609–1615, 2018.

[61] J. Xu, "Research on application of BIM 5D technology in central grand project," *Procedia Engineering*, vol. 174, pp. 600-610, 2017.

[62] W. C. Wang et al., "Integrating building information models with construction process simulations for project scheduling support," *Automation in Construction*, vol. 37, pp. 68-80, 2014.

[63] A. Fazeli, M. S. Dashti, F. Jalaei, and M. Khanzadi, "An integrated BIM-based approach for cost estimation in construction projects," *Engineering, Construction and Architectural Management*, vol. 28, no. 9, pp. 2828-2854, 2021.

[64] F. H. Abanda, B. Kamsu-Foguem, and J. H. M. Tah, "BIM–New rules of measurement ontology for construction cost estimation," *Engineering Science and Technology, an International Journal*, vol. 20, no. 2, pp. 443-459, 2017.

[65] S. O. Babatunde, S. Perera, D. Ekundayo, and T. E. Adeleye, "An investigation into BIM-based detailed cost estimating and drivers to the adoption of BIM in quantity surveying practices," *Journal of Financial Management of Property and Construction*, vol. 25, no. 1, pp. 61-81, 2019.

[66] M. Mayouf, M. Gerges, and S. Cox, "5D BIM: an investigation into the integration of quantity surveyors within the BIM process," *Journal of Engineering, Design and Technology*, vol. 17, no. 3, pp. 537-553, 2019.

[67] H. Kim, K. Anderson, S. Lee, and J. Hildreth, "Generating construction schedules through automatic data extraction using open BIM (building information modeling) technology," *Automation in Construction*, vol. 35, pp. 285-295, 2013.

[68] K. J. Park and J. H. Ock, "Structuring a BIM Service Scoping, Tendering, Executing, and Wrapping-Up (STEW) Guide for Public Owners," *Applied Sciences*, vol. 12, no. 7, 3275, 2022.

[69] S. L. M. Correa and E. T. Santos, "BIM support in the tendering phase of infrastructure projects," in Proceedings of the 18th International Conference on Computing in Civil and Building Engineering: ICCCBE 2020, Springer International Publishing, 2021, pp. 383-392.

[70] S. S. Kumar and J. C. Cheng, "A BIM-based automated site layout planning framework for congested construction sites," *Automation in Construction*, vol. 59, pp. 24-37, 2015.

[71] R. Amiri, J. M. Sardroud, and B. G. De Soto, "BIM-based applications of metaheuristic algorithms to support the decision-making process: Uses in the planning of construction site layout," *Procedia Engineering*, vol. 196, pp. 558-564, 2017.

[72] A. A. Latiffi, S. Mohd, and J. Brahim, "Application of building information modelling (BIM) in the Malaysian construction industry: a story of the first

government project," *Applied Mechanics and Materials*, vols. 773–774, pp. 943–948, 2015.

[73] B. J. Park, S. K. Yoo, J. H. Kim, and J. J. Kim, "The Study on the Application of BIM at the Pre-design Stage of Public Projects-Through Case Studies," in CTBUH 2011 World Conference, 2011, pp. 625-630.

[74] C. Boton, "Supporting constructability analysis meetings with Immersive Virtual Reality-based collaborative BIM 4D simulation," *Automation in Construction*, vol. 96, pp. 1-15, 2018.

[75] A. Fadoul, W. Tizani, and C. A. Osorio-Sandoval, "A knowledge-based model for constructability assessment of buildings design using BIM," in International Conference on Computing in Civil and Building Engineering, Cham: Springer International Publishing, 2020, pp. 147-159.

[76] B. S. Lee, S. Y. Ji, and H. J. Jun, "An implementation of knowledge-based BIM system for representing design knowledge on massing calculation in architectural pre-design phase," *Korean Journal of Computational Design and Engineering*, vol. 21, no. 3, pp. 252–266, 2016.

[77] Y. Liu, S. Van Nederveen, and M. Hertogh, "Understanding effects of BIM on collaborative design and construction: An empirical study in China," *International Journal of Project Management*, vol. 35, no. 4, pp. 686-698, 2017.

[78] S. Zhang et al., "BIM-based collaboration platform for the management of EPC projects in hydropower engineering," *Journal of Construction Engineering and Management*, vol. 143, no. 12, 04017087, 2017.

[79] W. Fan et al., "Safety management system prototype/framework of deep foundation pit based on BIM and IoT," *Advances in Civil Engineering*, 2021, pp. 1-19.

[80] G. Ma and Z. Wu, "BIM-based building fire emergency management: combining building users' behavior decisions," *Automation in Construction*, vol. 109, 102975, 2020.

[81] M. D. Martínez-Aires, M. López-Alonso, and M. Martínez-Rojas, "Building information modeling and safety management: A systematic review," *Safety Science*, vol. 101, pp. 11-18, 2018.

[82] M. A. Hossain et al., "Design-for-safety knowledge library for BIM-integrated safety risk reviews," *Automation in Construction*, vol. 94, pp. 290-302, 2018.

[83] S. Durdyev et al., "Barriers to the implementation of Building Information Modelling (BIM) for facility management," *Journal of Building Engineering*, vol. 46, 103736, 2022.

[84] M. Kassem et al., "BIM in facilities management applications: a case study of a large university complex," *Built Environment Project and Asset Management*, vol. 5, no. 3, pp. 261-277, 2015.

[85] M. K. Dixit et al., "Integration of facility management and building information modeling (BIM): A review of key issues and challenges," *Facilities*, vol. 37, nos. 7/8, pp. 455-483, 2019.

[86] S. N. Naghshbandi, "BIM for facility management: challenges and research gaps," *Civil Engineering Journal*, vol. 2, no. 12, pp. 679–684, 2016.

[87] A. GhaffarianHoseini et al., "Application of nD BIM Integrated Knowledge-based Building Management System (BIM-IKBMS) for inspecting post-construction energy efficiency," *Renewable and Sustainable Energy Reviews*, vol. 72, pp. 935–949, 2017.

[88] A. Chong et al., "Continuous-time Bayesian calibration of energy models using BIM and energy data," *Energy and Buildings*, vol. 194, pp. 177–190, 2019.

[89] N. Bui, C. Merschbrock, and B. E. Munkvold, "A Review of Building Information Modelling for Construction in Developing Countries," *Procedia Engineering*, vol. 164, pp. 487–494, 2016.

[90] D. Silva et al., "Interdisciplinary Framework: A Building Information Modeling Using Structural Equation Analysis in Lean Construction Project Management," *Frontiers in Artificial Intelligence and Applications*.

[91] J. M. C. Ongpeng, "Assessment of Time and Costs of Two Formwork Methodologies in the Philippines using BIM Simulation," *International Journal on Advanced Science, Engineering and Information Technology*, vol. 8, no. 3, pp. 911, 2018.

[92] L. Chang, "A psychometric evaluation of 4-point and 6-point Likert-type scales in relation to reliability and validity," *Applied Psychological Measurement*, vol. 18, no. 3, pp. 205-215, 1994.

[93] P. J. Lavrakas, *Encyclopedia of Survey Research Methods*, Sage Publications, 2008.

[94] N. S. Azman et al., "Relative importance index (RII) in ranking of quality factors on industrialised building system (IBS) projects in Malaysia," in AIP Conference Proceedings, vol. 2129, no. 1, AIP Publishing, 2019.

[95] J. D. Gibbons and S. Chakraborti, *Nonparametric Statistical Inference*, CRC Press, 2020.

[96] N. J. Salkind, *Encyclopedia of Research Design*, Sage Publications, United States of America, 2010.

[97] Philippine Institute of Civil Engineers, "PICE history," [Philippines]; [accessed January 26, 2022]. Available: https://pice.org.ph/about-us/

[98] United Architects of the Philippines, "Profile," [Philippines]; [accessed January 26, 2022]. Available: https://united-architects.org/about/profile/

[99] Philippine Society of Mechanical Engineers, "PSME, Through the Years," [Philippines]; [accessed January 26, 2022]. Available: https://psme.org.ph/page/About

[100] Institute of Integrated Electrical Engineers of the Philippines, Inc., "About us," [Philippines]; [accessed January 26, 2022]. Available: https://iiee.org.ph/

[101] Philippine Society of Sanitary Engineers, Inc., "History of PSSE," [Philippines]; [accessed January 26, 2022]. Available: https://psse.org.ph/index.php/history/

REMOVAL OF METHYLENE BLUE DYE IN AQUEOUS SYSTEM USING POLYVINYL ALCOHOL AND CHEMICALLY MODIFIED-ALUMINIUM FOIL BLEND

Aliyu Danmusa MOHAMMED[1]* (iD), **Abubakar IBRAHIM TSAGERO[1]** (iD)

[1] *Department of Chemistry, Umaru Musa Yar'adua University, Katsina, Katsina State, Nigeria,*
aly27moh27@gmail.com, ich170443@students.umyu.edu.ng
* *Corresponding author*

ABSTRACT

Aqueous solution containing different concentrations of methylene blue dye was treated with chemically modified aluminium foil/PVA blends. There have been impressive decolourisation of the dye molecules in the aqueous system treated with the blends. Contact time and amount of composite facilitate more decolourisation of the dye solution. 97 % dye removal has been recorded at optimum conditions of the experiment. Energy dispersive X-ray fluorescence (EDXRF) analysis was used to determine the elemental composition of the aluminium foil and FTIR analysis was used to ascertain the composite formation between the foil and PVA. The blends have shown an impressive swelling property in aqueous system and poor to moderate in other organic solvents.

1   INTRODUCTION

Composites are often produced to have superior characteristics than their parent materials. The physico-chemical changes that come along the blend formation provides some additional properties to the starting materials. The component materials in the composites may be described as having synergistic effects that provide better and desirable properties in the final product [1]. Mixing of different materials to construct materials of targeted applications have been a common breakthrough in different industries today. Polymers, both synthetic and natural are widely used with different materials to construct new products with impressive properties [2,3]. Nanocomposites from polymers and metal ions, biomolecules and other materials are impressively used in healthcare system and tissue engineering [4,5].

Polyvinyl alcohol (PVA), being a synthetic polymer with remarkable properties such as good chemical resistance low price and hydrophilicity, is widely used in different industrial applications such as textile, adhesives, agricultural and pharmaceuticals. The polymer is also used in food industry for packaging purposes and in medical industry for drug delivery, cancer therapeutics and wound healing [6,7,8,9]. The structural features of PVA such as the presence of OH groups in its molecule and small molecular size (Figure 1) are responsible for most of the properties that identify the polymer. For instance, hydrophilicity and impressive mechanical stability [10]. PVA blends with alginate (natural polymer) are reported to be used in waste water treatment, dye absorption and in bioremediation [11,12,13,14].

Water contamination due to human activities and population expansion have become an issue of great concern to environmentalists. Different techniques are employed in waste water remediation and purification. Cost, limited-hazard and recyclability are among the important factors that are being considered in making the choice. Aluminium is one of the common elements that are found in almost every urban household in form of kitchen wires, cans, doors, pie plates and wrapping packages [15]. Among the most common source of aluminium contamination into the environment is aluminium foil (Al-foil). It's widely used today in many industries, households and eateries. The foil is not easily degradable or easy to recycle, it can

only be disposed of using an incinerator or disposed in landfills. Water contamination from organic dyes usually comes from industries such textile, leather, cosmetics or ink industry. The presence of colourants in water can be hazardous when the dye molecule is toxic on its own or by releasing toxic molecules when it is degraded. Moreover, even when the colorants are made from non-toxic substances, their presence may lead to poor sunlight penetration and low oxygen level in the water. These may lead to termination of life activities in the water environment [16].
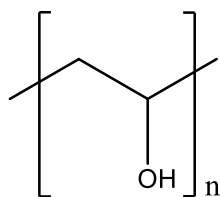
Figure 1. *Structure of polyvinyl alcohol.*

2   EXPERIMENTAL MATERIALS

2.1   Chemical Modification of Aluminium Foil Sample

Procedure reported by Narayana and Shafirovich (2014) [17] was used with little modification. Aluminium foil waste was obtained from domestic sources in the waste bins, the samples were washed, dried, and then shredded to an average 10 × 10 mm size. 5.0 g of the small pieces of aluminium waste was accurately weighed and transferred into 500 cm^3 beaker. 250 cm^3 of 1.5 M KOH was added to the 500 cm^3 beaker containing the aluminium pieces. The mixture was heated to 200 °C for 30 minutes. Bubbles of hydrogen was observed from the reaction of aluminium and aqueous KOH. The reaction was observed to be complete when the hydrogen evolution ceased and there were no visible pieces of aluminium metal. The solution was filtered to remove solid residue. The clear filtrate was transferred into a clean 500 cm^3 beaker and allowed to cool. 100 cm^3 of 9.0 M H_2SO_4 was added to the solution and stirred gently. The reaction beakers were set into the ice-water bath to chill for about 30 minutes. As the mixture became cold, crystals of aluminium salts began to form in few minutes. Further crystallization of the mixture was carried out using 50% ethanol/water mixture. The crystals formed was filtered from the solution and dried

for 48 hours in an oven at 50 °C. The modified aluminium foil was obtained and labelled as M-Al-foil. The overall reaction is represented in the scheme 1.

$$2Al_{(s)} + 2KOH_{(aq)} + 4H_2SO_{4(aq)} + 22H_2O_{(aq)} \text{-------->} 2KAl(SO_4)_2 .12H_2O_{(s)} + 3H_{2(g)}$$
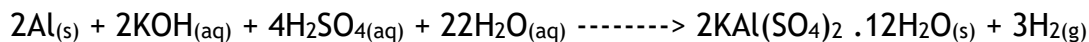
Scheme 1: Production of M-Al-foil from aluminium foil.

2.2 Preparation of PVA/ M-Al-foil Blend Hydrogel via Freezing and Thawing Method

0.2 g of synthesized aluminium salts crystals were weighed and transferred into a 100 mL beaker labelled as A. Distilled water (10 mL) was added into the beaker and stirred gently for 1hr at ambient temperature. PVA (1 g) was transferred into a 100 mL beaker and labelled as B. Distilled water (10 mL) was added to the beaker and heated to 80 °C for 1hr. After allowing the mixture to cool, the two solutions (A and B) were combined and gently mixed at room temperature using a magnetic stirrer until homogeneity was achieved. The mixture was then poured on a petri dish and exposed to the atmospheric pressure to degas. The Hydrogel formed was frozen for 12 hrs and then thawed. The mass of dried blend was measured.

2.3 Characterization

2.3.1 Ultraviolet spectroscopy

UV-VIS Pye Unicam Spectrophotometer Type Sp 8- 200 was used in this experiment. All spectrophotometric measurements were carried out at ambient temperature.

2.3.2 Energy dispersive X-Ray florescence (EDXRF)

A Jeol 5400 (Japan) scanning electron microscope with energy dispersive X-ray (EDX) attachment was used to determine the uptake of the different elements by different substrates.

EDXRF analysis is designed to analyze groups of elements simultaneously. This type of XRF instrumentation separates the characteristics x-rays of different elements into a complete fluorescence energy spectrum which is then processed for qualitative or quantitative analysis.

2.3.3 FTIR analysis

FTIR spectrophotometer model Mattson 100, made by Unicam, (UK) was used for the FTIR measurements over the range 500-4000 cm^{-1}. The FTIR spectra of the samples were obtained using ATR mode.

The Thermal properties and structural characterization were carried out using TGA and SEM analyses respectively.

2.4   Solvents Absorption and Retention of the Blend

20 mg of the sample was soaked in 25 mL of different solvents for 24 h at room temperature. The samples were then removed and blotted on filter paper to remove excess water/solvent on the surface. The swelling (%) was calculated according to the following equation:

$$\text{Swelling \%} = \frac{W2}{W1} \times 100 \qquad (1)$$

where W1: initial weight of the sample and W2: final weight of the swollen sample.

2.5   Adsorption of Methylene Blue Dye

Procedure reported by Karaoglu and Ugurlu (2010) [18] was used with little modifications. Methylene blue dye stock solution was prepared by dissolving 1 g of the dye in 1000 cm^3 distilled H_2O. Different targeted concentrations were obtained in the experiment by diluting the stock solution prepared. Different operating conditions such as contact time, dose of blend, dye concentration and pH were respectively studied. The pH adjustments were made by the controlled addition of 1 M, NaOH and 1 M HCl. The varying amounts of methylene blue concentration (5 mg/L to 100 mg/L) were prepared. 100 mL of the dye solution was used in each batch experiment at ambient temperature. In each case the dye uptake was determined by measuring the light absorption of the residual dye solution after contact with the blend. The dye sorption by samples was determined according to equation (2):

$$\text{Dye uptake\%} = \text{Dye conc. on sample / initial dye conc. X 100} \qquad (2)$$

3 RESULTS and DISCUSSION

3.1 FT-IR Analysis

Figure 2 shows the FT-IR spectroscopy of pure PVA sample before blending with the aluminium crystals. The IR spectrum showed absorption bands at 3265 cm-1 and at 1699 cm-1due to OH stretching and bending modes respectively. Absorption bands at 2907 and 1080 cm-1 are due to C-H stretching and bending respectively. In Figure 3, the FTIR spectrum of the PVA/M-Al blends show reasonable adjustment of peaks. The OH stretching vibration at around 3265 cm-1 has now been shifted to 3324 cm-1 and C-H bending vibration has changed from 1699 to 1658 cm-1 in the blend. This changes in absorption peaks are associated with the presence of other substances from the alum in the blend.
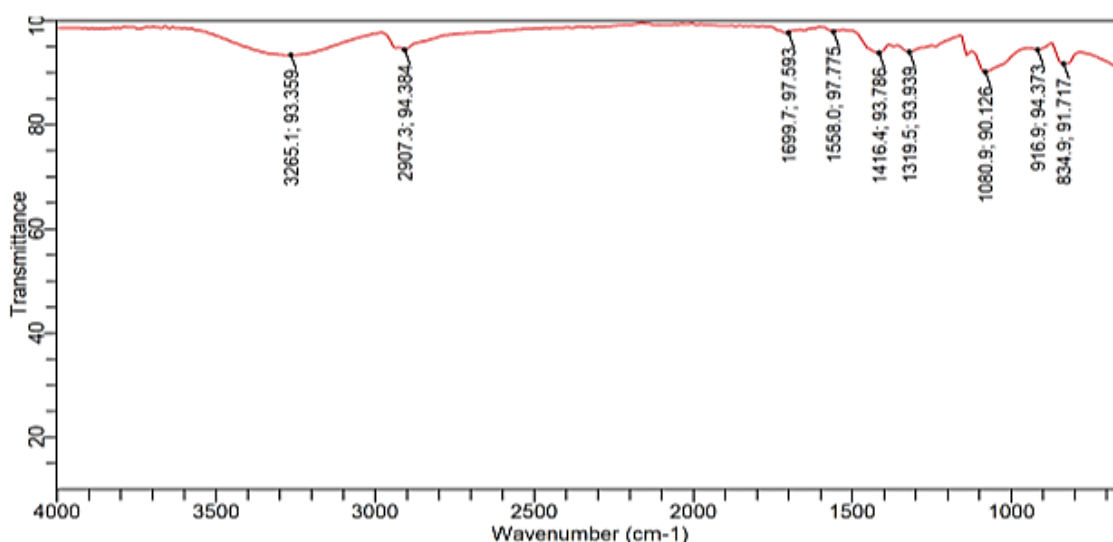
Figure 2. *FTIR spectra of PVA virgin sample.*
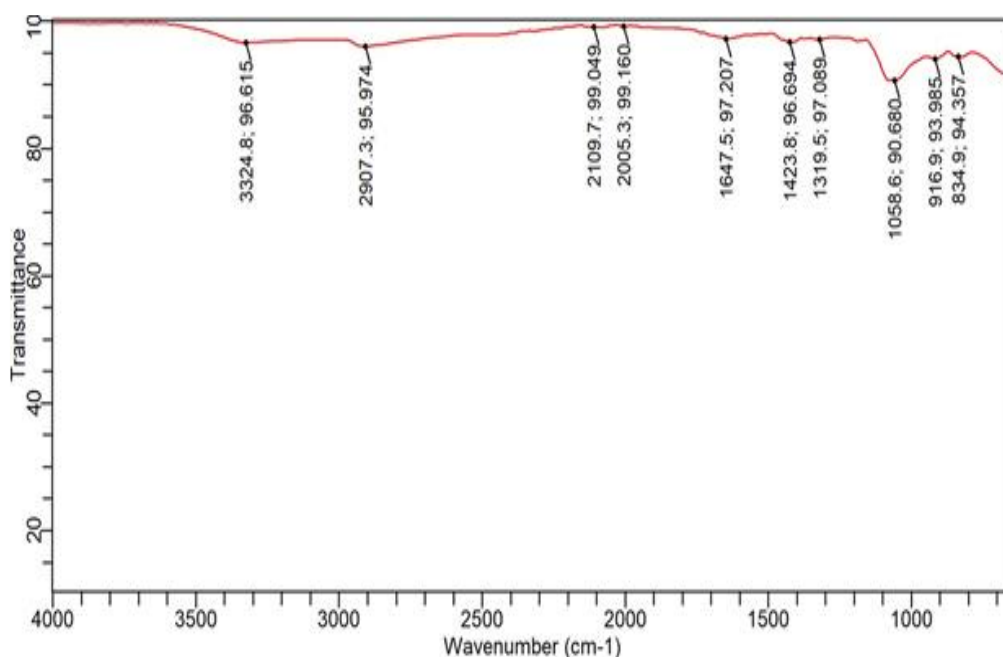
Figure 3. FTIR spectrum of PVA/M-Al blend.

3.2 EDXRF Analysis of Alum Crystals

Table 1 shows the elemental composition and oxides present in the extracted alum from the aluminium foil. The results showed high amount of aluminium, Sulphur and potassium and their respective oxides. Presence of these elements further confirms that aluminium salt (alum) has been successfully prepared from aluminium foil. Other elements and their oxides that are in a negligible quantity are also presented.

Table 1. EDXRF results showing the composition of some elements present in alum crystals.

Elements	%Elements	Oxides	% Oxides
Fe	0.02375	Fe_2O_3	0.03396
Na	0.136	Na_2O	0.183
Al	6.605	Al_2O_3	12.480
Si	0.7736	SiO_2	1.655
P	0.1338	P_2O_5	0.3067
S	19.098	SO_3	47.688
K	8.452	K_2O	10.181

3.3   Swelling Properties of the Blend

The swelling property of the blend in water and other solvents was carried out by immersing the blend in different solvent for 24 hours. The swelling property of the blend in each solvent is shown in Table 2. From the result it can be observed that the blend has a high tendency to swell in water and moderately in other solvents with high polarity and dielectric constants than in nonpolar solvents [19]. The trend goes in the following order: water >DMF>ethylacetate>n-hexane>benzene.

Table 2. Swelling of PVA/M-Al blend in organic solvent and water after 24hours.

Solvents	%Swelling
Water	236
Benzene	75
Dimethylformamide	146
Ethylacetate	97
n-hexane	78

3.4   Studies on Dye Removal from Waste Water

3.4.1 Effect of contact time

Figure 4 shows the trend in dye adsorption by the blend in percentage with contact time. The results obtained showed the highest dye adsorption at 35 minutes. However, there wasn't significant dye adsorption with further increase of time. This can be attributed to the fact that, at the initial stage the number of free adsorption sites was higher and the slow or constant adsorption rate in the later stage was due to slower diffusion of solute into the interior of the adsorbent.
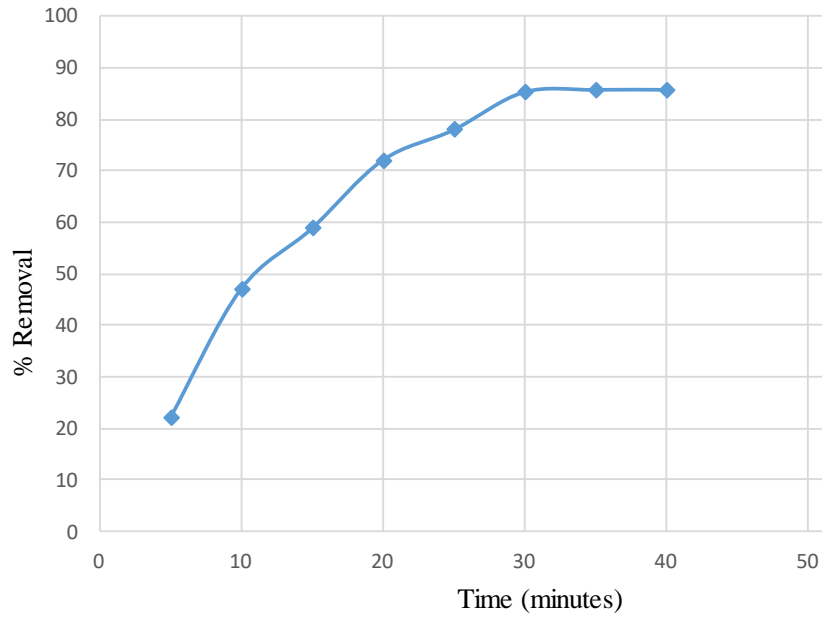
Figure 4. Effect of contact time.

3.4.2 Effect of dye concentration

In Figure 5, the dye uptake has been shown to decrease with increase in the dye concentration. This is as a result of excess dye molecules would have limited active contact with the blend's surface. Hence, the free dye molecules would remain in the solution without being adsorbed. In this research work, it is observed that the blend adsorbent degraded 85.29 % of methylene blue at initial concentration of 20 mg/L.
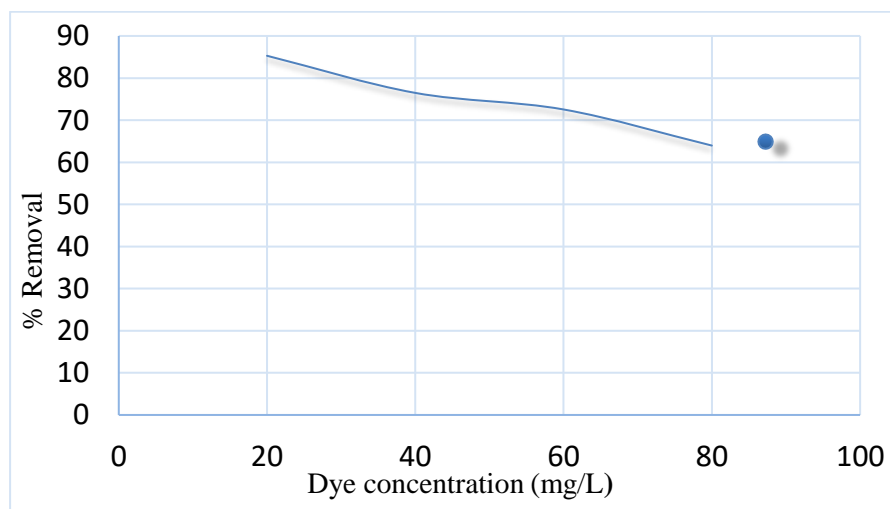
Figure 5. Effect of dye concentration.

3.4.3 Effect of amount of composite

The effect of composite dosage on the adsorption of methylene blue is shown in Figure 6. There is a general increase in the dye uptake with more amount of the composite sample until it reached a stage where it levelled-off and then started decreasing. High amount of composite would lead to a more active contact between the dye molecules and the surface of the composites. Thus, more dye uptake. In this experiment, 97.05% removal was observed at optimum adsorbent dosage of 1.5 g.
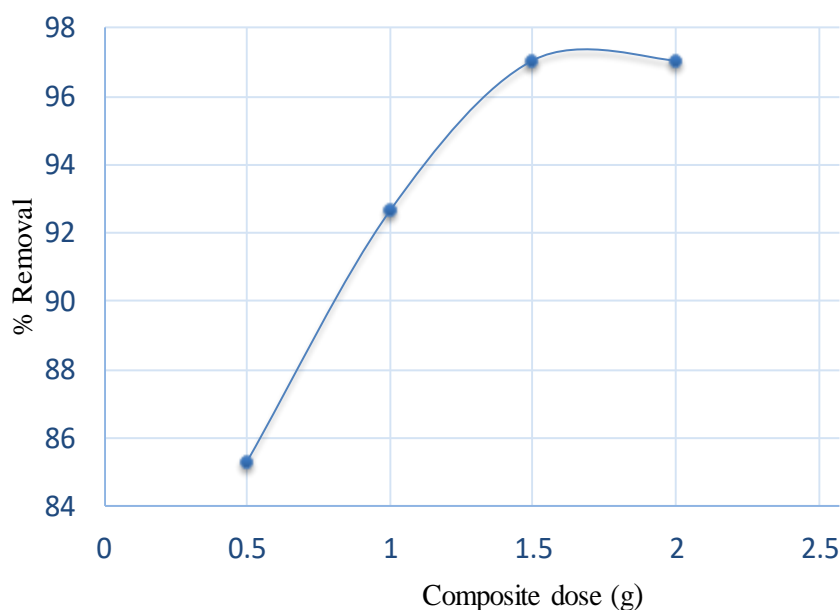
Figure 6. *Effect of composite dose*.

3.4.4 Effect of pH on dye adsorption

The effect of pH on the percentage of the methylene blue dye removal is shown in Figure 7. There was a general increase in the dye uptake with increase in pH. The adsorption was observed to reach its optimum at a pH slightly less than 7. In this work, it can be concluded that at a more acidic or alkaline pH there is a general decrease in the dye uptake.
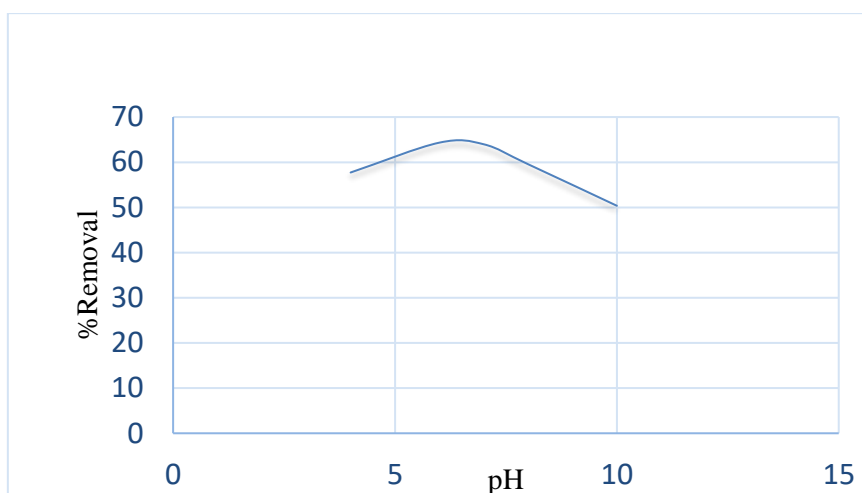
Figure 7. *Effect of pH on dye uptake*.

4 CONCLUSION

In this study, methylene blue dye in aqueous solution was treated with PVA/M-Al foil blend as adsorbent. FTIR and EDXRF results showed that Aluminium foil have been successfully incorporated onto the polyvinyl alcohol. The results showed that PVA/M-Al foil blend proved to be a very effective adsorbent in the removal of methylene blue dye from waste water. The adsorption performance is strongly affected by parameters such as contact time, initial dye concentration, adsorbent dosage and pH. The maximum removal of methylene blue observed was 97.05% for 1.5 g of PVA/M-Al foil blend adsorbent at neutral solution. The optimum conditions of PVA/M-Al foil experiment are 30 minutes of contact time, 1.5 g adsorbent dose and PH of solution in between 6 and 7. It was also observed that, the percentage adsorption of methylene blue decreases with increase in the dye concentration and the amount of dye uptake increases with the increasing of adsorbent dose.

Conflict of Interest

There is no conflict of interest between the authors.

Authors contributions

Aliyu Danmusa Mohammed contributed with the Project proposal and title. Moreover, interpretations of results obtained in the manuscript were carried out by him. He also designed the article format in accordance with the journal guidelines.

On the other hand, Abubakar Tsagero contributed to the sample collections and preparation.

Acknowledgment and support

The authors gratefully acknowledge the support from Umaru Musa Yar'adua University, Katsina, Katsina state, Nigeria.

Statement of research and publication ethics

The study is complied with research and publication ethics.

REFERENCES

[1] A. Gbaguidi, S. Namilae, and D. Kim, "Synergy effect in hybrid nanocomposites based on carbon nanotubes and graphene nanoplatelets," *Nanotechnology*, vol. 31, no. 25, p. 255704, 2020.

[2] V. Shanmugam *et al.*, "Potential natural polymer-based nanofibres for the development of facemasks in countering viral outbreaks," *J. Appl. Polym. Sci.*, vol. 138, no. 27, p. 50658, 2021.

[3] M. Silva, F. N. Ferreira, N. M. Alves, and M. C. Paiva, "Biodegradable polymer nanocomposites for ligament/tendon tissue engineering," *J. Nanobiotechnology*, vol. 18, no. 1, p. 23, 2020.

[4] M. F. Maitz, "Applications of synthetic polymers in clinical medicine," *Biosurf. Biotribol.*, vol. 1, no. 3, pp. 161–176, 2015.

[5] X. Tang *et al.*, "Polymeric biomaterials in tissue engineering and regenerative medicine," in *Natural and Synthetic Biomedical Polymers*, Elsevier, 2014, pp. 351–371.

[6] M. S. B. Husain, A. Gupta, B. Y. Alashwal, and S. Sharma, "Synthesis of PVA/PVP based hydrogel for biomedical applications: a review," *Energy Sources Recovery Util. Environ. Eff.*, vol. 40, no. 20, pp. 2388–2393, 2018.

[7] A. Kumar and S. S. Han, "Enhanced mechanical, biomineralization, and cellular response of nanocomposite hydrogels by bioactive glass and halloysite nanotubes for bone tissue regeneration," *Mater. Sci. Eng. C Mater. Biol. Appl.*, vol. 128, no. 112236, p. 112236, 2021.

[8] A. Kumar, Y. S. Negi, N. K. Bhardwaj, and V. Choudhary, "Synthesis and characterization of methylcellulose/PVA based porous composite," *Carbohydr. Polym.*, vol. 88, no. 4, pp. 1364–1372, 2012.

[9] C. C. Thong, D. C. L. Teo, and C. K. Ng, "Application of polyvinyl alcohol (PVA) in cement-based composite materials: A review of its engineering properties and microstructure behavior," *Constr. Build. Mater.*, vol. 107, pp. 172–180, 2016.

[10] M. Aslam, M. A. Kalyar, and Z. A. Raza, "Polyvinyl alcohol: A review of research status and use of polyvinyl alcohol based nanocomposites," *Polym. Eng. Sci.*, vol. 58, no. 12, pp. 2119–2132, 2018.

[11] X. Gao, C. Guo, J. Hao, Z. Zhao, H. Long, and M. Li, "Adsorption of heavy metal ions by sodium alginate based adsorbent-a review and new perspectives," *Int. J. Biol. Macromol.*, vol. 164, pp. 4423–4434, 2020.

[12] Y. Zvulunov and A. Radian, "Alginate composites reinforced with polyelectrolytes and clay for improved adsorption and bioremediation of formaldehyde from water," *ACS ES T Water*, vol. 1, no. 8, pp. 1837–1848, 2021.

[13] B. Aderibigbe and B. Buyana, "Alginate in wound dressings," *Pharmaceutics*, vol. 10, no. 2, p. 42, 2018.

[14] M. Bahadoran, A. Shamloo, and Y. D. Nokoorani, "Development of a polyvinyl alcohol/sodium alginate hydrogel-based scaffold incorporating bFGF-encapsulated microspheres for accelerated wound healing," *Sci. Rep.*, vol. 10, no. 1, p. 7342, 2020.

[15] O. A. Buryakovskaya, E. A. Meshkov, M. S. Vlaskin, E. I. Shkolnokov, and A. Z. Zhuk, "Utilization of aluminum waste with hydrogen and heat generation," *IOP Conf. Ser. Mater. Sci. Eng.*, vol. 250, p. 012007, 2017.

[16] S. Ibrahim, I. Fatimah, H.-M. Ang, and S. Wang, "Adsorption of anionic dyes in aqueous solution using chemically modified barley straw," *Water Sci. Technol.*, vol. 62, no. 5, pp. 1177–1182, 2010.

[17] A. K. Narayana Swamy and E. Shafirovich, "Conversion of aluminum foil to powders that react and burn with water," *Combust. Flame*, vol. 161, no. 1, pp. 322–331, 2014.

[18] M. H. Karaoğlu and M. Uğurlu, "Studies on UV/NaOCl/TiO2/Sep photocatalysed degradation of Reactive Red 195," *J. Hazard. Mater.*, vol. 174, no. 1–3, pp. 864–871, 2010.

[19] A. D. Mohammed, D. A. Young, and H. C. M. Vosloo, "Synthesis of high-performance superabsorbent glycerol acrylate-cross-linked poly (acrylic acid)," *Res. Chem. Intermed.*, vol. 43, no. 4, pp. 2187–2200, 2017.

ACCURACY DETECTION IN SOME SPORTS TRAINING USING COMPUTER VISION AND DEEP LEARNING TECHNIQUES

Nurettin ACI[1] [iD] **, Muhammed Fatih KULUÖZTÜRK[2],*** [iD]

[1] *Bitlis Eren University, Graduate Education Institute, Turkey,* nurettin.aci@adalet.gov.tr
[2] *Bitlis Eren University, Electrical-Electronics Engineering Department, Turkey,*
mfkuluozturk@beu.edu.tr
* *Corresponding author*

ABSTRACT

In this study, the performance of the MediaPipe Pose Estimation model in estimating body position in different sports activities was investigated in the light of biomechanical parameters. Additionally, the performance of the model was evaluated by comparing the real-time data obtained from the camera with different machine learning algorithms (regression, classification, etc.). The results showed that the MediaPipe Pose Estimation model is a suitable and effective tool for sports biomechanics. The model was able to estimate body position with high accuracy in different sports activities. Additionally, the performance of the model was improved by using different machine learning algorithms. This study is a pioneer research on the applicability of computer vision-supported deep learning techniques in sports training and pose estimation. The model has been developed into an application that can be used to improve the performance of athletes.

1   INTRODUCTION

Every year, a large number of athletes are injured as a result of participation in strenuous physical activity. These injuries can be costly to treat and can also lead to long-term health problems [1]. The frequency of these injuries can be reduced by proper training, technique, and fitness, which can help to identify factors that may make an athlete susceptible to injury [2]. Additionally, efforts to reduce these injuries require both efforts to ensure the long-term health of athletes and efforts to reduce medical costs [3].

The movements of living things are of interest to many researchers. Studies in this field include biomechanical analyses, performance analyses, person recognition, identification of movement disorders, and virtual human animation in computer graphics. These studies are based on the biomechanical properties of sports activities such as walking, running, and jumping. Biomechanics has emerged with the use of structural, physical, and mathematical models for the understanding and analysis of human movements [4].

The emergence of biomechanics has also been influenced by the challenges of numerically expressing and giving meaning to the factors that cause movement, as well as the high degree of freedom in the human body. The analysis and definition of human movements is a very challenging process and the development of biomechanics has been necessary [5].

The development of biomechanics has been greatly influenced by the integration of mathematics, physical principles, and engineering methodologies. The combination of these disciplines has contributed to the diversification and development of the application areas of biomechanics. The main purpose of biomechanics is to understand, analyse, and optimize human movements. In this direction, simple models can be used to represent the movements and explain some basic mechanical properties, while sports biomechanics is used for more complex motion structures. Sports biomechanics plays an important role in understanding the human movement capacity, the evaluation of the principles of injury and prevention mechanics, and the treatment of muscle and skeletal problems. The benefits of

technology are also used to get the maximum output from the movements made with sports biomechanics [6].

Human movements are studied by using kinematic and kinetic data of body members. For this purpose, computer vision-based human pose estimation models have been developed. Human pose estimation aims to find human body parts with the data obtained from images and videos, and to create a three-dimensional human body skeleton [7].

The analysis of human movements is not limited to the evaluation of large data sets obtained by motion analysis systems with basic statistical methods [8]. Researchers perform motion analysis based on the observation that the positions of the joints that make up the human body parts do not change randomly over time and show a regular behaviour, even though they move at the point of high degree of freedom using different techniques [9].

Human pose estimation has been attracting increasing interest in recent years. Although deep learning-based solutions provide high performance in human pose estimation, there are still challenges such as insufficient training data, depth uncertainties, and occlusions [10].

"There are people familiar with using YouTube content and fitness applications to exercise at home. However, these individuals may exercise based on incorrect information from non-professionals, which can increase the risk of injury by performing exercises with incorrect posture or without considering their physical abilities [11]. While exercising at home may be convenient, it can be harmful to the body as it is difficult to monitor proper posture. Therefore, this article proposes a program that guides users while exercising at home without the need for a fitness instructor. This program utilizes MediaPipe Pose's landmark model to estimate body posture and displays instructions on the screen when the user's posture does not conform to proper exercise criteria. If the user's posture is correct, the number of exercises performed according to the displayed instructions increases."

The aim of this article is to systematically analyse the accuracy rates of sports activities performed using real-time images through computer vision-based deep learning solutions for human pose estimation from the perspective of sports biomechanics.

1.1 Relationship between Computer Vision and Deep Learning

Computer vision is a field that aims to transfer the vision processes of the human brain to the machine. The main goal in this field is to be able to identify and group objects in digital images by understanding the content of the images. In this way, the machine can perform extraction of an object, text or model on the image [12].

Deep learning is a type of machine learning. This method performs feature extraction and transformation operations using many nonlinear processing unit layers. Each consecutive layer takes the output of the previous layer as input. The algorithms can be used for both supervised learning (such as classification) and unsupervised learning (such as pattern analysis) [13].

Deep learning algorithms are used to distinguish objects in the field of computer vision and image processing. The most commonly used deep learning algorithm is the convolutional neural network algorithm, which provides an effective method for distinguishing objects in images. The basic components of this algorithm are convolutional, pooling and fully-connected layers. In the model training process, weights and bias values are optimized with repeated layers, forward and backward propagation operations, and object recognition tasks can be performed [14].

There are many algorithms used in the field of computer vision and deep learning, in addition to convolutional neural networks (CNN). Algorithms such as artificial neural networks (ANN), recurrent neural networks (RNN), long short-term memory (LSTM), deep belief networks (DBN) and learning-based classifier systems are preferred for different tasks. The choice of algorithm depends on the properties of the problem to be applied and the structure of the data set. The deep learning field is rapidly developing and new algorithms are constantly being discovered or existing algorithms are being developed [15].

1.2 Human Pose Estimation with Computer Vision

Human pose estimation is a computer vision technique in which a person's movements and positions are represented graphically using deep learning techniques. This technique uses a model-based approach to estimate the positions of a person's body parts or joint positions using 2D or 3D data. Pose estimation models

are able to detect human poses using 2D and 3D pose estimation techniques. 2D pose estimation estimates the positions of body joints using X and Y coordinates, while 3D pose estimation estimates the object's true spatial location using an additional Z dimension. 3D pose estimation poses a significant challenge for machine learning engineers due to the need to create data sets and algorithms [16].

There are three main methods for solving the human pose estimation problem: Absolute Pose Estimation, Relative Pose Estimation, and Proportional Pose Estimation. Pose estimation algorithms are designed to estimate a person's position relative to the background using the human pose and direction. Models can be designed using bottom-up or top-down approaches, and the encoder-decoder architecture is frequently used. There are five popular deep learning-based pose estimation libraries for human pose estimation, and these libraries are used in the development of customized human pose estimation applications [17].

OpenPose: OpenPose is a free human joint detection library that can run in real time. It can simultaneously detect a total of 135 key points by detecting important points for body, face, hand, and foot estimation. It uses a bottom-up approach and provides an open source API, supporting different hardware architectures. OpenPose is widely used in various application areas [18].

Pose Detection: Pose detection is an open source library that can detect human poses in real time. This architecture, built on TensorFlow.js, allows the detection of body parts such as elbows, hips, wrists, knees, ankles, etc. for single or multiple poses. It is efficiently designed for light devices (browsers, mobile devices) and offers three different models, such as MoveNet, BlazePose, and PoseNet [19].

DensePose: Dense human pose estimation is an open source library that can match all human pixels in RGB images with the body's 3D surface-based model in real time. It runs on a Caffe2-supported detector framework and is used for single or multiple pose estimation problems [20].

AlphaPose: Alphapose is an open source, real time, and multi-person pose estimation library. It uses a top-down approach and helps to detect poses in case of misdetection of human bounding boxes. It uses the most appropriate architecture by determining human poses with the detected bounding boxes. It also provides

PoseFlow, an online pose tracker that can correctly detect single-person and multi-person key points in real time [21].

HRNet (High Resolution Network): HRNet is an architecture used for human pose estimation. It is used to determine key points based on specific objects or people in the image and estimates a very accurate key point heat map by preserving high resolution representations. HRNet is also suitable for detecting human poses in sports broadcast on television and has also been used in other dense estimation tasks [22].

1.3   Selection of Appropriate Human Pose Estimation for Sports Training

2D artificial learning models are generally successful, but sharper inferences are required for the perception of 3D objects. Mediapipe library, offered by Google as open source, is a tool that can be used in real time in many different areas that can make more detailed inferences such as size, position and orientation. This library can perform many operations from face detection to iris tracking, and works in a way that is compatible with different devices, resources and hardware.

Mediapipe library classifies human poses by detecting human body. This allows the accuracy of sports training to be determined using mathematical methods. The detection of body lines provided by Mediapipe is an important tool that can be used to evaluate the accuracy of sports training [23].

The key points of the user's body can be detected using the MediaPipe library. A list corresponding to the X, Y and Z coordinates of these points indicates the location of the body parts in the input image. MediaPipe's output contains the coordinates of a total of 33 key points (Figure 1). These points can be used to create a skeleton orientation. MediaPipe is an open source and customizable machine learning solution for real-time media streaming. The library is supported on different platforms such as Android, iOS, Python, JavaScript. MediaPipe's output provides a rough estimate of the human body structure and orientation in the given image or video stream. This output is obtained at a speed of 30 frames per second as specified by the frame rate [24].
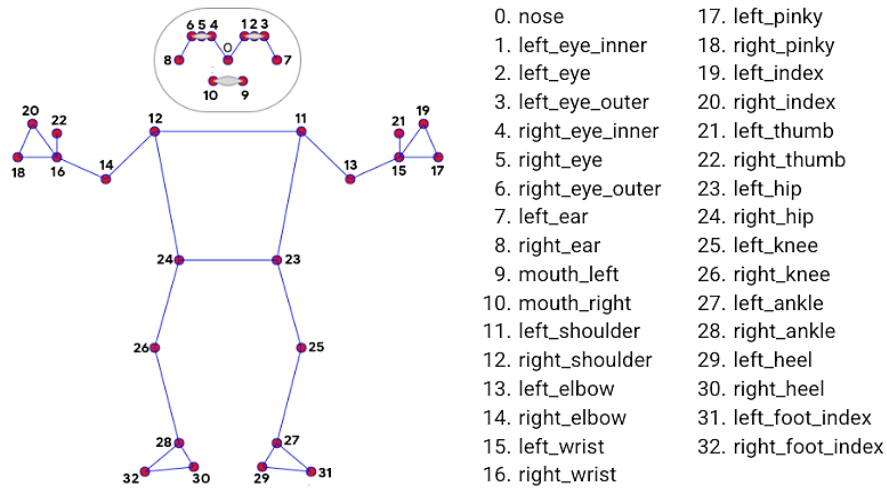
Figure 1. *Key points noted in the MediaPipe Library.*

1.4   MediaPipe Library Model Architecture

The MediaPipe library uses heatmaps for image processing and analysis. Heatmaps are a method of visually representing how a certain feature or measurement changes over time. MediaPipe creates various models using heatmaps, especially for complex objects such as the human body and face. These models can be used for tasks such as hand gesture recognition, face recognition, body motion tracking, and image classification.

The MediaPipe library provides various tools and methods, such as data collection, data preprocessing, and machine learning techniques, to create models that achieve high accuracy and performance within the scope of deep learning algorithms, while it is creating models with the heatmaps method.

The models created are used to detect, track, and analyse specific features and objects with the combined use of heatmaps. The MediaPipe library is also useful for the detection and tracking of detailed objects, especially the human body (Figure 2). In addition to offering an easy-to-use and customizable interface, it allows users to combine and configure different models that support different functions according to their needs. These models offered by MediaPipe can be used in a variety of application scenarios, as well as being an ideal tool for the detection and tracking of objects with various details. [23]
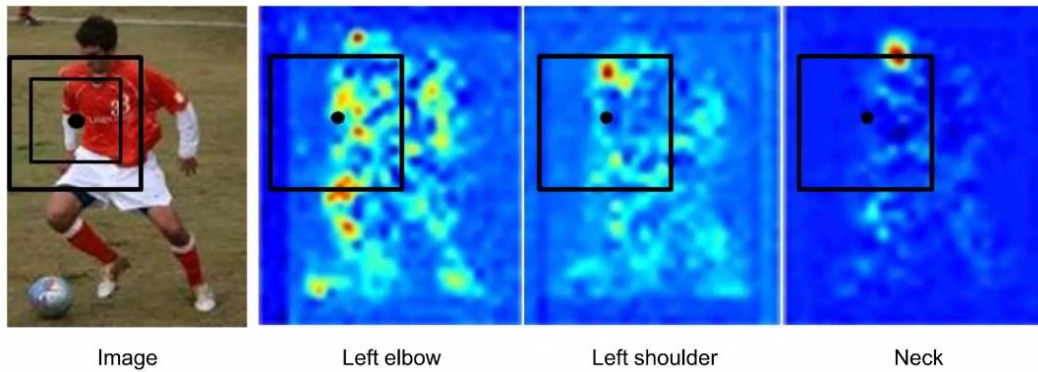
Figure 2. *Use of Mediapipe Library Heatmaps.*

The MediaPipe library offers a new topology of 33 key points for the detection of the human body. This topology is a superset of the key points used in the BlazeFace, BlazePalm, and COCO datasets, and provides consistency between different datasets and models [24].

The MediaPipe topology allows it to estimate the rotation, size, and location of the relevant region with high accuracy and efficiency, using a minimum number of key points on the face, hands, and feet, compared to other popular topologies such as OpenPose and Kinect. The model reduces computational complexity and increases detection speed, as it uses only the necessary key points[25].

The MediaPipe topology is designed to provide suitable, accurate, and efficient person detection for a variety of applications, from augmented reality to sports analytics [26].

In contrast to other pose estimation solutions that detect key points using heatmaps, the underlying solution in MediaPipe is to initially perform a pose alignment.

The MediaPipe training dataset contains 60,000 images with one or several people, as well as 25,000 images of a single person doing sports exercises. The dataset is limited to cases where the entire person is visible or the hip and shoulder key points are clearly obtained. In addition, significant occlusion simulation augmentation is used to ensure that the model supports heavy occlusions that are not present in the dataset [27].

2 MATERIALS AND METHODS

2.1 Application for Movement Analysis for Sports Biomechanics

This study presents an application that detects the accuracy rate of sports activities using human pose estimation data obtained from real-time images. The application analyses the data collected using the MediaPipe Pose Estimation model in the scope of machine learning algorithms.

The application converts the input images created by a computer webcam or ready-made video files to RGB images from BGR images using OpenCV. Using the MediaPipe Pose Estimation model, it detects and records the body landmarks required for postural analysis. The position of the analysed position is compared with the pre-trained model in accordance with the x, y, z coordinates, the angle of the posture is calculated and it is verified whether it meets the criteria of the correct exercise posture. If the user's posture criteria are not met, appropriate warnings are displayed on the screen. If the posture is correct, the number of correction trainings is increased and the output is given on the screen (Figure3).

This study has shown that deep learning techniques can be used in addition to traditional methods in the field of sports biomechanics. This new approach aims to increase the usability and accuracy of athletes' performance and injury risk assessment. For our program, the most suitable exercises, squat (squat) and deadlift, were selected.
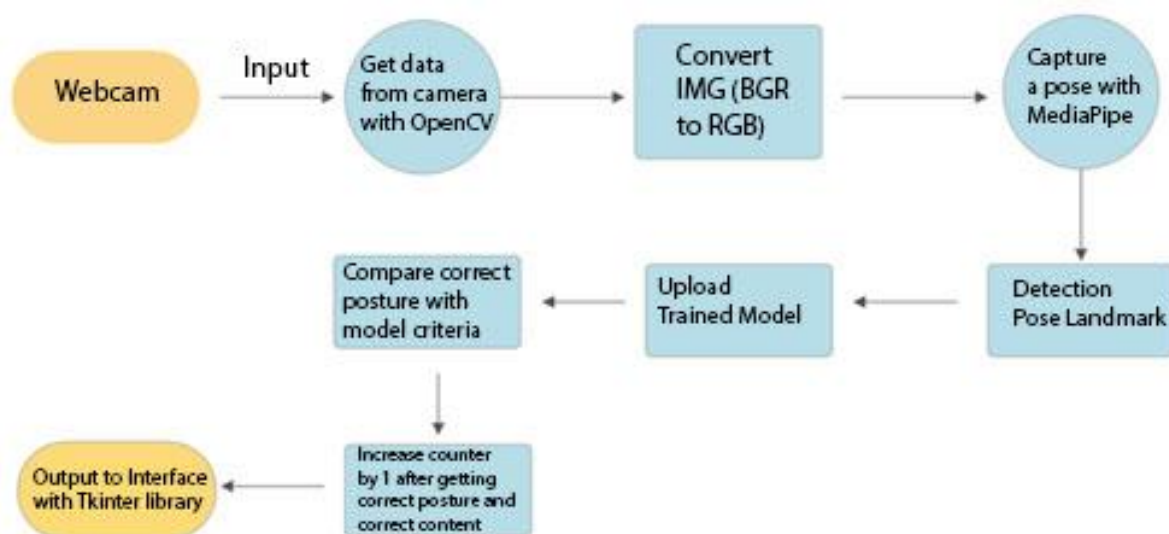
Figure 3. *Correct position detection application processes from camera or video file.*

2.2   Creating a Dataset from Video Files

Deep learning models often require large amounts of labelled data. This data is usually called a dataset and is used to train the model. However, it can sometimes be difficult to find a suitable dataset [28]. In these cases, the method of creating a dataset from video files can be used.

In this study, the following steps was followed to create a dataset from video files:

1. The images were extracted from the video recordings frame by frame.
2. The correct label was determined for each image.
3. The images were saved as a comma-separated values (CSV) file.

When labelling the images, kinematic data was used determined by the **American College of Sports Medicine (ACSM).** According to ACSM, the position where the hips are at the lowest level in the deadlift exercise is the most effective and the hip angle should be between 120-140 degrees in this position [29]. In addition, the knee angle should also be between 100-120 degrees. In the squat exercise, the hip angle should be between 120-130 degrees [30]. The knee angle should be between 100-110 degrees. The back should be kept straight and the chest open. In addition, the head should be prevented from bending forward [31].

The dataset created consists of 7795 lines. Each line is labelled with 33 joint points and related kinematic data. The dataset has been used to achieve the correct position in the deadlift and squat exercises (Figure 4).
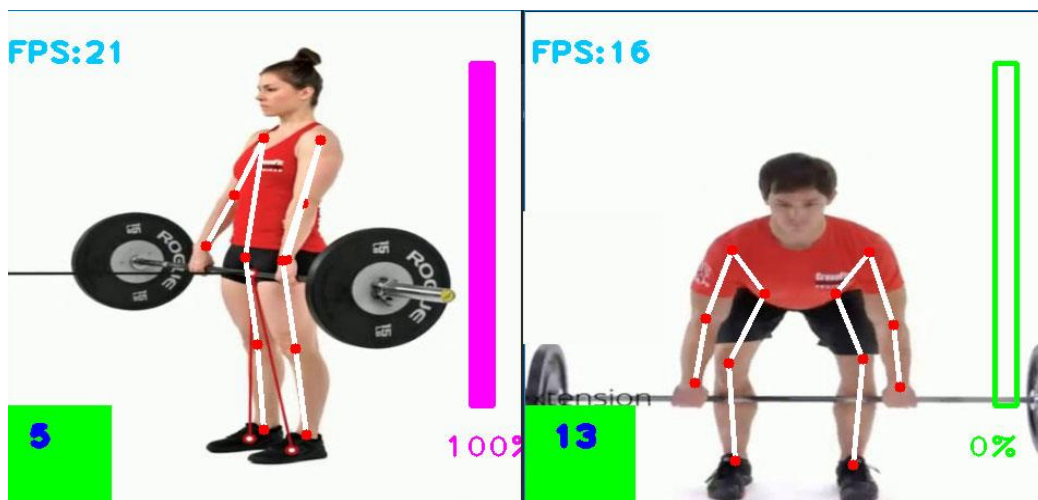
Figure 4. *Dataset creation within kinematic measurements.*

The MediaPipe joint points models used as base points to determine whether the correct posture conditions were met for both Deadlift and Squat. As can be seen in Figure 5, the camera angles of the right and left hips can be different, so the hip angle calculated by taking the average of the two values. Figure 5 shows the key points of the Mediapipe Pose Estimation model that used in the conditions to verify the correct squat and deadlift postures (Figure5).

Figure 5. Kinematic angle values obtained from a certain camera angle.

The hip angle (left knee (25), left hip (23), left shoulder (11)) and the right hip angle (right knee (26), right hip (24), right shoulder (12)) are calculated as follows based on the data obtained (Figure6):

$$\text{Hip Angle} = (\text{Right Hip Angle} + \text{Left Hip Angle}) / 2 \qquad (1)$$

The elbow angle (left wrist (15), left elbow (13), left shoulder (11)) and the right elbow angle (right wrist (16), right elbow (14), right shoulder (12)) are calculated as follows based on the data obtained (Figure6):

$$\text{Elbow Angle} = (\text{Right Elbow Angle} + \text{Left Elbow Angle}) / 2 \qquad (2)$$
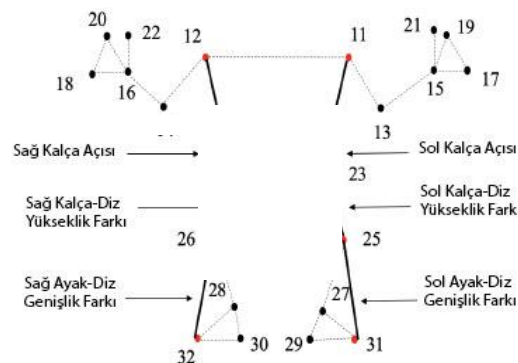
Figure 6. Joint Points for Correct Posture Validity in Squat and Deadlift.

For human pose estimation from a camera or video file, the x, y, and z coordinates are used to calculate the angle between three points. Figure 7 shows the angle between three points. Let the three points be A, B, and C. And the angle to be obtained is θ. The dot product of vectors was used to obtain θ.
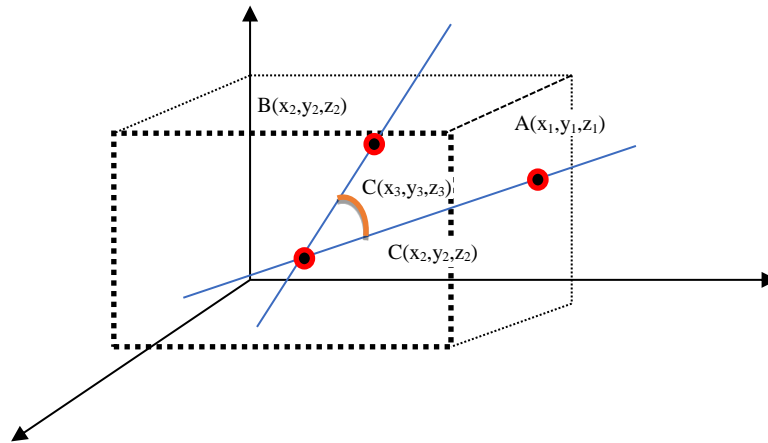
Figure 7. Angle between three points.

The vector with the viewpoint at point C and the endpoint at point A is denoted by $\overrightarrow{CA}$, and the vector with the viewpoint at point C and the endpoint at point B is denoted by $\overrightarrow{CB}$. The vectors $\overrightarrow{CA}$ and $\overrightarrow{CB}$, are defined as (3.2.1).

$$\overrightarrow{CA} = (x1 - x3, y1 - y3, z1 - z3)$$

$$\overrightarrow{CB} = (x2 - x3, y2 - y3, z2 - z3)$$

(3)

So θ is obtained by substituting the inner formula of the vector. In this way, the angle between three points can be defined as (3.2.2).

$$\overrightarrow{CA} \cdot \overrightarrow{CB} = \left|\overrightarrow{CA}\right|\left|\overrightarrow{CA}\right| \cos(\theta)$$

$$\theta = \cos^{-1} \frac{\overrightarrow{CA} \cdot \overrightarrow{CB}}{\left|\overrightarrow{CA}\right|\left|\overrightarrow{CA}\right|}$$

(4)

2.3   Data Modelling with Dataset

Dataset modelling is an approach that is often used in areas such as machine learning and artificial intelligence. This approach is the process of creating a model using the examples in a dataset. This model is then used to classify, predict, or explore new data [32].

In this study, the following steps was followed to do dataset modelling with the dataset prepared in csv file format in the light of kinematic data:

1. Our dataset was divided into 80% training and 20% test data.
2. The training data was used in the model's learning process.
3. The test data was used to measure the performance of the model.
4. A model was created using the features of the dataset.
5. The best performing algorithm was obtained by using different classifier algorithms such as Logistic Regression, Ridge Classifier, Random Forest Classifier and Gradient Boosting Classifier.
6. The performance of the model was calculated with performance metrics such as accuracy, precision and recall (Table 1).
7. The model was saved to be suitable for future predictions and to be used later as a Pickle file.

Table 1. *Model training dataset validation metric values.*

Algorithm	Accuracy	Precision	Recall
Logistik Regression	1.0	1.0	1.0
Ridge Classifier	1.0	1.0	1.0
Random Forest Classifier	0.998	0.996	0.994
Gradient Boosting Classifier	0.955	0.994	0.988

Pickle is very useful in cases where objects need to be serialized and saved. For example, the training of a machine learning model can take a long time, and the model obtained as a result of the training may be desired to be saved for future predictions. In this case, after the training of the model is completed, the model can be serialized using the Pickle module and can be used again later [33].

After completing the training of the model with the pickle library used for serialization of objects in the Python programming language, the csv file, which contains the attributes of **33 joint points** obtained using the Mediapipe pose estimation model and **7795** lines indicating whether the movement is upward or

downward, and occupies approximately **8.22 Megabytes of space**, was saved in a smaller format using the Pickle module. The file obtained in this way was made suitable for the machine learning model by taking up **219 Kilobytes of space**.

2.4 Model Testing Phase

The model was tested our model in Python code after converting it to an appropriate format taking into account factors such as the quality, size and balance of the dataset. Our Python code uses the MediaPipe Pose Estimation model to detect the position of the human body by taking the video stream and converts this positioning into a data frame to test a model that recognizes body language. Then, this data frame is given to the classification model, which is pre-trained and saved as a pickle file, and tries to predict to which class the body language belongs.

This specific code provides a mechanism that counts the number of times the user stands up and squats properly in the deadlift or squat exercise defined above, in line with the movements the user makes. It detects the body language that the user shows during the "up" and "down" movements and keeps the number of "up" movements. This information is displayed in a box displayed on the screen. During the video stream, the class predicted by the model as well as the prediction probabilities are displayed (Figure 8).

Figure 8. *Testing the obtained model*.

2.5   Interface Development and Accuracy Evaluation

In this study, an interface has been developed to evaluate the accuracy of sports exercises. The interface uses machine learning algorithms that provide real-time feedback by processing data from a camera or video file.

The interface uses a webcam to view the user's movement in real time and defines the body position through the Mediapipe Library. Then, it evaluates the predictions using a previously created machine learning model. The components, labels, buttons, and images in the interface are designed in a specific layout so as not to distract the user and to display the feedback and statistics when the user does not make the correct movements.

The graphic interface code includes the Tkinter, Pandas, Numpy, Pickle, Mediapipe, OpenCV and PIL modules. The program takes the video stream, defines the body structure, and predicts the accuracy of a specific posture. The results are shown in the user interface with the appropriate screen instructions, whether the movement is "up" or "down" based on the 33 joint points of the Mediapipe Pose Estimation model, with a similarity of 70% or more.

The interface is designed to help users perform their exercises correctly. The interface can help users learn the correct posture and reduce the risk of injury (Figure9).
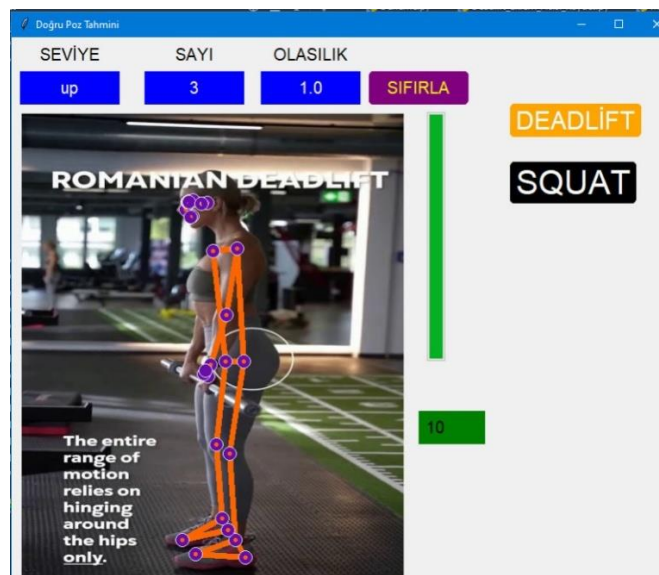
Figure 9. *Model interface design screen.*

3   RESULTS AND DISCUSSION

3.1   Applicability of Mediapipe Human Pose Prediction to Sports Biomechanics

Sports biomechanics is not only a branch of science that investigates the mechanical aspects of the most complex movements of athletes and moving objects by examining them to fine details, but also measures the changes that occur in the body during movement by examining movements specific to the characteristics of athletes [34].

In addition, sports biomechanics is applied for different purposes by using it in fields such as sports sciences, physiotherapy, rehabilitation, orthopaedics in the study of human movement [35].

There has been an interest in the study of human-specific movements since ancient times and many researches have been conducted in this field. In the 1830s, under the leadership of the Weber brothers, the modern study of human movements began. The Weber brothers played an important role in the first gait analysis studies by using modern methods [36]. Most of the research carried out today continues under the influence of Winter's work [37].

Braune and Fischer, who were among the pioneers of biomechanical studies, proposed the use of high-speed recording systems for the study of human and athlete movements. In parallel with the advances in technology, the advancement of electronic and computer systems has enabled the development of new methods in the analysis of athlete movements [38].

In the field of sports biomechanics, there are many software and commercial motion analysis systems for athlete health and sports studies. Examples such as TASS (TNO Automotive Safety Solitiouns), LifeMOD, The AnyBody Modelling System, OpenSim and CATIA are some of the systems used as ergonomic design and analysis modules. Systems developed by APAS (Ariel Dynamics, Inc.), CODA (Charnwood Dynamics Ltd.), ELITE (Bioengineering Technology and Systems), OPTOTRACK (Northern Digital, Inc.), PEAK (Peak Performance Technologies, Inc.), QUALISYS (Qualisys Medical AB) and VICON (Vicon Motion Systems Ltd.) are among the most widely known in the field of motion analysis [39].

Again, Sim Mechanics is a software that combines Simulink and MATLAB (The MathWorks) tools to analyse uncomplicated athlete movements. HUBAG, designed by Hacettepe University biomechanics research group, is a Three Dimensional Motion Analysis software designed for academics, engineers and physicians. The software, which runs in MATLAB environment, is designed for users who want to analyse musculoskeletal systems. HUBAG aims to analyse the movements of athletes and improve athlete technique [40].

However, since the terms and methods used to describe and analyse the movements performed during exercises have an important place in movement analysis, it has become possible to perform these operations with computer vision in order to use these processes more effectively and efficiently with today's technologies. When the concept of computer vision is included in the field of sports biomechanics, it has become clear that even the most complex movements can be analysed and physiological changes can be measured during movements.

With technological advances, machine learning algorithms have made human pose detection and tracking possible. With the widespread commercialization of human pose estimation technology, it has significant implications in various fields such as security, business, health, entertainment and autonomous driving.

In addition, various applications of human pose estimation include human activity and motion estimation, augmented reality (AR) and virtual reality (VR) applications, robotics, animation and games. Human pose estimation has a wide range of application potential, from sports training to sign language communication.

While machine learning models developed today generally focus on 2D perception, Google's open-source Mediapipe library, a deep learning-based model pipeline tool for 3D object perception, is used in the application part of our study as it can perform many operations such as real-time pose estimation applications, face detection, iris tracking.

Deep learning models usually require large amounts of labelled data. This data is often referred to as a dataset and is used for model training. However, sometimes it can be difficult to find a suitable dataset [41]. In these cases, the method of creating a dataset from video files can be used. In this study, this method was used to create our own dataset.

While creating the dataset from video files, images were extracted from video recordings frame by frame and labelled these images. In addition, this method is especially used in areas such as object recognition, face recognition, human activity recognition.

Using the characteristics of the dataset, different classifier algorithms were used different classifier algorithms such as Logistic Regression [42], Ridge Classifier [43], Random Forest Classifier [44], Gradient Boosting Classifier [45], which are popular today and generally perform the best, to obtain our own model and transfer it to the application interface.

Our application shows that deep learning techniques can be used in addition to traditional methods in the field of sports biomechanics. Since it aims to increase the usability and accuracy of this new approach to assess athletes' performance and injury risk, a new approach was presented to the usability of human pose estimation data obtained using the MediaPipe Pose Prediction model in the field of sports biomechanics by determining the accuracy rate of sports activities.

3.2   Human Pose Estimation Libraries Comparison

Nowadays, as the demand for Human Pose Estimation has increased, many skeleton-based Human Pose Estimation algorithms have been developed and Human Pose Estimation algorithms have been packaged into libraries to provide ease of use for researchers. Since the performance of Human Pose Estimation libraries is important to ensure the reliability of the different practical applications they are integrated into, Jen-Li Cung et al. in their study *"Comparative Analysis of Skeleton-Based Human Pose Estimation"* conducted a comparative analysis of four state-of-the-art Human Pose Estimation libraries, namely PoseNet, MoveNet, OpenPose, and MediaPipe Pose, based on images and videos, despite challenges such as camera position and self-shutdown [46].

In this study, the performance of human pose estimation algorithms oflibraries is crucial in terms of the reliability of different applications. To this end, four state-of-the-art human pose estimation libraries, namely PoseNet [47], MoveNet [48], OpenPose [49], and MediaPipe Pose [50] have been comparatively analysed. These libraries employ the keypoint detection approach, which is divided into two classes:

top-down and bottom-up methods. In the top-down method, the number of individuals is determined from the input, and each person is assigned to a separate bounding box sequentially [51]. Subsequently, unlike the top-down method where keypoint estimation is performed in each bounding box, the bottom-up method performs keypoint detection in the initial step. After this stage, keypoints are grouped according to human instances [52].

The datasets used in the experiment for image and video sources are the Microsoft Common Objects in Context (COCO) [53] and Penn Action [54] datasets, respectively. COCO is a commonly used dataset for human pose estimation, containing 330,000 images and 1.5 million object instances. It also provides additional annotations for body keypoint detection, where each person is labelled with 17 keypoint locations. The COCO dataset and the Penn Action video dataset were used to compare the performance of the human pose estimation libraries. Data pre-processing was performed to eliminate irrelevant data in the experiments. The quality of the human pose estimation libraries was measured using the formula of Percentage of Detected Joints. The formula is as follows:

$$d(x - y) = \sqrt{(x_1 - x_2)^2 + (y_1 - y_2)^2} \; pixel \tag{5}$$

$$body \; diameter = \sqrt{(x_{ls} - x_{rh})^2 + (y_{ls} - y_{rh})^2} \tag{6}$$

$$percentage \; of \; detected \; joints = \frac{\sum_{i=1}^{n} bool(d_i < 0.05 * body \; diameter}{n} \tag{7}$$

The Euclidean distance calculation, denoted as d(x, y), between the ground truth key points (x_1, y_1) and the estimated key points (x_2, y_2) is shown in Equation (5). A threshold of 0.05 is used for the detected joint percentage based on the body diameter value. The body diameter is calculated as the Euclidean distance between the left shoulder and the right hip, represented by the coordinates (x_{ls}, y_{ls}) and (x_{rh}, y_{rh}), respectively, as shown in Equation (6). If the Euclidean distance d(x, y) between the estimated key points and the ground truth key points is below the threshold, the estimated key points are considered correctly detected. Therefore, the detected joint percentage is calculated as shown in Equation (7). The variable "n" represents the total number of estimated joints.

Table 2. Number of images detected by human pose estimation in each specific proportion of detected joint percentage

	0% < DJP ≤ 25%		25% < DJP ≤ 50%	50% < DJP ≤ 75%	75% < DJP ≤ 100%
MediaPipe Poz	240	342	116	127	275
OpenPoz	8	87	85	252	668
PoseNet	30	128	185	323	434
MoveNet	5	33	68	247	747

The performance of human pose estimation libraries is affected by challenges such as image clarity and inappropriate camera positioning. In this experiment, the performance of three different libraries, MoveNet, MediaPipe Pose, and PoseNet, was compared (Table 2). MoveNet achieved a higher value for the Detected Joint Percentage (DJP) compared to the other libraries. MediaPipe Pose obtained the highest maximum and median values for the Detected Joint Percentage. Consequently, MediaPipe Pose performed well on the video dataset, while MoveNet showed the best overall performance (Figure10).
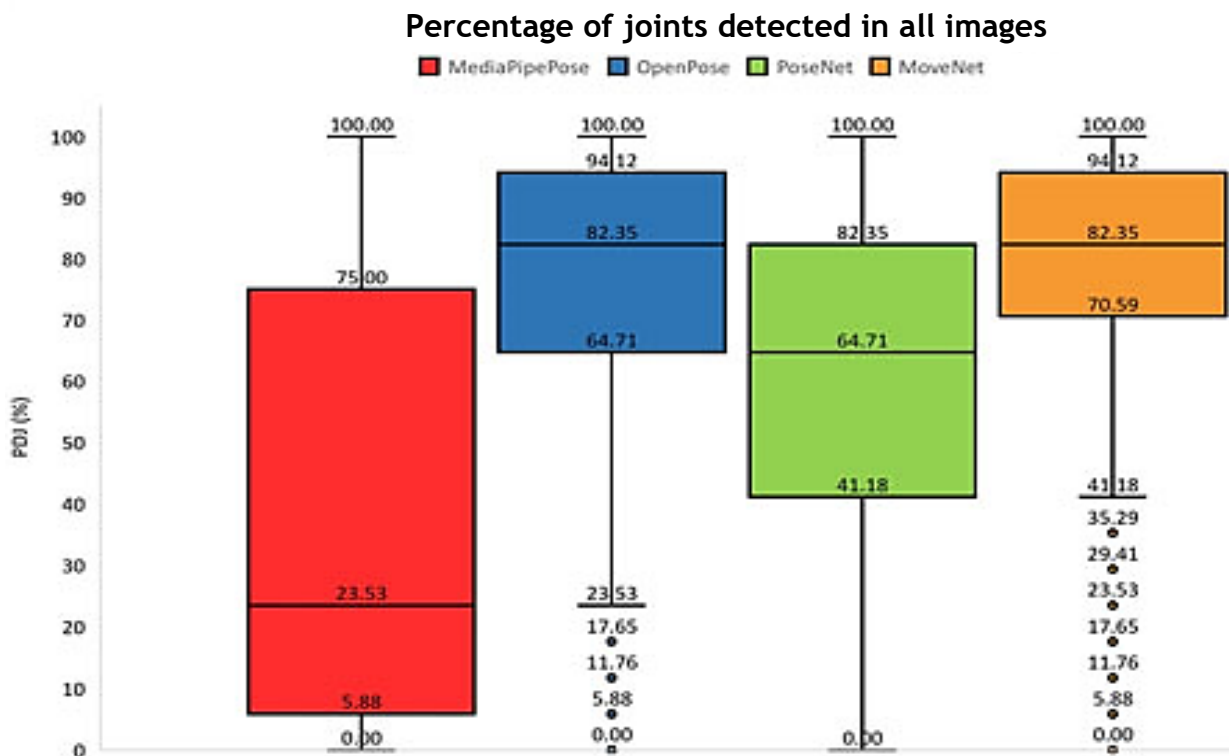
Figure 10. Box plot of the number of joints detected for the images in the dataset.

Also, in another study the Mediapipe library trained two models using a subset of the Augmented Reality (AR) and Yoga datasets to compare and evaluate the quality of the BlazePose model against OpenPose. Both models were trained using the common 17-point MS Coco topology, and their performance was assessed using the Percentage of Correct Points formula. On the AR dataset, the BlazePose model performed slightly worse than the OpenPose model. However, in Yoga/Fitness use cases, the BlazePose Full model outperformed OpenPose. Furthermore, the BlazePose model demonstrated significantly faster processing speeds, ranging from 25 to 75 times faster than a 20-core desktop processor on an intermediate-level phone CPU, depending on the desired quality (Table 3).

Table 3. BlazePose and OpenPose comparison.

Model	FPS	AR Dataset, PCK@0.2	Yoga Dataset, PCK@0.2
OpenPose (only body)	0.4	**87.8**	83.4
BlazePose Full	10	84.1	**84.5**
BlazePose Lite	31^2	79.6	88.6

4 RESULTS AND DISCUSSION

In recent years, the use of artificial intelligence, machine learning, and deep learning technologies has been increasing in the analysis of athlete movements. These technologies enable a more detailed and accurate analysis of athlete movements. In this context, the deep learning-based MediaPipe Pose Estimation model is used to analyse real-time images and obtain human pose estimation data.

In this study, the accuracy rate of deadlift and squat activities were aimed to predict in the field of sports biomechanics. For this purpose, it was used the MediaPipe Pose Estimation module, Numpy, Pandas, and Scikit-Learn Python libraries to process human pose data from real-time or video and images, calculate the angles, and use machine learning algorithms to select the most suitable classifier model and analyse. In addition, this study is an example of the joint use of the MediaPipe Pose Estimation module and Python libraries for human pose estimation in the field of sports biomechanics.

In this context, our application is a program that calculates the kinematic angles for deadlift and squat sports exercises and records the "up" and "down" movements as a CSV dataset consisting of 7795 rows and 33 columns. The program was trained on four machine learning algorithms and compared with performance measurements such as accuracy, precision, and recall scores. The classification algorithm that gave the best result in the comparison was used to evaluate the accuracy of sports exercises. In addition, the processing and memory performance of the machine learning model created using the kinematic angles was tested. The analysis results show that the machine learning method performs better than the processing and memory performance of the kinematic data. These results are visually presented in Figure 11 and Figure 12.
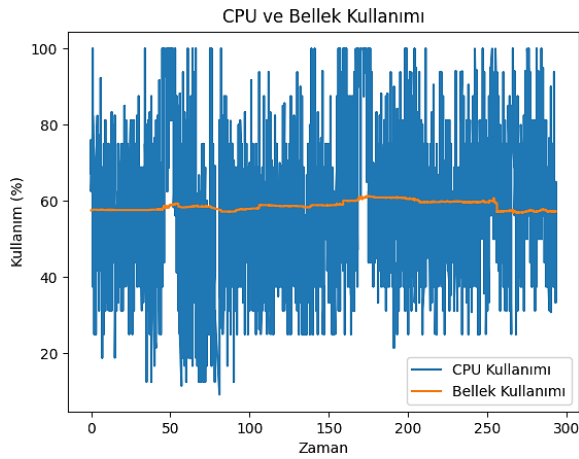
Figure 11. *Kinematic angle measurements performance*.
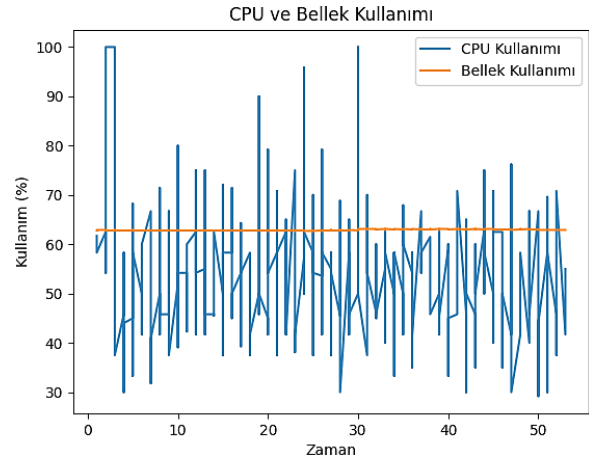
Figure 12. *Machine learning performance*.

Thanks to the program created in this way, people will be able to do sports activities with the correct posture at home or in any suitable environment without the help of a professional trainer and get the economic benefit of sports activity.

In addition, it has the advantage that the time required for posture analysis is short and the user can receive immediate feedback.

Our system created in this direction will make it easier to exercise without the need for a special trainer and will reduce injuries due to incorrect technique. In addition, by comparing the BlazePose model used by the Mediapipe library with other models, it is suggested that this library can be used effectively in the field of sports biomechanics due to its advantages as opposed to its disadvantages. By moving the

system to an Android or IOS application and creating a personalised account to monitor progress, a wider audience be able to be reached in the future. In addition, the emergence of depth sensors in smartphones will also help to improve the accuracy of detecting the pose much more precisely, which will help to create a more accurate posture for comparison.

Conflict of Interest

There is no conflict of interest between the authors.

Authors contributions

[Muhammed Fatih KULUÖZTÜRK]: Played a leading role in identifying the main design and research questions of the article. He was involved in the data collection process and provided management of the analyses. He also played a key role in making sense of the methodology and results.

[Nurettin ACI]: Conducted in-depth studies during the literature review phase and contributed significantly to the organization and style of the manuscript. He led the critical appraisal of the results of the analysis.

Task Sharing:

Design and Concept: [Muhammed Fatih KULUÖZTÜRK]

Data Collection and Analysis: [Muhammed Fatih KULUÖZTÜRK]

Literature Review: [Nurettin ACI]

Writing and Editing: [Nurettin ACI]

Methodology Development: [Muhammed Fatih KULUÖZTÜRK]

Interpretation of Analysis Results: [Nurettin ACI]

Statement of Research and Publication Ethics

The study is complied with research and publication ethics.

REFERENCES

[1]   Ö. Çevik, Oğuzhanoglu, N. K., & Gülbas, Z., "Spor Yaralanmaları: Önleme ve Tedavi," *Türk fiziksel tıp ve rehabilitasyon dergisi,* vol. 64, no.3, pp. 266-273, 2018.

[2]   I. Shrier, "Strategic Assessment of Risk and Risk Tolerance (StARRT) framework for return-to-play decision-making," *British journal of sports medicine,* vol. 49, no.19, pp. 1311-1315, 2015.

[3]   R. Bahr, & Holme, I, "Risk factors for sports injuries-a methodological approach," *British journal of sports medicine,* vol. 37, no. 5, pp. 384-392, 2003.

[4]   Y. Çakır, "Biyomekaniksel Analizler," İstanbul Medipol Üniversitesi, Sağlık Bilimleri Enstitüsü, Fizyoterapi ve Rehabilitasyon Anabilim Dalı, 2019.

[5]   İ. Sarı, "Biyomekanik ve Fiziksel Performansın Biyomekanik Analizi," *Hacettepe Spor Bilimleri Dergisi,* vol. 25, no. 4, pp. 153-167, 2014.

[6]   S. Mülayim, "Spor Biyomekaniği," *Ankara Üniversitesi Beden Eğitimi ve Spor Yüksekokulu Dergisi,* vol. 19, no. 3, pp. 183-192, 2019.

[7]   Y. Güneri, "Biyomekanik, sağlık bilimleri ve spor bilimleri açısından önemi," *Türkiye Klinikleri Journal of Sports Sciences,* vol. 11, no.1, pp. 16-22, 2019.

[8]   D. A. Winter, "Biomechanics and motor control of human movement," *John Wiley & Sons,* 2019.

[9]   V. M. Zatsiorsky, & Seluyanov, V. N, "The mass and inertia characteristics of the main segments of the human body," *Biomechanics VIII-B,* pp. 115-122, 1983.

[10]   F. Muradlı, "Derin Öğrenme Kullanılarak Görüntülerden İnsan Duruş Tespiti," *Sakarya Üniversitesi Fen Bilimleri Enstitüsü Yüksek Lisans Tezi,* 2021.

[11]   A. Özdemir, & Özdemir, A, "MediaPipe Pose ile Evde Egzersiz Yaparken Duruş Tespiti ve Rehberlik Etme,"*International Journal of Informatics Technologies,* vol. 14. no. 2, pp. 123-132, 2021.

[12]   M. Dersuneli, T. Gündüz, and Y. Kutlu, "Bul-Tak Oyuncağı Şekillerinin Klasik Görüntü İşleme ve Derin Öğrenme Yöntemleri ile Tespiti,"*Bitlis Eren Üniversitesi Fen Bilimleri Dergisi,* vol. 10, no. 4, pp. 1290-1303, 2021.

[13]   L. Deng and D. Yu, "Deep learning: methods and applications,"*Foundations and trends® in signal processing,* vol. 7, no. 3–4, pp. 197-387, 2014.

[14]   A. Yaman, S. Abdulkadir, B. Ümit, and E. Sami, "Deep learning-based face liveness detection in videos," in *Proceedings of the IEEEInternational Artificial Intelligence and Data Processing Symposium (IDAP), Malatya, Turkey,* 2017, pp. 16-17.

[15]   Y. LeCun, Y. Bengio, and G. Hinton, "Deep learning," *nature,* vol. 521, no. 7553, pp. 436-444, 2015.

[16]   C.-H. Chen and D. Ramanan, "3d human pose estimation= 2d pose estimation+ matching," in *Proceedings of the IEEE conference on computer vision and pattern recognition,* 2017, pp. 7035-7043.

[17]   C. Zheng *et al.*, "Deep Learning-Based Human Pose Estimation: A Survey," *ACM Computing Surveys,* 2019.

[18]   Z. Cao, T. Simon, S.-E. Wei, and Y. Sheikh, "Realtime multi-person 2d pose estimation using part affinity fields," in *Proceedings of the IEEE conference on computer vision and pattern recognition,* 2017, pp. 7291-7299.

[19]   M. H. BC, R. Prathibha, and S. Kumari, "YOGA AI TRAINER USING TENSORFLOW. JS POSENET."

[20]   R. Guler, N. Neverova, and I. DensePose, "Dense human pose estimation in the wild," in *Proceedings of the IEEE Conference on Computer Vision and Pattern Recognition, Salt Lake City, UT, USA*, 2018, pp. 18-23.

[21]   H.-S. Fang *et al.*, "Alphapose: Whole-body regional multi-person pose estimation and tracking in real-time," *IEEE Transactions on Pattern Analysis and Machine Intelligence,* 2022.

[22]   K. Sun, B. Xiao, D. Liu, and J. Wang, "Deep high-resolution representation learning for human pose estimation," in *Proceedings of the IEEE/CVF conference on computer vision and pattern recognition*, 2019, pp. 5693-5703.

[23]   S. Garg, A. Saxena, and R. Gupta, "Yoga pose classification: a CNN and MediaPipe inspired deep learning approach for real-world application," *Journal of Ambient Intelligence and Humanized Computing*, pp. 1-12, 2022.

[24]   H. H. Pham, H. Salmane, L. Khoudour, A. Crouzil, S. A. Velastin, and P. Zegers, "A unified deep framework for joint 3d pose estimation and action recognition from a single rgb camera," *Sensors,* vol. 20, no. 7, p. 1825, 2020.

[25]   A. Howard *et al.*, "Searching for mobilenetv3," in *Proceedings of the IEEE/CVF international conference on computer vision*, 2019, pp. 1314-1324.

[26]   Z. Cao, T. Simon, S.-E. Wei, and Y. Sheikh, "Realtime multi-person 2d pose estimation using part affinity fields," in *Proceedings of the IEEE conference on computer vision and pattern recognition*, 2017, pp. 1302-1310.

[27]   K. Su, D. Yu, Z. Xu, X. Geng, and C. Wang, "Multi-person pose estimation with enhanced channel-wise and spatial information," in *Proceedings of the IEEE/CVF conference on computer vision and pattern recognition*, 2019, pp. 5674-5682.

[28]   M. Orescanin, L. N. Smith, S. Sahu, P. Goyal, and S. R. Chhetri, "Editorial: Deep learning with limited labeled data for vision, audio, and text," (in English), *Frontiers in Artificial Intelligence,* Editorial vol. 6, 2023-June-13 2023, doi: 10.3389/frai.2023.1213419.

[29]   A. C. o. S. Medicine, *ACSM's guidelines for exercise testing and prescription*. Lippincott williams & wilkins, 2013.

[30]   R. F. Escamilla, G. S. Fleisig, T. M. Lowry, S. W. Barrentine, and J. R. Andrews, "A three-dimensional biomechanical analysis of the squat during varying stance widths," *Medicine and science in sports and exercise,* vol. 33, no. 6, pp. 984-998, 2001.

[31]   R. F. Escamilla, A. C. Francisco, A. V. Kayes, K. P. Speer, and C. T. Moorman 3rd, "An electromyographic analysis of sumo and conventional style deadlifts," *Medicine and science in sports and exercise,* vol. 34, no. 4, pp. 682-688, 2002.

[32]   Z. Cömert and A. KOCAMAZ, "A study of artificial neural network training algorithms for classification of cardiotocography signals," *Bitlis Eren University journal of science and technology,* vol. 7, no. 2, pp. 93-103, 2017.

[33]   M. Pilgrim, "Serializing Python Objects," in *Dive Into Python 3*: Springer, 2009, pp. 205-223.

[34]   N. Çetin, Biyomekanik, *Setma Baskı Ankara, vol.* 1, pp.4-41, 1997.

[35]   C. Açıkada, H. Demirel, Biyomekanik ve Hareket Bilgisi, *AÜAÖFEskişehir,* pp. 15,1993.

[36]   G. Yavuzer, The use of computerized gait analysis in the assessment of neuromusculoskeletal disorders, *Journal Of Physical Medicine And Rehabilitation Sciences*, vol. 10, no: 2, pp. 043-045, 2007.

[37]   DA Winter, Biomechanics And Motor Control Of Human Movement, *2nd Edition, John Wiley & Sons Canada*, 1990.

[38]   W. Braüne, O. Fischer, The Human Gait (Ceviri: Maquet P Furlong R), *Springer-Verlag Heidelberg Almanya*, 1987.

[39]   YI Abdel-Aziz, HM Karara, Direct linear transformation from comparator coordinates ınto object space coordinates in close-range photogrammetry proceedings of the asp/ui, *Symposium on Close-range Photogrammetry American Society of Photogrammetry,* Falls Church VA, s 1-18, 1971.

[40]   E. Civek, Comparison of kinematic results between Metu-kiss & Ankara University-vicon gait analysis systems, *Y Lisans Tezi, Odtü Makina Mühendisliği Bölümü*, 2006.

[41]   M. Orescanin, L. N. Smith, S. Sahu, P. Goyal, and S. R. Chhetri, "Editorial: Deep learning with limited labeled data for vision, audio, and text," (in English), *Frontiers in Artificial Intelligence,* Editorial vol. 6, 2023-June-13 2023, doi: 10.3389/frai.2023.1213419.

[42]   Ö. Çokluk, "Lojistik regresyon analizi: Kavram ve uygulama.", *Kuram ve uygulamada eğitim bilimleri,* vol.10, no: 3, pp. 1357-1407, 2010.

[43]   C.F. İşçen et al, "Su Kalitesi Değişimine Etki Eden Değişkenlerin Lojistik Regresyon, Lojistik-Ridge Ve Lojistik-Lasso Yöntemleri İle Tespiti.", *Biyoloji Bilimleri Araştırma Dergisi*, vol. 14, no: 1, pp. 1-12.

[44]   F. Erdem, et al., "Rastgele orman yöntemi kullanılarak kıyı çizgisi çıkarımı İstanbul örneği.", *Geomatik 3.2,*pp. 100-107, 2018.

[45]   N. Chakrabarty, et al., "Flight arrival delay prediction using gradient boosting classifier.", *Emerging Technologies in Data Mining and Information Security: Proceedings of IEMIS* 2018, Volume 2. Springer Singapore, 2019, 2018.

[46]   J.-L. Chung, L.-Y. Ong, and M.-C. Leow, "Comparative Analysis of Skeleton-Based Human Pose Estimation," *Future Internet,* vol. 14, no. 12, p. 380, 2022. [Online]. Available: https://www.mdpi.com/1999-5903/14/12/380.

[47]   C. Lugaresi *et al.*, "Mediapipe: A framework for building perception pipelines," *arXiv preprint arXiv:1906.08172,* 2019.

[48]   G. Papandreou *et al.*, "Towards accurate multi-person pose estimation in the wild," in *Proceedings of the IEEE conference on computer vision and pattern recognition*, 2017, pp. 4903-4911.

[49]   B. Jo and S. Kim, "Comparative analysis of OpenPose, PoseNet, and MoveNet models for pose estimation in mobile devices," *Traitement du Signal,* vol. 39, no. 1, p. 119, 2022.

[50]   F. Duman, T. D. İpek, and M. Saraçlar, "Unsupervised Discovery of Fingerspelled Letters in Sign Language Videos," in *2021 29th Signal Processing and Communications Applications Conference (SIU)*, 2021: IEEE, pp. 1-4.

[51]   M. Mundt, Z. Born, M. Goldacre, and J. Alderson, "Estimating Ground Reaction Forces from Two-Dimensional Pose Data: A Biomechanics-Based Comparison of AlphaPose, BlazePose, and OpenPose," *Sensors,* vol. 23, no. 1, p. 78, 2022.

[52]   L. Song, G. Yu, J. Yuan, and Z. Liu, "Human pose estimation and its application to action recognition: A survey," *Journal of Visual Communication and Image Representation,* vol. 76, p. 103055, 2021.

[53]   L. Pishchulin *et al.*, "Deepcut: Joint subset partition and labeling for multi person pose estimation," in *Proceedings of the IEEE conference on computer vision and pattern recognition*, 2016, pp. 4929-4937.

[54]   T.-Y. Lin *et al.*, "Microsoft coco: Common objects in context," in *Computer Vision–ECCV 2014: 13th European Conference, Zurich, Switzerland, September 6-12, 2014, Proceedings, Part V 13*, 2014: Springer, pp. 740-755.

[55]   D. C. Luvizon, D. Picard, and H. Tabia, "2d/3d pose estimation and action recognition using multitask deep learning," in *Proceedings of the IEEE conference on computer vision and pattern recognition*, 2018, pp. 5137-5146.

MOLECULAR DYNAMICS STUDY ON THE FORMATION OF ORDERED ARRANGEMENT OF Ba-Ba ATOMIC PAIRS IN THE SiO₂-Al₂O₃-CaO-BaO GLASS-CERAMIC

Fatih Ahmet ÇELİK[1] (iD)

[1] *Bitlis Eren University, Department of Physics, Turkey, facelik@beu.edu.tr*

ABSTRACT

In this study, the barium-calcium aluminosilicate (BaO-CaO-Al₂O₃-SiO₂) glass-ceramic system (BCAS) was modelled by using classical molecular dynamics (MD) simulation method based on Born-Mayer-Huggins (BMH) potential for interatomic interactions. The model system was heated to 5000 K and cooled to 300 K for obtaining a glassy structure. Then the temperature of the system was increased to 400 K, 500 K and 600 K temperatures for observing more ordered structure. For understanding of order formation, the structural development was analyzed by partial radial distribution function (PRDF). The results demonstrated that the PRDF peaks of Ba-Ba became sharper than other bond pairs with the increasing of annealing temperature. These sharp peaks at distant atomic distances represent the occurrence of ordered arrangement in Ba-Ba interactions.

1   INTRODUCTION

In recent years, new generation glass-ceramics have exhibited a number of remarkable physical characteristics when compared to the traditional ceramics and glasses [1-5]. Also, experimental studies have revealed the superior mechanical properties of these materials such as toughness, high flexural strength and fracture [6-8]. Therefore, they have a wide range of interesting technological and industry applications [9-12] because they are easily formed under different heat-treatment conditions via experimental methods [13-15]. At the end of these processes, these materials contain one or more embedded crystalline phases apart from remaining glass matrix. Recently, many studies have been carried out in different types of glass ceramics [16-20]. Among them, the $XO–BaO–SiO_2$-type glass ceramics (X = Mg, Zn and Ca) have attracted the attention for solid oxide fuel cell performance [21-23]. The $Sr/BaO–Al_2O_3–SiO_2–B_2O_3–La_2O_3$ systems have been investigated to understand how Ba/Sr content takes a role on coefficient of thermal expansion [1]. The effect of nucleating agents on glassy structure of $XO–Al_2O_3–SiO_2–B_2O_3$ glasses (R = Ba, Ca and Mg) have been investigated by Lahl et al. [24].

The several-type glass-ceramics have been fabricated for a variety of technological innovations. These studies show that one of the most important features expected from glass for glass-ceramic production is the ability to form suitable crystals without the need for long crystallization times [21-24]. Crystallization is facilitated when the network structure-modifying oxides are present in high amounts in the glass structure by adding CaO and BaO metal oxides. The addition of CaO and BaO to Al_2O_3-SiO_2 system causes various nucleation and crystallization processes [18, 21]. Therefore, the BaO- Al_2O_3-SiO_2 (BAS) glass ceramic materials have properties such as low thermal expansion and dielectric constant, high strength and corrosion resistance, and the CaO-Al_2O_3-SiO_2 (CAS) glass ceramic system is used in many industrial areas due to its good refractoriness, mechanical properties and optics [20-25]. In addition, barium–calcium aluminosilicate (BaO-CaO-Al_2O_3-SiO_2-BCAS) glass-ceramic appears to be very promise for use of chemical compatibility in a glass with metallic interconnects [26]. Specially, many researchers have focused on the BCAS systems by using experimental tools for fuel cell applications [1, 26].

Inspired by these experimental studies, we have also reported that the powerful computational methods are needed for understanding physical behaviors of these-type materials in the nanosized range [27]. The molecular dynamic (MD) simulation methods are a major tool for investigating the electronic, mechanical, optical, structural and phase transition processes of various materials at a nanoscale perspective [28-32]. However, in the literature, there are a few studies on the crystallization behaviors in nano-sized BCAS glass-ceramics under heat-treatment to detect the effect of XO addition on the structure of $YO-SiO_2-Al_2O_3$ system (X = Ba, Y = Ca, K, Mg).

In this study, the crystallization mechanism of BCAS glass-ceramic system have been investigated by using MD calculations based on the two-body BMH potential function. Its structural evaluation was carried out by radial distribution function (RDF) to understand the phase change mechanism during the annealing process.

2 MATERIALS AND METHODS

MD calculations are performed via SCIGRESS [34], a multiplatform molecular design, modeling and dynamics software. The potential energy function is selected as two-body BMH potential in Eq. 1 [35-37].

$$U_{ij(r)} = \frac{q_i q_j}{r_{ij}} + A_{ij} \exp\left(-B_{ij} r\right) - \frac{c_{ij}}{r_{ij}^6} \tag{1}$$

Where, r_{ij} denotes the distance between i and j atoms, $U_{ij}(r)$ is the interatomic-pair potential; $q_i q_j / r_{ij}$ is the long-range and, $A_{ij} \exp(-B_{ij} r)$ represents the short-range repulsion interactions. The initial MD simulation box consisted of randomly distributed $CaOwt\%46-SiO_2wt\%46-Al_2O_3wt\%5-BaOwt3\%$ which included 6000 total atoms and had a 2.854 g/cm^3 density [33] applying periodic boundary conditions along with all three directions. The time-step has chosen to be 1 fs with the NVT ensemble and the Nosé-Hoover thermostat [38] have been used during the simulation. The system held initial temperature of 5000 K for 50 ps for mixing of the system, and then the system was cooled to 300 K within 60 ps. Finally, the temperature of the system increased from 300 K to 400, 500, 600 K and the temperature was maintained at these temperatures for 90 ps to obtain an equilibrium state. A schematic diagram of the variation of temperature and potential

energy with simulation time is shown in Figure 1. After the relaxation process of the system, the equilibrium state of the model system at 5000 K temperature continued about 110 ps and then, the system was annealed to different temperatures from 300K.
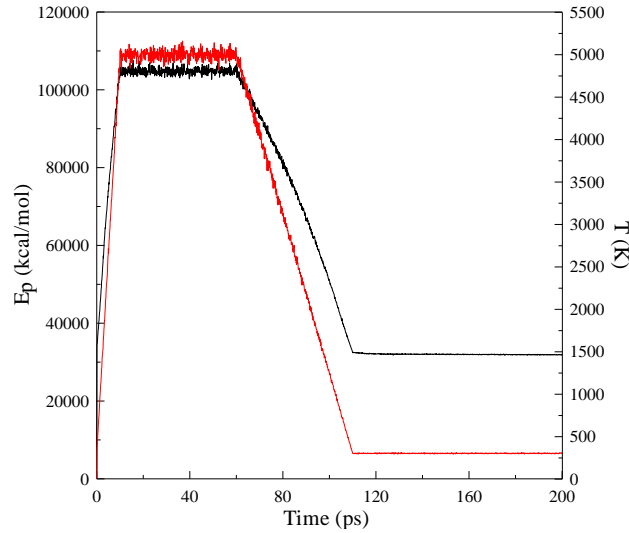
Figure 1. *The schematic diagram of potential energy and temperature variation with simulation time.*

3   RESULTS AND DISCUSSION

In MD simulations, RDF or g(r) is one of the important structural analysis methods to examine the local order of a system during phase transition processes [39, 40]. The total RDF is defined as follows.

$$g(r) = \frac{V}{N^2}\left\langle\sum_{i=1}^{n}\frac{n(r)}{4\pi r^2\Delta r}\right\rangle \qquad (2)$$

where N represents the total number of atoms, V is the volume of the MD box, and n(r) is the number of particles in the shell between r and r+Δr [41]. Figure 2 shows the total RDF curves at 5000 and 300 K for BCAS system. At high temperature, the RDF curves exhibit broader than crystal structure, which is typical behavior characteristic of liquid. Also, the height of the first peak is less than that of glass or amorphous and crystal because there are very few atoms in the first neighborhood shell. At 300 K, the height of the first peak of RDF increases due to formation of the short-range clusters in the glass system. A minor splitting occurred in the second peak of RDF at 300 K upon the development of disordered structures in the second

neighborhood. Figure 3 shows the MD simulation result of the atomic positions of SiO_2-Al_2O_3-CaO-BaO glass ceramic model system at 300 K.
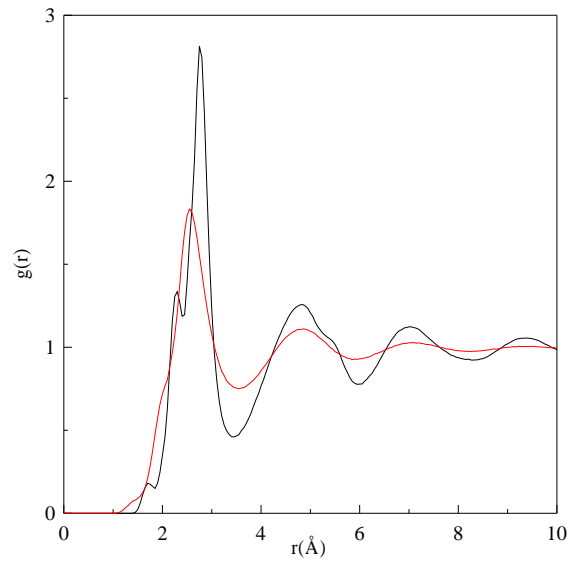
Figure 2. *The total RDF curves for the system at 5000 K and 300 K temperatures (red lines represent 5000 K, black lines represent 300 K).*
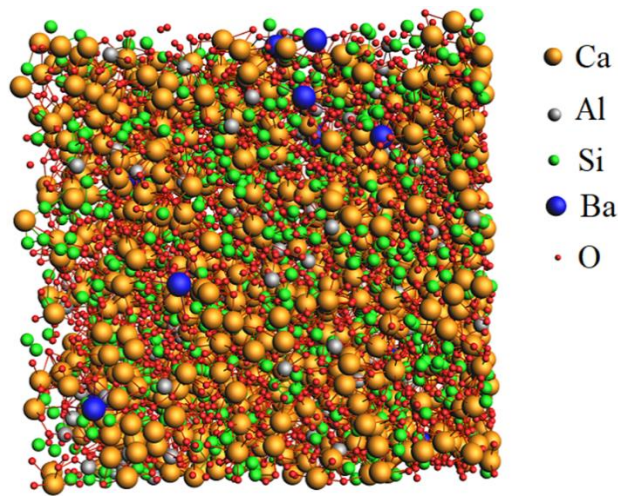
Figure 3. *The simulation result of SiO_2-Al_2O_3-CaO-BaO glass ceramic model system at 300 K (Al, Si, Ba, Ca, and O atoms are shown in grey, green, blue, yellow and red, respectively).*

Some computed partial RDF's (PRDF) for BCAS system with different atomic bonded pairs at various annealing temperatures are shown in Figure 4 (a-b), Figure 5 (a-b), Figure 6 (a-b) and Figure 7 (a-b). As can be seen in these figures, we can be said that the PRDF curves exhibit a short-range order because there are no peaks at distant atomic positions [40] and they have strong first peak.
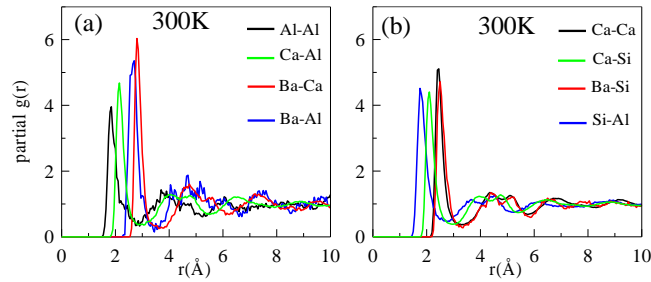
Figure 4. *The PRDFs of atomic bonded pairs at 300 K annealing temperature a) Al-Al, Ca-Al, Ba-Ca and Ba-Al pairs b) Ca-Ca, Ca-Si, Ba-Si and Si-Al pairs.*
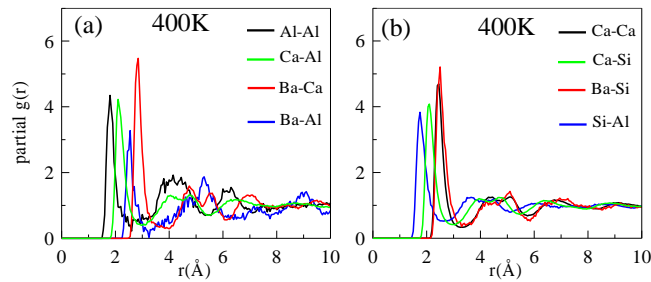
Figure 5. *The PRDFs of atomic bonded pairs at 400 K annealing temperature a) Al-Al, Ca-Al, Ba-Ca and Ba-Al pairs b) Ca-Ca, Ca-Si, Ba-Si and Si-Al pairs.*
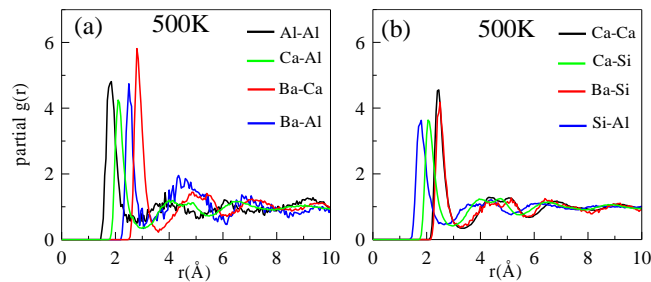
Figure 6. *The PRDFs of atomic bonded pairs at 500 K annealing temperature a) Al-Al, Ca-Al, Ba-Ca and Ba-Al pairs b) Ca-Ca, Ca-Si, Ba-Si and Si-Al pairs.*
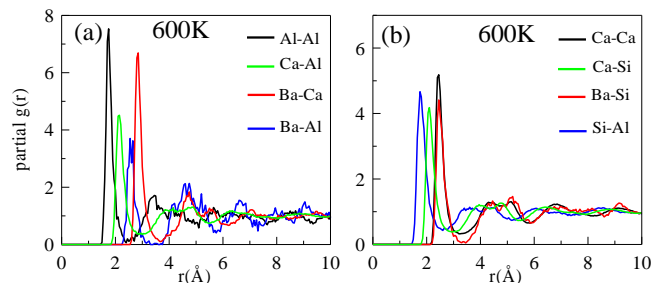
Figure 7. *The PRDFs of atomic bonded pairs at 600 K annealing temperature a) Al-Al, Ca-Al, Ba-Ca and Ba-Al pairs b) Ca-Ca, Ca-Si, Ba-Si and Si-Al pairs.*

Figure 8 shows the PRDFs of the bonded pairs in Ba-Ba interactions at various temperatures. The peaks in the PRDFs are sharper and have more distant atomic distances compared to the other bonded pairs. Especially, the height of the first peak of PRDF for Ba-Ba pairs is higher because the ordered periodic arrangement is dominant between Ba-Ba pairs array in the glassy structure. It was observed that the increasing of annealing temperature causes in better-defined ordered peaks for Ba-Ba interactions. From the position of the first peak in partial g (r)Ba-Ba, it can be asserted that the Ba-Ba nearest-neighbor distances are calculated as 3.35 Å, 3.35 Å, 3.11 Å and 3.52 Å for 300 K, 400 K, 500 K and 600 K temperatures, respectively. This crystallization tendency between Ba-Ba atomic pairs can be explained with other studies on the BCAS glass ceramic. In recent years, a few studies have investigated how the content of Ba affects the crystallization behaviors of BCAS system. The addition of Ba to BCAS can decrease the viscosity of the mold flux [33]. The formation of ordered arrangements of Ba atoms can be reason behind this decrement in viscosity for BCAS system. Also, Bansal et al., [26] investigated the crystallization kinetics of a BCAS system by using experimental tools. They found that the crystallization activation energy of 259 kJ/mol for BCAS glass is much lower compared to other glass systems. This difference in activation energy have been evaluated as the silicate crystallization based on Ba which is formed firstly in BCAS glass different from other various glasses. In fact, the formation of this-type ordered array of Ba-Ba atomic pairs in a glass-ceramic has a complex microstructure with one or more crystalline phases [27]. Therefore, a basic modeling approach can help us close the gap between ordered formation observations in glassy structure in microscopic and macroscopic levels of materials.
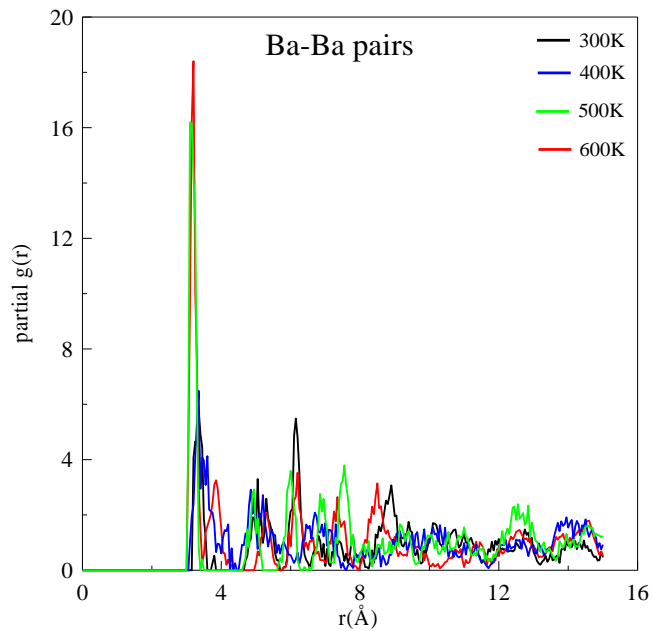
Figure 8*. The variation of partial RDFs of Ba-Ba bonded pairs with annealing temperatures.*

4   CONCLUSIONS

We conducted a classical molecular dynamics simulation on barium–calcium aluminosilicate (BaO-CaO-Al$_2$O$_3$-SiO$_2$) glass-ceramic system by using BMH potential function. The results of molecular dynamics indicated that while the height of the first peak of PRDF for Ba-Ba pairs was very sharp because of ordered structure between Ba-Ba pairs, the peak of the other pairs was not sharp because of glassy structure. The Ba-Ba nearest-neighbor distances were determined as 3.35 Å, 3.35 Å, 3.11 Å and 3.52 Å for 300 K, 400 K, 500 K and 600 K temperatures, respectively. The study is helpful in building up a modeling approach to understand the crystal formation behaviors in BCAS glass-ceramics at nanoscale.

Acknowledgment and support

Statement of Research and Publication Ethics

The study is complied with research and publication ethics.

REFERENCES

[1] S. Ghosh, A. D. Sharma, P. Kundu, S. Mahanty, and R. N. Basu, "Development and characterizations of BaO–CaO–Al2O3–SiO2 glass–ceramic sealants for intermediate temperature solid oxide fuel cell application," *Journal of Non-Crystalline Solids*, vol. 354, no. 34, pp. 4081-4088, 2008.

[2] R. Ota, N. Mishima, T. Wakasugi, and J. Fukunaga, "Nucleation of Li2O- SiO2 glass and its interpretation based on a new liquid model," *Journal of Non-Crystalline Solids*, vol. 219, pp. 70-74, 1997.

[3] B. T. Hoa et al., "Structure, Morphology and Bioactivity of Bioactive Glasses SiO2–CaO–P2O5 Doped with ZnO Synthesized by Green Synthesis," *Glass Physics and Chemistry*, vol. 48, no. 4, pp. 273-279, 2022.

[4] R. D. Rawlings, J. P. Wu, and A. R. Boccaccini, "Glass-ceramics: their production from wastes—a review," *Journal of Materials Science*, vol. 41, pp. 733-761, 2006.

[5] H. R. Fernandes et al., "Crystallization process and some properties of Li2O–SiO2 glass-ceramics doped with Al2O3 and K2O," *Journal of the American Ceramic Society*, vol. 91, no. 11, pp. 3698-3703, 2008.

[6] V. E. Pautkin, "Use of alkaline glass in micromechanical sensor structures," *Glass and Ceramics*, vol. 76, nos. 3-4, pp. 142-144, 2019.

[7] H. Chen, T. Hong, and Y. Jing, "The mechanical, vibrational and thermodynamic properties of glass-ceramic lithium thiophosphates Li4P2S6," *Journal of Alloys and Compounds*, vol. 819, 152950, 2020.

[8] T. Sugawara et al., "Na2O activity and thermodynamic mixing properties of SiO2–Na2O–CaO melt," *Journal of Non-Crystalline Solids*, vol. 371, pp. 58-65, 2013.

[9] D. Herman, T. Okupski, and W. Walkowiak, "Wear resistance glass-ceramics with a gahnite phase obtained in CaO-MgO-ZnO-Al2O3-B2O3-SiO2 system," *Journal of the European Ceramic Society*, vol. 31, no. 4, pp. 485-492, 2011.

[10] H. Masai et al., "Surface crystallization of CaO–Bi2O3-B2O3–Al2O3–TiO2 glass using IR furnace," *Journal of Non-Crystalline Solids*, vols. 356, nos. 52-54, pp. 2977-2979, 2010.

[11] C. Thieme et al., "Effect of Al2O3 on phase formation and thermal expansion of a BaO-SrO-ZnO-SiO2 glass ceramic," *Ceramics International*, vol. 44, no. 2, pp. 2098-2108, 2018.

[12] K. El-Egili, "Infrared studies of Na2O–B2O3–SiO2 and Al2O3–Na2O–B2O3–SiO2 glasses," *Physica B: Condensed Matter*, vol. 325, pp. 340-348, 2003.

[13] W. Zheng et al., "Effect of complex nucleation agents on preparation and crystallization of CaO-MgO-Al2O3-SiO2 glass-ceramics for float process," *Journal of Non-Crystalline Solids*, vol. 450, pp. 6-11, 2016.

[14] Q. C. Yu et al., "Effect of Fe2O3 on non-isothermal crystallization of CaO–MgO–Al2O3–SiO2 glass," *Transactions of Nonferrous Metals Society of China*, vol. 25, no. 7, pp. 2279-2284, 2015

[15] R. G. Duan, K. M. Liang, and S. R. Gu, "Effect of changing TiO2 content on structure and crystallization of CaO-Al2O3-SiO2 system glasses," *Journal of the European Ceramic Society*, vol. 18, no. 12, pp. 1729-1735, 1998.

[16] C. Başaran et al., "The crystallization kinetics of the MgO–Al2O3–SiO2–TiO2 glass ceramics system produced from industrial waste," *Journal of Thermal Analysis and Calorimetry*, vol. 125, pp. 695-701, 2016.

[17] S. C. Von Clausbruch et al., "The effect of P2O5 on the crystallization and microstructure of glass-ceramics in the SiO2–Li2O–K2O–ZnO-P2O5 system," *Journal of Non-Crystalline Solids*, vol. 263, pp. 388-394, 2000.

[18] J. Partyka, "Effect of BaO ratio on the structure of glass–ceramic composite materials from the SiO2–Al2O3–Na2O-K2O–CaO system," *Ceramics International*, vol. 41, no. 8, pp. 9337-9343, 2015.

[19] E. Tkalcec, S. Kurajica, and H. Ivankovic, "Crystallization behavior and microstructure of powdered and bulk ZnO–Al2O3–SiO2 glass-ceramics," *Journal of Non-Crystalline Solids*, vol. 351, nos. 2, pp. 149-157, 2005.

[20] Z. E. Biskri et al., "Computational study of structural, elastic and electronic properties of lithium disilicate (Li2Si2O5) glass-ceramic," *Journal of the Mechanical Behavior of Biomedical Materials*, vol. 32, pp. 345-350, 2014.

[21] J. Kang et al., "Crystallization behavior and properties of CaO-MgO-Al2O3-SiO2 glass-ceramics synthesized from granite wastes," *Journal of Non-Crystalline Solids*, vol. 457, pp. 111-115, 2017.

[22] W. Zheng et al., "CaO–MgO–Al2O3–SiO2 glass-ceramics from lithium porcelain clay tailings for new building materials," *Journal of Non-Crystalline Solids*, vol. 409, pp. 27-33, 2015.

[23] X. Guo et al., "Crystallization and microstructure of CaO–MgO–Al2O3–SiO2 glass-ceramics containing complex nucleation agents," *Journal of Non-Crystalline Solids*, vol. 405, pp. 63-67, 2014.

[24] N. Lahl et al., "Crystallisation kinetics in AO-Al2O3-SiO2-B2O3 glasses (A= Ba, Ca, Mg)," *Journal of Materials Science*, vol. 35, pp. 3089-3096, 2000.

[25] Z. Yang et al., "Effect of CaO/SiO2 ratio on the preparation and crystallization of glass-ceramics from copper slag," *Ceramics International*, vol. 40, no. 5, pp. 7297-7305, 2014.

[26] N. P. Bansal and E. A. Gamble, "Crystallization kinetics of a solid oxide fuel cell seal glass by differential thermal analysis," *Journal of Power Sources*, vol. 147, nos. 1-2, pp. 107-115, 2005.

[27] B. Deng et al., "Molecular dynamics simulations on fracture toughness of Al2O3-SiO2 glass-ceramics," *Scripta Materialia*, vol. 162, pp. 277-280, 2019.

[28] M. Celtek, S. Sengul, and U. Domekeli, "Glass formation and structural properties of Zr50Cu50-xAlx bulk metallic glasses investigated by molecular dynamics simulations," *Intermetallics*, vol. 84, pp. 62-73, 2017.

[29] S. Sengul, M. Celtek, and U. Domekeli, "Molecular dynamics simulations of glass formation and atomic structures in Zr60Cu20Fe20 ternary bulk metallic alloy," *Vacuum*, vol. 136, pp. 20-27, 2017.

[30] F. A. Celik and E. T. Korkmaz, "Molecular dynamic investigation of the effect of atomic polyhedrons on crystallization mechanism for Cu-based Cu-Pd and Cu-Pt alloys," *Journal of Molecular Liquids*, vol. 314, 113636, 2020.

[31] F. A. Celik, A. K. Yildiz, and S. Ozgen, "A molecular dynamics study to investigate the local atomic arrangements during martensitic phase transformations," *Molecular Simulation*, vol. 37, no. 05, pp. 421-429, 2011.

[32] S. Kazanc, F. A. Celik, and S. Ozgen, "The investigation of solid–solid phase transformation at CuAlNi alloy using molecular dynamics simulation," *Journal of Physics and Chemistry of Solids*, vol. 74, no. 12, pp. 1836-1841, 2013.

[33] Z. Piao et al., "Effect of BaO on the viscosity and structure of fluorine-free calcium silicate-based mold flux," *Journal of Non-Crystalline Solids*, vol. 542, 120111, 2020.

[34] SCIGRESS, Fujitsu Limited., Tokyo, Japan, 2021.

[35] D. K. Belashchenko, "Computer simulation of the structure and properties of non-crystalline oxides," *Russian Chemical Reviews*, vol. 66, no. 9, pp. 733, 1997.

[36] J. Kieffer and C. A. Angell, "Structural incompatibilities and liquid–liquid phase separation in molten binary silicates: A computer simulation," *The Journal of Chemical Physics*, vol. 90, no. 9, pp. 4982-4991, 1989.

[37] K. Hirao and K. Kawamura, *Materials Design Using Personal Computer*, Shokabo, Tokyo, 1994, p. 52.

[38] S. Nosé, "A unified formulation of the constant temperature molecular dynamics methods," *The Journal of Chemical Physics*, vol. 81, no. 1, pp. 511-519, 1984.

[39] X. Li et al., "Tension-compression asymmetry of grain-boundary sliding: A molecular dynamics study," *Materials Letters*, vol. 325, 132822, 2022.

[40] C. Li et al., "The concealed solid-solid structural phase transition of Fe70Ni10Cr20 under high pressure," *Materials Today Communications*, vol. 33, 104499, 2022.

[41] S. Özgen and E. Duruk, "Molecular dynamics simulation of solidification kinetics of aluminium using Sutton–Chen version of EAM," *Materials Letters*, vol. 58, no. 6, pp. 1071-1075, 2004.

A GENERALIZATION OF THE REGULAR TRIBONACCI-LUCAS MATRIX

Gonca KIZILASLAN[1],* (ID), **Zinnet SARAL ACER[1]** (ID)

[1] *Kırıkkale University, Department of Mathematics, Turkey, goncakizilaslan@gmail.com,*
mat.saral53@gmail.com
***** *Corresponding author*

ABSTRACT

We define a generalization of a regular Tribonacci-Lucas matrix and give some factorizations by some special matrices. We find the inverse and the k-th power of the matrix. We also present several identities and a relation between an exponential of a matrix and the defined matrix.

1 INTRODUCTION

There have been several studies about Fibonacci and Lucas numbers and their generalizations as they have many applications on several fields, see [8, 9, 12−14, 16, 17]. The Fibonacci sequence $\{F_n\}_{n\geq 0}$ is defined by the recurrence

$$F_{n+2} = F_{n+1} + F_n$$

with initial conditions $F_0 = 0, F_1 = 1$. The Lucas sequence $\{L_n\}_{n\geq 0}$ is defined by $L_0 = 2, L_1 = 1$ and

$$L_{n+2} = L_{n+1} + L_n.$$

A third order generalization of these sequences are called as Tribonacci sequence $\{t_n\}_{n\geq 0}$ and Tribonacci-Lucas sequence $\{v_n\}_{n\geq 0}$. These sequences are defined by the recurrences

$$t_{n+3} = t_{n+2} + t_{n+1} + t_n$$

with initial conditions $t_0 = 0, t_1 = 1, t_2 = 1$ and

$$v_{n+3} = v_{n+2} + v_{n+1} + v_n$$

with initial conditions $v_0 = 3, v_1 = 1, v_2 = 3$, respectively. The first few terms of $\{t_n\}_{n\geq 0}$ and $\{v_n\}_{n\geq 0}$ are given in Table 1.

Table 1. The first few terms of the Tribonacci and Tribonacci-Lucas sequences.

n	0	1	2	3	4	5	6	7	8	9	10	11	12
t_n	0	1	1	2	4	7	13	24	44	81	149	274	504
v_n	3	1	3	7	11	21	39	71	131	241	443	815	1499

There are many studies on Tribonacci and Tribonacci-Lucas numbers and their various properties in the literature. Several sums formulas of these sequences such as

$$\sum_{k=1}^{n} t_k = \frac{t_{n+2} + t_n - 1}{2}$$

$$\sum_{k=1}^{n} v_k = \frac{v_{n+2} + v_n - 6}{2}$$

are also obtained, see [4−6, 10, 11, 20, 24−28, 30].

Matrices whose entries are chosen from special numbers are also found interesting and some factorizations of these matrices have been considered by many researchers, see [1, 2, 7, 19, 21, 32]. In [31], a matrix of order $n + 1$ with entries $[t_{i,j}]$

$$t_{i,j} = \begin{cases} \dfrac{2t_j}{t_{i+2} + t_i - 1}, & \text{if } 0 \leq j \leq i \\ 0, & \text{otherwise} \end{cases} \tag{1}$$

is defined and the Tribonacci space sequences $\ell_p(T)$ are introduced. In [22], a two variables generalization of the matrix given in (1) is defined and some factorizations of the defined matrix are obtained.

Recently, a new regular Tribonacci-Lucas matrix $V = [v_{i,j}]$ is defined by

$$v_{i,j} = \begin{cases} \dfrac{2v_j}{v_{i+2} + v_i - 6}, & \text{if } 0 \leq j \leq i \\ 0, & \text{otherwise} \end{cases} \tag{2}$$

see [18]. They give some relations and inclusion results between the defined matrix and some well-known summability matrices. In this paper, we define a generalization of the matrix given in (2) and present several properties. We obtain some factorizations of the defined matrix and give a relation with an exponential of a special matrix.

2 A GENERALIZATION OF THE REGULAR TRİBONACCİ-LUCAS MATRİX

We define a generalization of the matrix (2) for two variables. Let $V_n(x, y) = [v_{i,j}(x, y)]$ be the matrix of order $n + 1$ with entries

$$v_{i,j}(x,y) = \begin{cases} \dfrac{2v_j}{v_{i+2} + v_i - 6}x^{i-j}y^j, & \text{if } 0 \leq j \leq i, \\ 0, & \text{otherwise.} \end{cases}$$

Here $v_{i,j}(x,y)$ will be zero for x or y is zero and so we assume that x and y are non-zero real numbers. It is clear that for $x = y = 1$ we have

$$v_{i,j}(1,1) = v_{i,j}$$

and so, in this case we obtain the regular Tribonacci-Lucas matrix (2).

Example 1. For $n = 5$, the matrix $V_5(x,y)$ will be of the form

$$V_5(x,y) = \begin{bmatrix} 1 & 0 & 0 & 0 & 0 & 0 \\ \dfrac{1}{4}x & \dfrac{3}{4}y & 0 & 0 & 0 & 0 \\ \dfrac{1}{11}x^2 & \dfrac{3}{11}xy & \dfrac{7}{11}y^2 & 0 & 0 & 0 \\ \dfrac{1}{22}x^3 & \dfrac{3}{22}x^2y & \dfrac{7}{22}xy^2 & \dfrac{11}{22}y^3 & 0 & 0 \\ \dfrac{1}{43}x^4 & \dfrac{3}{43}x^3y & \dfrac{7}{43}x^2y^2 & \dfrac{11}{43}xy^3 & \dfrac{21}{43}y^4 & 0 \\ \dfrac{1}{49}x^5 & \dfrac{3}{49}x^4y & \dfrac{7}{49}x^3y^2 & \dfrac{11}{49}x^2y^3 & \dfrac{21}{49}xy^4 & \dfrac{39}{49}y^5 \end{bmatrix}$$

2.1 Properties of the Tribonacci-Lucas Matrices $V_n(x,y)$

We give some interesting properties and applications of the matrix $V_n(x,y)$. Throughout the paper, we will denote the (i,j) entry of a matrix A as $(A)_{i,j}$. For $n, j \in \mathbb{N}$, we define

$$(x \oplus y)_j^n := \sum_{k=0}^{n} v_{k+j,k+j}x^{n-k}y^k.$$

Theorem 2.1. For any positive integer n and any real numbers x, y, z and w, we have

$$(V_n(x,y)V_n(w,z))_{i,j} = \left(V_n\big((x \oplus yw)_j, yz\big)\right)_{i,j}. \tag{3}$$

Proof. It is clear from the definition that $v_{i,j+1}v_{j+1,j} = v_{j+1,j+1}v_{i,j}$. Then we have

$$
\begin{aligned}
(V_n(x,y)V_n(w,z))_{i,j} &= \sum_{k=j}^{i} v_{i,k}(x,y)v_{k,j}(w,z) \\
&= v_{i,j}v_{j,j}x^{i-j}y^j z^j + v_{i,j+1}v_{j+1,j}x^{i-j-1}y^{j+1}wz^j + \cdots + v_{i,i}v_{i,j}y^i w^{i-j}z^j \\
&= v_{i,j}y^j z^j (v_{j,j}x^{i-j} + v_{j+1,j+1}x^{i-j-1}yw + \cdots + v_{i,i}y^{i-j}w^{i-j}) \\
&= v_{i,j}y^j z^j (x \oplus yw)_j^{i-j} \\
&= \left(V_n((x \oplus yw)_j, yz)\right)_{i,j}.
\end{aligned}
$$

We can obtain the $k-$ th power of the matrix $V_n(x,y)$ by using Theorem 2.1. For $w = x$ and $z = y$ in (3), we get

$$
(V_n^2(x,y))_{i,j} = \left(V\big(x(1 \oplus y)_j, y^2\big)\right)_{i,j}.
$$

Using formula (3) again, multiplying $V_n^2(x,y)$ and $V_n(x,y)$, we get

$$
(V_n^3(x,y))_{i,j} = \left(V\left(x\big((1 \oplus y)_j \oplus y^2\big)_j, y^3\right)\right)_{i,j}.
$$

Then using the mathematical induction method, we have

$$
(V_n^k(x,y))_{i,j} = \left(V\left(x\left(\big(\cdots\big((1 \oplus y)_j \oplus y^2\big)_j \oplus y^3\big)_j \cdots \oplus y^{k-1}\right)_j, y^k\right)\right)_{i,j}.
$$

The inverse of the Tribonacci-Lucas matrix $V_n(x,y)$ which is denoted by $V_n^{-1}(x,y) = [v_{i,j}^{-1}(x,y)]$ is given by the following theorem.

Theorem 2.2. The $(i,j)-$ entry of the inverse of the matrix $V_n(x,y)$ is

$$
v_{i,j}^{-1}(x,y) =
\begin{cases}
\dfrac{v_{i+2} + v_i - 6}{2v_j y^i}, & \text{if } i = j, \\[2ex]
\dfrac{-(v_{i+2} + v_i - 6)x}{2v_{j+2} y^i}, & \text{if } i = j + 1, \\[2ex]
0, & \text{otherwise.}
\end{cases}
$$

Proof. It is clear that $(V_n(x,y)V_n^{-1}(x,y))_{i,j} = 0$ in the case of $i \neq j$ and $i \neq j + 1$. For $i = j$, we obtain that

$$(V_n(x,y)V_n^{-1}(x,y))_{i,i} = \sum_{k=i}^{i} v_{i,k}(x,y)v_{k,i}^{-1}(x,y) = v_{ii}(x,y)v_{ii}^{-1}(x,y)$$

$$= \frac{2v_i y^i}{v_{i+2} + v_i - 6} \frac{v_{i+2} + v_i - 6}{2v_i y^i} = 1$$

and for $i = j + 1$ we get

$$(V_n(x,y)V_n^{-1}(x,y))_{i,j} = \sum_{k=j}^{i} v_{i,k}(x,y)v_{k,j}^{-1}(x,y)$$

$$= v_{ij}(x,y)v_{jj}^{-1}(x,y) + v_{i,j+1}(x,y)v_{j+1,j}^{-1}(x,y)$$

$$= \frac{2v_j x^{i-j} y^j}{v_{i+2} + v_i - 6} \frac{v_{j+2} + v_j - 6}{2v_j y^j} + \frac{2v_{j+1} x^{i-j-1} y^{j+1}}{v_{i+2} + v_i - 6} \frac{(v_{j+2} + v_j - 6)(-x)}{2v_{j+1} y^{j+1}}$$

$$= \frac{(v_{j+2} + v_j - 6)x^{i-j}}{v_{i+2} + v_i - 6} - \frac{(v_{j+2} + v_j - 6)x^{i-j}}{v_{i+2} + v_i - 6}$$

$$= 0.$$

Thus, the result follows.

2.2 Factorizations of the Tribonacci-Lucas Matrices $V_n(x,y)$

We give some factorizations of the matrix $V_n(x,y)$. For this purpose, we need to define the following matrices of order $n + 1$

$$(S_n(x,y))_{i,j} = \begin{cases} v_{i,j+1}(x,y)v_{j,j-1}^{-1}(x,y) + v_{i,j}(x,y)v_{j-1,j-1}^{-1}(x,y), & \text{if } 0 \leq j \leq i, \\ 0, & \text{otherwise} \end{cases}$$

$$\bar{V}_{n-1}(x,y) = \begin{bmatrix} 1 & 0 \\ 0 & V_{n-1} \end{bmatrix},$$

$$G_k = \begin{bmatrix} I_{n-k-1} & 0 \\ 0 & S_k \end{bmatrix} \text{ for } 1 \leq k \leq n-1, \text{ and } G_n(x,y) = S_n(x,y).$$

Lemma 2.1. For any positive integer n and any real numbers x and y, we have

$$V_n(x,y) = S_n(x,y)\bar{V}_{n-1}(x,y).$$

Proof. We denote the inverse of the matrix $\bar{V}_n(x,y)$ as $\bar{V}_n^{-1}(x,y) := [\bar{v}_{i,j}^{-1}(x,y)]$. Then

$$(V_n(x,y)\bar{V}_{n-1}^{-1}(x,y))_{i,j} = \sum_{k=j}^{i} v_{i,k}(x,y)\bar{v}_{k,j}^{-1}(x,y) = \sum_{k=j}^{i} v_{i,k}(x,y)v_{k-1,j-1}^{-1}(x,y).$$

Here the sum is nonzero only for $k - 1 = j - 1$ and $k - 1 = j$. So we get

$$\sum_{k=j}^{i} v_{i,k}(x,y)v_{k-1,j-1}^{-1}(x,y) = v_{i,j+1}(x,y)v_{j,j-1}^{-1}(x,y) + v_{i,j}(x,y)v_{j-1,j-1}^{-1}(x,y) = S_n(x,y).$$

Example 2.

$S_5(x,y)\bar{V}_4(x,y) =$

$$
\begin{bmatrix}
1 & 0 & 0 & 0 & 0 & 0 \\
\frac{1}{4}x & \frac{3}{4}y & 0 & 0 & 0 & 0 \\
\frac{1}{11}x^2 & \frac{2}{33}xy & \frac{28}{11}y & 0 & 0 & 0 \\
\frac{1}{22}x^3 & \frac{1}{33}x^2y & \frac{32}{231}xy & \frac{11}{14}y & 0 & 0 \\
\frac{1}{43}x^4 & \frac{2}{129}x^3y & \frac{64}{903}x^2y & -\frac{26}{301}xy & \frac{42}{43}y & 0 \\
\frac{1}{49}x^5 & \frac{2}{147}x^4y & \frac{64}{1029}x^3y & -\frac{26}{343}x^2y & \frac{8}{343}xy & \frac{559}{343}y
\end{bmatrix}
\begin{bmatrix}
1 & 0 & 0 & 0 & 0 & 0 \\
0 & 1 & 0 & 0 & 0 & 0 \\
0 & \frac{1}{4}x & \frac{3}{4}y & 0 & 0 & 0 \\
0 & \frac{1}{11}x^2 & \frac{3}{11}xy & \frac{7}{11}y^2 & 0 & 0 \\
0 & \frac{1}{22}x^3 & \frac{3}{22}x^2y & \frac{7}{22}xy^2 & \frac{11}{22}y^3 & 0 \\
0 & \frac{1}{43}x^4 & \frac{3}{43}x^3y & \frac{7}{43}x^2y^2 & \frac{11}{43}xy^3 & \frac{21}{43}y^4
\end{bmatrix}
$$

$$
=
\begin{bmatrix}
1 & 0 & 0 & 0 & 0 & 0 \\
\frac{1}{4}x & \frac{3}{4}y & 0 & 0 & 0 & 0 \\
\frac{1}{11}x^2 & \frac{3}{11}xy & \frac{7}{11}y^2 & 0 & 0 & 0 \\
\frac{1}{22}x^3 & \frac{3}{22}x^2y & \frac{7}{22}xy^2 & \frac{11}{22}y^3 & 0 & 0 \\
\frac{1}{43}x^4 & \frac{3}{43}x^3y & \frac{7}{43}x^2y^2 & \frac{11}{43}xy^3 & \frac{21}{43}y^4 & 0 \\
\frac{1}{49}x^5 & \frac{3}{49}x^4y & \frac{7}{49}x^3y^2 & \frac{11}{49}x^2y^3 & \frac{21}{49}xy^4 & \frac{39}{49}y^5
\end{bmatrix}
$$

$=V_5(x,y).$

Theorem 2.3. The matrix $V_n(x,y)$ can be factorized as

$$V_n(x,y) = G_n(x,y)G_{n-1}(x,y)\ldots G_1(x,y).$$

In particular,

$$V_n = G_n G_{n-1} \ldots G_1$$

where $V_n := V_n(1,1), G_k := G_k(1,1), k = 1,2,\ldots,n.$

Proof. By the definition of the matrices $G_k(x,y)$ and Lemma 2.1, we get the desired decomposition of the matrix $V_n(x,y)$.

It is clear that the inverse matrix $V_n^{-1}(x,y)$ can be factorized as

$$V_n^{-1}(x,y) = G_1^{-1}(x,y)G_2^{-1}(x,y)\ldots G_n^{-1}(x,y).$$

Example 3. Since

$$V_5(x,y) = \begin{bmatrix} 1 & 0 & 0 & 0 & 0 & 0 \\ \frac{1}{4}x & \frac{3}{4}y & 0 & 0 & 0 & 0 \\ \frac{1}{11}x^2 & \frac{3}{11}xy & \frac{7}{11}y^2 & 0 & 0 & 0 \\ \frac{1}{22}x^3 & \frac{3}{22}x^2y & \frac{7}{22}xy^2 & \frac{11}{22}y^3 & 0 & 0 \\ \frac{1}{43}x^4 & \frac{3}{43}x^3y & \frac{7}{43}x^2y^2 & \frac{11}{43}xy^3 & \frac{21}{43}y^4 & 0 \\ \frac{1}{49}x^5 & \frac{3}{49}x^4y & \frac{7}{49}x^3y^2 & \frac{11}{49}x^2y^3 & \frac{21}{49}xy^4 & \frac{39}{49}y^5 \end{bmatrix}$$

we can factorize this matrix as

$$G_5(x,y)G_4(x,y)G_3(x,y)G_2(x,y)G_1(x,y)=$$

$$\begin{bmatrix} 1 & 0 & 0 & 0 & 0 & 0 \\ \frac{1}{4}x & \frac{3}{4}y & 0 & 0 & 0 & 0 \\ \frac{1}{11}x^2 & \frac{2}{33}xy & \frac{28}{11}y & 0 & 0 & 0 \\ \frac{1}{22}x^3 & \frac{1}{33}x^2y & \frac{32}{231}xy & \frac{11}{14}y & 0 & 0 \\ \frac{1}{43}x^4 & \frac{2}{129}x^3y & \frac{64}{903}x^2y & -\frac{26}{301}xy & \frac{42}{43}y & 0 \\ \frac{1}{49}x^5 & \frac{2}{147}x^4y & \frac{64}{1029}x^3y & -\frac{26}{343}x^2y & \frac{8}{343}xy & \frac{559}{343}y \end{bmatrix} \begin{bmatrix} 1 & 0 & 0 & 0 & 0 & 0 \\ 0 & 1 & 0 & 0 & 0 & 0 \\ 0 & \frac{1}{4}x & \frac{3}{4}y & 0 & 0 & 0 \\ 0 & \frac{1}{11}x^2 & \frac{2}{33}xy & \frac{28}{11}y & 0 & 0 \\ 0 & \frac{1}{22}x^3 & \frac{1}{33}x^2y & \frac{32}{231}xy & \frac{11}{14}y & 0 \\ 0 & \frac{1}{43}x^4 & \frac{2}{129}x^3y & \frac{64}{903}x^2y & -\frac{26}{301}xy & \frac{42}{43}y \end{bmatrix}$$

$$\begin{bmatrix} 1 & 0 & 0 & 0 & 0 & 0 \\ 0 & 1 & 0 & 0 & 0 & 0 \\ 0 & 0 & 1 & 0 & 0 & 0 \\ 0 & 0 & \frac{1}{4}x & \frac{3}{4}y & 0 & 0 \\ 0 & 0 & \frac{1}{11}x^2 & \frac{2}{33}xy & \frac{28}{11}y & 0 \\ 0 & 0 & \frac{1}{22}x^3 & \frac{1}{33}x^2y & \frac{32}{231}xy & \frac{11}{14}y \end{bmatrix} \begin{bmatrix} 1 & 0 & 0 & 0 & 0 & 0 \\ 0 & 1 & 0 & 0 & 0 & 0 \\ 0 & 0 & 1 & 0 & 0 & 0 \\ 0 & 0 & 0 & 1 & 0 & 0 \\ 0 & 0 & 0 & \frac{1}{4}x & \frac{3}{4}y & 0 \\ 0 & 0 & 0 & \frac{1}{11}x^2 & \frac{2}{33}xy & \frac{28}{11}y \end{bmatrix} \begin{bmatrix} 1 & 0 & 0 & 0 & 0 & 0 \\ 0 & 1 & 0 & 0 & 0 & 0 \\ 0 & 0 & 1 & 0 & 0 & 0 \\ 0 & 0 & 0 & 1 & 0 & 0 \\ 0 & 0 & 0 & 0 & 1 & 0 \\ 0 & 0 & 0 & 0 & \frac{1}{4}x & \frac{3}{4}y \end{bmatrix}.$$

We can also separate the variables x and y from the matrices $V_n(x,y)$ and $V_n(-x,y)$.

Theorem 2.4. Let $D_n(x) := \operatorname{diag}(1, x, x^2, x^3, \dots, x^n)$ be a diagonal matrix. For any positive integer k and any non-zero real numbers x and y, we have

$$V_k(x,y) = V_k(x,1)D_k(y),$$
$$V_k(-x,y) = V_k(-x,1)D_k(y).$$

Now, we present a relation between the matrices $V_n(x, ay)$ and $V_n(x, -y)$ for a nonzero real number a.

Theorem 2.5. For a nonzero real number a, the matrices $V_n(x, ay)$ and $V_n(x, -y)$ satisfy the following

$$V_n\left(x, \frac{y}{a}\right)^{-1} = V_n^{-1}(x, -y)V_n(x, ay)V_n^{-1}(x, -y).$$

Proof. The proof can be done easily by definition of the matrices and matrix multiplication.

Theorem 2.6. Let $K_n(x, y) = [k_{i,j}]$ be a matrix with entries $k_{i,j} = v_j x^{i-j} y^j$ and $D'_n = [d'_{i,j}]$ be a diagonal matrix with diagonal entries $d'_{i,i} = \frac{2}{v_{i+2}+v_i-6}$. Then we have

$$V_n(x, y) = D'_n K_n(x, y).$$

Proof. By matrix multiplication, we have

$$(D'_n K_n(x, y))_{i,j} = \sum_{k=0}^{n} d'_{i,k} k_{k,j}(x, y) = d'_{i,i} k_{i,j}(x, y)$$
$$= \frac{2}{v_{i+2} + v_i - 6} v_j x^{i-j} y^j$$
$$= \frac{2v_j}{v_{i+2} + v_i - 6} x^{i-j} y^j = (V_n(x, y))_{i,j}.$$

Example 4. For $n = 5$, we have

$$V_5(x, y) = \begin{bmatrix} 1 & 0 & 0 & 0 & 0 & 0 \\ \frac{1}{4}x & \frac{3}{4}y & 0 & 0 & 0 & 0 \\ \frac{1}{11}x^2 & \frac{3}{11}xy & \frac{7}{11}y^2 & 0 & 0 & 0 \\ \frac{1}{22}x^3 & \frac{3}{22}x^2y & \frac{7}{22}xy^2 & \frac{11}{22}y^3 & 0 & 0 \\ \frac{1}{43}x^4 & \frac{3}{43}x^3y & \frac{7}{43}x^2y^2 & \frac{11}{43}xy^3 & \frac{21}{43}y^4 & 0 \\ \frac{1}{49}x^5 & \frac{3}{49}x^4y & \frac{7}{49}x^3y^2 & \frac{11}{49}x^2y^3 & \frac{21}{49}xy^4 & \frac{39}{49}y^5 \end{bmatrix}$$

$$
= \begin{bmatrix} 1 & 0 & 0 & 0 & 0 & 0 \\ 0 & \dfrac{1}{4} & 0 & 0 & 0 & 0 \\ 0 & 0 & \dfrac{1}{11} & 0 & 0 & 0 \\ 0 & 0 & 0 & \dfrac{1}{22} & 0 & 0 \\ 0 & 0 & 0 & 0 & \dfrac{1}{43} & 0 \\ 0 & 0 & 0 & 0 & 0 & \dfrac{1}{49} \end{bmatrix} \begin{bmatrix} 1 & 0 & 0 & 0 & 0 & 0 \\ x & 3y & 0 & 0 & 0 & 0 \\ x^2 & 3xy & 7y^2 & 0 & 0 & 0 \\ x^3 & 3x^2y & 7xy^2 & 11y^3 & 0 & 0 \\ x^4 & 3x^3y & 7x^2y^2 & 11xy^3 & 21y^4 & 0 \\ x^5 & 3x^4y & 7x^3y^2 & 11x^2y^3 & 21xy^4 & 39y^5 \end{bmatrix}
$$

$$
= D_5' K_5(x, y).
$$

3 SOME APPLICATIONS OF THE TRIBONACCI-LUCAS MATRIX $V_n(x,y)$

The following result gives the sum of squares of the first n Tribonacci-Lucas numbers.

Lemma 3.1 ([23]). For $n \geq 1$, the Tribonacci-Lucas numbers v_n satisfy

$$
\sum_{k=1}^{n} v_k^2 = \frac{-v_{n+1}^2 - v_{n-1}^2 + v_{2n+3} + v_{2n-2} - 4}{2}.
$$

Now, we consider a matrix whose Cholesky factorization includes the matrix $V_n(1,1)$.

Theorem 3.1. A matrix $Q_n = [c_{i,j}]$ with entries

$$
c_{i,j} = \frac{2(-v_{k+1}^2 - v_{k-1}^2 + v_{2k+3} + v_{2k-2} - 4)}{(v_{i+2} + v_i - 6)(v_{j+2} + v_j - 6)},
$$

where $k = \min\{i,j\}$, is a symmetric matrix and its Cholesky factorization is $V_n(1,1)V_n(1,1)^T$.

Proof. Since

$$
c_{i,j} = \frac{2(-v_{k+1}^2 - v_{k-1}^2 + v_{2k+3} + v_{2k-2} - 4)}{(v_{i+2} + v_i - 6)(v_{j+2} + v_j - 6)} = c_{j,i}
$$

the matrix Q_n is symmetric. We now show that $Q_n = V_n(1,1)V_n(1,1)^T$.

$$V_n(1,1)V_n(1,1)^T = \sum_{k=0}^{n} v_{i,k}v_{j,k} = \sum_{k=0}^{n} \frac{2v_k}{v_{i+2} + v_i - 6}\frac{2v_k}{v_{j+2} + v_j - 6}$$

$$= \frac{4}{(v_{i+2} + v_i - 6)(v_{j+2} + v_j - 6)}\sum_{k=0}^{n} v_k^2$$

$$= \frac{4}{(v_{i+2} + v_i - 6)(v_{j+2} + v_j - 6)}\frac{-v_{n+1}^2 - v_{n-1}^2 + v_{2n+3} + v_{2n-2} - 4}{2}$$

$$= \frac{2(-v_{k+1}^2 - v_{k-1}^2 + v_{2k+3} + v_{2k-2} - 4)}{(v_{i+2} + v_i - 6)(v_{j+2} + v_j - 6)}$$

$$= Q_n.$$

Hence, we obtain the result.

For any square matrix M, the exponential of M is defined to be the matrix

$$e^M = I + M + \frac{M^2}{2!} + \frac{M^3}{3!} + \cdots + \frac{M^k}{k!} + \cdots$$

Thus, we have the following result for a square matrix M.

Theorem 3.2 ([3, 29]). (i) For any numbers r and s, we have $e^{(r+s)M} = e^{rM}e^{sM}$.

(ii) $(e^M)^{-1} = e^{-M}$.

(iii) By taking the derivative with respect to x of each entry of e^{Mx}, we get the matrix $\frac{d}{dx}e^{Mx} = Me^{Mx}$.

In the last part of this section, we will give a relation between the matrix $V_n(x,y)$ and the exponential of a special matrix.

Definition 1. The matrix $M_n = [m_{i,j}]$ is defined by

$$m_{i,j} = \begin{cases} \frac{v_j}{v_i}, & \text{if } i = j + 1, \\ 0, & \text{otherwise.} \end{cases} \tag{4}$$

We want to obtain a relation between $V_n(x,y)$ and $e^{M_n x}$, so we prove the following auxiliary result.

Lemma 3.2. For every nonnegative integer k, the entries of the matrix M_n^k are given by

$$(M_n^k)_{i,j} = \begin{cases} \dfrac{v_j}{v_i}, & \text{if } i = j + k \\ 0, & \text{otherwise.} \end{cases}$$

Theorem 3.3. For $n \in \mathbb{N}$ and $x \in \mathbb{R}$, we have

$$(V_n^{-1}(0,1)V_n(x,1))_{i,j} = (i-j)! \, (e^{M_n x})_{i,j}.$$

Proof. Suppose that there is a matrix Y_n such that $(V_n^{-1}(0,1)V_n(x,1))_{i,j} = (i-j)! \, (e^{M_n x})_{i,j}$. Then we have

$$\frac{d}{dx}(V_n^{-1}(0,1)V_n(x,1))_{i,j} = Y_n(i-j)(e^{Y_n x})_{i,j} = Y_n(V_n^{-1}(0,1)V_n(x,1))_{i,j}$$

and so

$$\frac{d}{dx}(V_n^{-1}(0,1)V_n(x,1))_{i,j}\Big|_{x=0} = Y_n.$$

Thus, there is at most one matrix Y_n such that $(V_n^{-1}(0,1)V_n(x,1))_{i,j} = (i-j)! \, (e^{Y_n x})_{i,j}$. It can be easily seen that $Y_n = M_n$, where M_n is the matrix given Definition 1, by calculating $\frac{d}{dx}(V_n^{-1}(0,1)V_n(x,1))_{i,j}\Big|_{x=0}$. We conclude that $M_n^k = 0$ for $n+1 \le k$, thus

$$e^{M_n x} = \sum_{k=0}^{n} M_n^k \frac{x^k}{k!}.$$

For $i < j$, we see that $(e^{M_n x})_{i,j} = 0$ and we also have $(e^{M_n x})_{i,i} = 1$. Now, suppose that $i > j$ and let $i = j + k$

$$(e^{M_n x})_{i,j} = (M_n^k)_{i,j} \frac{x^k}{k!} = \frac{v_j}{v_{j+k}} \frac{x^k}{k!} = \frac{1}{k!}(V_n^{-1}(0,1)V_n(x,1))_{i,j}.$$

Example 5. We obtain the matrix $\frac{d}{dx}(V_5^{-1}(0,1)V_5(x,1))$ by taking the derivative of each entry of the matrix $V_5^{-1}(0,1)V_5(x,1)$ with respect to x. Thus,

$$\frac{d}{dx}(V_5^{-1}(0,1)V_5(x,1)) = \begin{bmatrix} 0 & 0 & 0 & 0 & 0 & 0 \\ \frac{1}{3} & 0 & 0 & 0 & 0 & 0 \\ \frac{2}{7}x & \frac{3}{7} & 0 & 0 & 0 & 0 \\ \frac{3}{11}x^2 & \frac{6}{11}x & \frac{7}{11} & 0 & 0 & 0 \\ \frac{4}{21}x^3 & \frac{9}{21}x^2 & \frac{14}{21}x & \frac{11}{21} & 0 & 0 \\ \frac{5}{39}x^4 & \frac{12}{39}x^3 & \frac{21}{39}x^2 & \frac{22}{39}x & \frac{21}{39} & 0 \end{bmatrix},$$

Hence, we have

$$M_5 = V_5^{-1}(0,1)\frac{d}{dx}V_5(x,1)\Big|_{x=0} = \begin{bmatrix} 0 & 0 & 0 & 0 & 0 & 0 \\ \frac{1}{3} & 0 & 0 & 0 & 0 & 0 \\ 0 & \frac{3}{7} & 0 & 0 & 0 & 0 \\ 0 & 0 & \frac{7}{11} & 0 & 0 & 0 \\ 0 & 0 & 0 & \frac{11}{21} & 0 & 0 \\ 0 & 0 & 0 & 0 & \frac{21}{39} & 0 \end{bmatrix}$$

and

$$M_5^2 = \begin{bmatrix} 0 & 0 & 0 & 0 & 0 & 0 \\ 0 & 0 & 0 & 0 & 0 & 0 \\ \frac{1}{7} & 0 & 0 & 0 & 0 & 0 \\ 0 & \frac{3}{11} & 0 & 0 & 0 & 0 \\ 0 & 0 & \frac{7}{21} & 0 & 0 & 0 \\ 0 & 0 & 0 & \frac{11}{39} & 0 & 0 \end{bmatrix}$$

$$M_5^3 = \begin{bmatrix} 0 & 0 & 0 & 0 & 0 & 0 \\ 0 & 0 & 0 & 0 & 0 & 0 \\ 0 & 0 & 0 & 0 & 0 & 0 \\ \dfrac{1}{11} & 0 & 0 & 0 & 0 & 0 \\ 0 & \dfrac{3}{21} & 0 & 0 & 0 & 0 \\ 0 & 0 & \dfrac{7}{39} & 0 & 0 & 0 \end{bmatrix}$$

$$M_5^4 = \begin{bmatrix} 0 & 0 & 0 & 0 & 0 & 0 \\ 0 & 0 & 0 & 0 & 0 & 0 \\ 0 & 0 & 0 & 0 & 0 & 0 \\ 0 & 0 & 0 & 0 & 0 & 0 \\ \dfrac{1}{21} & 0 & 0 & 0 & 0 & 0 \\ 0 & \dfrac{3}{39} & 0 & 0 & 0 & 0 \end{bmatrix}$$

$$M_5^5 = \begin{bmatrix} 0 & 0 & 0 & 0 & 0 & 0 \\ 0 & 0 & 0 & 0 & 0 & 0 \\ 0 & 0 & 0 & 0 & 0 & 0 \\ 0 & 0 & 0 & 0 & 0 & 0 \\ 0 & 0 & 0 & 0 & 0 & 0 \\ \dfrac{1}{39} & 0 & 0 & 0 & 0 & 0 \end{bmatrix}$$

Let M_n be the matrix defined in (4) and $U_n(x) = e^{M_n x}$. At the end of this section, we will find the explicit inverse of the matrix $R_n(x) = [I_n - \lambda U_n(x)]^{-1}$ for a real number λ such that $|\lambda| < 1$. To achieve this, we need the following result.

Lemma 3.3 ([15], Corollary 5.6.16). A matrix A of order n is nonsingular if there is a matrix norm $\|\cdot\|$ such that $\| I - A \| < 1$. If this condition is satisfied,

$$A^{-1} = \sum_{k=0}^{\infty} (I - A)^k.$$

Theorem 3.4. The matrix $R_n(x)$ is defined for real number λ such that $|\lambda| < 1$. The entries of the matrix are

$$(R_n(x))_{i,i} = \frac{1}{1 - \lambda}$$

and

$$(R_n(x))_{i,i} = (U_n(x))_{i,j} Li_{j-i}(\lambda),$$

183

for $i > j$, where $Li_n(z)$ is the polylogarithm function

$$Li_n(z) = \sum_{k=1}^{\infty} \frac{z^k}{k^n}.$$

Proof. By Lemma 3.3, for $|\lambda| < 1$, we have

$$(R_n(x))_{i,i} = \sum_{k=0}^{\infty} (U_n(x))^k \lambda^k = \sum_{k=0}^{\infty} (U_n(xk))_{i,j} \lambda^k = (U_n(x))_{i,j} \sum_{k=0}^{\infty} \lambda^k k^{i-j}.$$

We get the result by writing the sum for $i = j$ and $i > j$.

Example 6.

$$I_4 - \lambda U_4(x) = I_4 - \lambda \begin{bmatrix} 1 & 0 & 0 & 0 & 0 \\ \dfrac{x}{3} & 1 & 0 & 0 & 0 \\ \dfrac{x^2}{14} & \dfrac{3x}{7} & 1 & 0 & 0 \\ \dfrac{x^3}{66} & \dfrac{3x^2}{22} & \dfrac{7x}{11} & 1 & 0 \\ \dfrac{x^4}{528} & \dfrac{3x^3}{132} & \dfrac{7x^2}{44} & \dfrac{11x}{22} & 1 \end{bmatrix} = \begin{bmatrix} 1-\lambda & 0 & 0 & 0 & 0 \\ \dfrac{-\lambda x}{3} & 1-\lambda & 0 & 0 & 0 \\ \dfrac{-\lambda x^2}{14} & \dfrac{-3\lambda x}{7} & 1-\lambda & 0 & 0 \\ \dfrac{-\lambda x^3}{66} & \dfrac{-3\lambda x^2}{22} & \dfrac{-7\lambda x}{11} & 1-\lambda & 0 \\ \dfrac{-\lambda x^4}{528} & \dfrac{-3\lambda x^3}{132} & \dfrac{-7\lambda x^2}{44} & \dfrac{-11\lambda x}{22} & 1-\lambda \end{bmatrix}.$$

The inverse of this matrix equals

$$\begin{bmatrix} \dfrac{1}{1-\lambda} & 0 & 0 & 0 & 0 \\ \dfrac{\lambda x}{3(1-\lambda)^2} & \dfrac{1}{1-\lambda} & 0 & 0 & 0 \\ \dfrac{(\lambda+\lambda^2)x^2}{14(1-\lambda)^3} & \dfrac{3\lambda x}{7(1-\lambda)^2} & \dfrac{1}{1-\lambda} & 0 & 0 \\ \dfrac{(\lambda+4\lambda^2+\lambda^3)x^3}{66(1-\lambda)^4} & \dfrac{(\lambda+\lambda^2)3x^2}{22(1-\lambda)3} & \dfrac{7\lambda x}{11(1-\lambda)^2} & \dfrac{1}{1-\lambda} & 0 \\ \dfrac{(\lambda+11\lambda^2+11\lambda^3+\lambda^4)x^4}{528(1-\lambda)^5} & \dfrac{(\lambda+4\lambda^2+\lambda^3)3x^3}{132(1-\lambda)^4} & \dfrac{(\lambda+\lambda^2)7x^2}{44(1-\lambda)^3} & \dfrac{11\lambda x}{22(1-\lambda)^2} & \dfrac{1}{1-\lambda} \end{bmatrix}.$$

Conflict of Interest

There is no conflict of interest between the authors.

Authors contributions

All authors contributed equally.

Statement of Research and Publication Ethics

The study is complied with research and publication ethics.

REFERENCES

[1] M. Bayat and H. Teimoori, "The linear algebra of the generalized Pascal functional matrix", *Linear Algebra Appl.*, vol. 295, pp. 81-89, 1999.

[2] M. Bayat and H. Teimoori, "Pascal k-eliminated functional matrix and its property", *Linear Algebra Appl., vol.* 308 no. (1-3), pp. 65-75, 2000.

[3] G. S. Call and D. J. Velleman, "Pascal matrices", *Amer. Math. Monthly*, vol. 100, pp. 372-376, 1993.

[4] M. Catalani, "Identities for Tribonacci-related sequences", arXiv:math/0209179, https://doi.org/10.48550/arXiv.math/0209179

[5] E. Choi, "Modular Tribonacci numbers by matrix method", *J. Korean Soc. Math. Educ. Ser. B Pure Appl. Math.*, vol. 20, pp. 207-221, 2013.

[6] S. V. Devbhadra, "Some Tribonacci identities", *Math. Today*, vol. 27, pp. 1-9, 2011.

[7] A. Edelman and G. Strang, "Pascal matrices", *Amer. Math. Monthly*, vol. 111 no. 3, pp. 189-197, 2004.

[8] S. Falcon, and A. Plaza, "On the Fibonacci k-numbers", *Chaos, Solitons & Fractals*, vol. 32, pp. 1615-1624, 2007.

[9] S. Falcon, "On the k-Lucas Numbers", *International Journal of Contemporary Mathematical Sciences*, vol. 6 no. 21, pp. 1039-1050, 2011.

[10] M. Feinberg, "Fibonacci-Tribonacci", *Fibonacci Quart.*, vol. 1, pp. 71-74, 1963.

[11] R.Frontczak, "Sums of Tribonacci and Tribonacci-Lucas Numbers", *International Journal of Mathematical Analysis*, vol. 12 no. 1, pp. 19-24, 2018.

[12] A. F. Horadam, "Basic properties of a certain generalized sequence of numbers", *Fibonacci Quart.*, vol. 3, pp. 161-176, 1965.

[13] A. F. Horadam, "Special properties of the sequence $W_n(a, b;\ p, q)$", *Fibonacci Quart.*, vol. 5 no. 5, pp. 424-434, 1967.

[14] A. F. Horadam, "Jacobsthal representation numbers", *Fibonacci Quart.*, vol. 34 no. 1, 40-53, 1996.

[15] R. A. Horn and C. R. Johnson, "Matrix Analysis", Cambridge University Press, Cambridge, New York, New Rochelle, Melbourne, Sydney, Second Edition, 2013.

[16] F. T. Howard, "A Fibonacci Identity", *Fibonacci Quart.*, vol. 39, 352-357, 2001.

[17] D. Kalman and R. Mena, "The Fibonacci numbers-exposed", *Math. Mag.*, vol. 76 no. 3, 167-181, 2003.

[18] M. Karakas, "Some inclusion results for the new Tribonacci-Lucas matrix", *Bitlis Eren University Journal of Science and Technology*, vol. 11 no. 2, 76-81, 2021.

[19] C. Kızılateş, N. Terzioğlu, "On r-min and r-max matrices", *Journal of Applied Mathematics and Computing*, 1-30, 2022.

[20] E. Kilic, "Tribonacci Sequences with Certain Indices and Their Sums", *Ars Combinatoria*, vol. 86, 13-22, 2008.

[21] E. Kilic and T. Arikan, "Studying new generalizations of Max-Min matrices with a novel approach", *Turkish Journal of Mathematics*, vol. 43 no. 4, 2010-2024, 2019.

[22] G. Kizilaslan, "The Linear Algebra of a Generalized Tribonacci Matrix", *Commun. Fac. Sci. Univ. Ank. Ser. A1 Math. Stat.*, vol. 72 no. 1, 169-181, 2023.

[23] J. Li, Z. Jiang, and F. Lu, "Determinants, Norms, and the Spread of Circulant Matrices with Tribonacci and Generalized Lucas Numbers", *Abstract and Applied Analysis*, vol. 4, 1-9, 2014.

[24] S. Pethe, "Some identities for Tribonacci sequences", *Fibonacci Quart.*, vol. 26, 144-151, 1988.

[25] T. Piezas, "A tale of four constants", https://sites.google.com/site/tpiezas/0012

[26] A. Scott, T. Delaney, V. Hoggatt JR, "The Tribonacci sequence", *Fibonacci Quart.*, vol. 15, 193-200, 1977.

[27] W. Spickerman, "Binet's formula for the Tribonacci sequence", *Fibonacci Quart.*, vol. 20, 118-120, 1982.

[28] Y. Tasyurdu, "On the Sums of Tribonacci and Tribonacci-Lucas Numbers", *Applied Mathematical Sciences*, vol. 13 no. 24, 1201-1208, 2019.

[29] R. Williamson, H. Trotter, Multivariable Mathematics, second edition, Prentice-Hall, 1979.

[30] C. C. Yalavigi, "Properties of Tribonacci numbers", *Fibonacci Quart.*, vol. 10 no. 3, 231-246, 1972.

[31] T. Yaying and B. Hazarika, "On sequence spaces defined by the domain of a regular tribonacci matrix", *Mathematica Slovaca*, vol. 70 no. 3, 697-706, 2020.

[32] Z. Zhang, "The linear algebra of the generalized Pascal matrix", *Linear Algebra Appl.*, vol. 250, 51-60, 1997.

Noccaea anatolica SP. NOV. (BRASSICACEAE): A NEW SPECIES FROM EASTERN ANATOLIA, TÜRKİYE

Abdurrahman SEFALI[1],* (iD), Yakup YAPAR[2] (iD), İbrahim DEMİR[3] (iD)

[1] *Bayburt University, Faculty of Education, Department of Primary Education (Basic Education), Bayburt, Türkiye, asef4petal@gmail.com,*
[2] *Bingöl University, Department of Molecular Biology and Genetics, 12000 Bingöl, Türkiye, yyapar@bingol.edu.tr*
[3] *Bitlis Eren University, Department of Biology, Faculty of Arts and Sciences, Bitlis, Türkiye, hosap65@gmail.com*
*** Corresponding author*

ABSTRACT

Noccaea anatolica sp. nov. (Brassicaceae) is described and illustrated as a new species from Van Province in eastern Anatolia, Türkiye. Diagnostic morphological characteristics, a full description, detailed illustrations, and a distribution map are provided. It is morphologically similar to *Noccaea sintenisii* and *Noccaea valerianoides* but easily differs from these species by its fruit shape, seed characters, basal leaf shape, and also general habit.

1 INTRODUCTION

Although *Thlaspi* L. was first used by Linnaeus [1], Moench [2] first discussed the *Noccaea* Moench under the *Thlaspi*. After that, Meyer [3, 4] revised, based mostly on seed coat anatomy and embryonic aspect, and placed most of the older *Thlaspi* species in the genus *Noccaea*. Molecular evidence confirming Meyer's finding phylogenetically has been published [5, 6]. Since Meyer [3] began working on the genus *Thlaspi* in the early 1970s, he has consistently published a number of monographs on all his new genera (*Microthlaspi* Meyer, *Thlaspiceras* Meyer, *Noccidium* Meyer, *Kotschyella* Meyer, *Callothlaspi* Meyer, *Raparia* Meyer, *Atropatenia* Meyer, *Vania* Meyer, and *Masmenia* Meyer). A comprehensive volume focusing on *Noccaea* has been presented [7]. Recent floristic studies [8, 9, 10] have accepted that *Noccaea* is different from *Thlaspi*. Meyer [7] defined *Noccaea* as having 4 sections and 67 species. Although various improvements have been made to solve the taxonomic problems of *Noccaea*, complexity remains [11].

With the first revision of *Thlaspi* in Türkiye, 25 species and 2 subsp. records identified for Türkiye [12]. Since then, 26 new *Thlaspi* taxa, including subspecies, have been added [13, 14, 15, 16, 17]. Additionally, some anatomy and pollen morphology studies have been conducted on the genus [18, 19]. According to the study conducted by Al-Shehbaz [20], 51 *Noccaea* species grow naturally in Türkiye, and Mutlu [21] reported that there were 16 species according to the study [22].

The authors observed an interesting *Noccaea* population during a botanical trip in July 2021 to the Ispiriz Mountain, located in the Van-Başkale district. The authors noticed that this population has wide and semitriangular basal leaves. All examinations show that this population is distinct from all known species distributed in Türkiye and the neighboring countries (especially Iranian species).

2 MATERIAL AND METHODS

The material for the new species collected in Van province in the Eastern Anatolia region in 2022. Plants deposited at the Bingöl University Herbarium (BIN). We compared these specimens with relevant taxonomic literature [20, 16, 12, 14, 7, 17, 23] and with specimens held in the herbaria of E, B, and K (acronyms according

to Thiers [24]. Detailed morphological measurements performed using a stereo microscope (Leica EZ4). And the new species compared to the features of the closely related *Noccaea sintenisii* and *N. valerianoides*. During field studies, photographs of the living material of the new species and its related taxa taken with a Canon 60D digital camera. The general terminology used by Baytop [25].
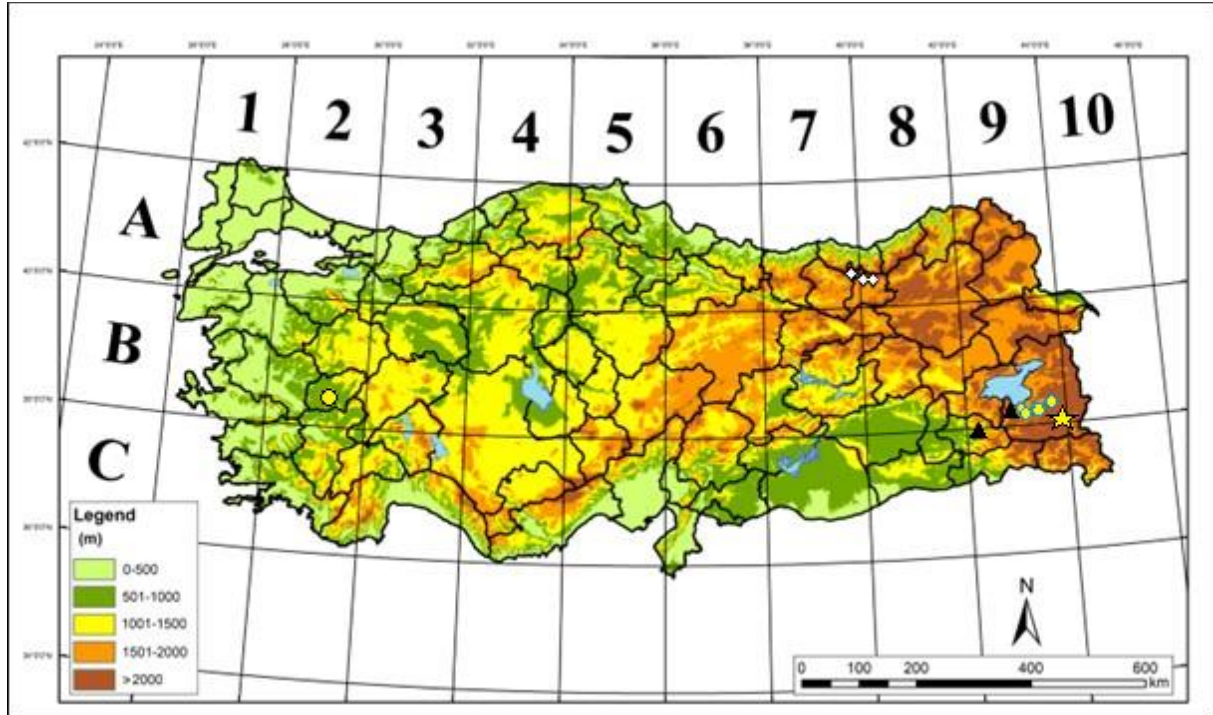
Figure 1. *Distribution map of Noccaea anatolica (☆), N. sintenisii (◊), N. valerianoides (▲), N. papillosa (◉) and N. kurdica (◉).*

3   RESULTS AND DISCUSSION

Noccaea anatolica Sefalı, Yapar & Demir sp. nova (Figures 2-4).

Type:—TÜRKİYE. Van: Başkale, Southern slopes of Ispiriz Mountain, stony places, 3500 m a.s.l., 13.07.2021, *A. Sefalı, Y. Yapar and İ. Demir* 13 (holotype: Bingöl University Herbarium (BIN))

Affinis: — *Noccaea anatolica* is characterized by its wider and semi-triangular basal leaves and wider stem leaves.

3.1 Description

Perennial, woody at base, c. 3 cm tall, glaucous, glabrous throughout. Stems erect, simple with sterile shoots. Basal leaves rosulate; sessile; spathulate or spathulate to elliptic. Margin entire sometimes with two angles near apex or semi triangular, 6–13×3–5 mm. Cauline leaves, sessile, a few, oblong, shortly auriculate, 6-10×c. 5 mm. Racemes ebracteate, lax 5–15 flowered, sterile fruit present, in fruit to 1.5 cm long. Fruiting pedicels 8 mm long (the bottom), slender, divaricate, straight, horizontal. Flowers unknown, probably white. When looking some dried flowers. Fruit slightly compressed, ovate, apex obtuse, basal truncate to obtuse, widest slightly basal, 7–8×3–4 mm, wingless, apical notch absent, style filiform, c. 1 mm long. Seeds yellowish brown, narrowly ovate, 2.5–3×1.4 mm, 1 in each loculus.

Flowering time:— June

Fruiting time:— July

Etymology:— The new species epithet is anatolica (in Turkish, Anadolu), refers to Anatolia, the Asian part of Türkiye.

3.2 Distribution and Ecology

Noccaea anatolica grows in stony and mobile slopes of the Ispiriz Mountain (Başkale, Van province), at 3500-3700 m (summit) a.s.l., together with *Allium oreophilum* C.A. Mey., *Androsace caduca* Ovcz., *Centaurea poluninii* Wagenitz, *Chondrilla spinosa* Lamond & V.A. Matthews, *Pastinaca vanensis* Demir, Sefalı & Yapar, *Didymophysa aucheri* Boiss., *Euprasia* sp., *Noccaea kurdica* (Hedge) Al-Shehbaz, *Draba* sp., *Vavilovia formosa* (Steven) Al. Fed. etc.

3.3 Conservation Status

According to IUCN [26] criteria, *Noccaea anatolica* should be labeled as "Critically Endangered" [CR B2ab(i, ii, iii)]. The area of occupancy estimated to be less than 10 km^2, and the number of mature individuals was about 50 in total.

3.4   Taxonomic Relationships

Noccaea anatolica is closely related to *N. sintenisii* and *N. valerianoides* about the general habit. It differs from the *N. sintenisii* and *N. valerianoides* basal leaves in shape, cauline leaf number, inflorescence density, fruit shape and length, and seed color and shape.

In the Flora of Turkey [12], *N. sintenisii* and *N. valerianoides* belong to the *Thlaspi* genus, sect. *Apterygium* Ledeb. This section had four species (*T. papillosum* Boiss., *T. sintenisii* Hausskn. Ex Bornm., *T. kurdicum* Hedge, and *T. valerianoides* Rech.) in Türkiye. These species have general fruit futures such as silicula, entire, acute at apex, not or slightly winged, and high alpine perennials. Therefore, the new species comprises not only *N. sintenisii* and *N. valerianoides* but also *N. papillosa* and *Noccaea kurdica*. *N. papillosa* has papillose on some leaf margins. *N. anatolica* throughoutly glabrose. *N. kurdica* has narrowly linear basal leaves, even though the new species has spathulate or spathulate to elliptic basal leaves. In addition, the fruit shape is quite different from this species.

Noccaea rubescens (Schott & Kotschy ex Boiss.) F.K.Mey. seems in a doctoral dissertation, "Revision of *Noccaea* Sensu Meyer Taxa Growing in Turkey" [23]. This species clearly differs from the new species in the petiolate basal leaves, elongating fruit, and cuneate base of fruit futures. *N. sintenisii* and *N. valerianoides* are closely related species and evaluated in the genus *Noccaea* in the last study [11]. Therefore, the new species (*N. anatolica*) described here appears to belong to the genus *Noccaea*.

In general, it can be seen that *N. anatolica* is more dwarf than related species and has more succulent rosette basal leaves. Considering the geographical distribution, it has been determined that *N. sintenisii* spreads in the northeastern and western regions, but *N. anatolica* is located in the eastern part of Türkiye.

Table 1. Morphological and habitat differences between Noccaea anatolica, N. sintenisii and N. valerianoides.

Characters	*Noccaea anatolica*	N. sintenisii	N. valerianoides
Plant height	c. 3 cm	c. 9 cm	c. 5 cm
Basal leaves size	6-13×3-5 mm.	10-22×4-6 mm.	4-15×c. 1-1.5 mm,
Basal leaves shape	Sessile, spathulate or spathulate to elliptic. Margin entire sometimes with two angles near apex or semi triangular.	Petiolate (c. 8 mm), oblanceolate, oblong-spathulate or obovate,	Petiolate (c. 12 mm), spatulate, apex obtuse. Margin entire.
Stem leaves	6-10×c. 5 mm. Sessile, a few, oblong, shortly auriculate.	3.5-12×1.5-7 mm. Sessile, a few, not or scarcely auriculate.	6-13×c. 5 mm. Sessile, dense, oblong, shortly auriculate.
Inflorescence	Lax, 5-15 flowered. Sterile fruit present.	Dense, 8-25 flowered. Sterile fruit absent.	Capitate, 8-15 flowered.
Pedicel length (the bottom)	8 mm	10 mm	6 mm
Fruit length	7-8×3-4 mm	5-9×c.5 mm	7-13.5×2-3 mm
Fruit shape	Slightly compressed, ovate, apex obtuse, basal truncate to obtuse.	Slightly compressed, oblong, attenuate at both ends.	Slightly compressed, linear-lanceolate to oblong, cuneate at both ends.
Stylus length	c. 1 mm	c. 2 mm	c. 1.5 mm
Seed characteristics	2.5-3×1.4 mm. Yellowish brown, narrowly ovate. 1 in each loculus.	2.2-2.7×1.5-1.8 mm. Reddish brown, ovate or ovate to elliptic. 2 in each loculus	2-2.5×1.25-1.5 mm. Greenish brown, ovate. 2 in each loculus
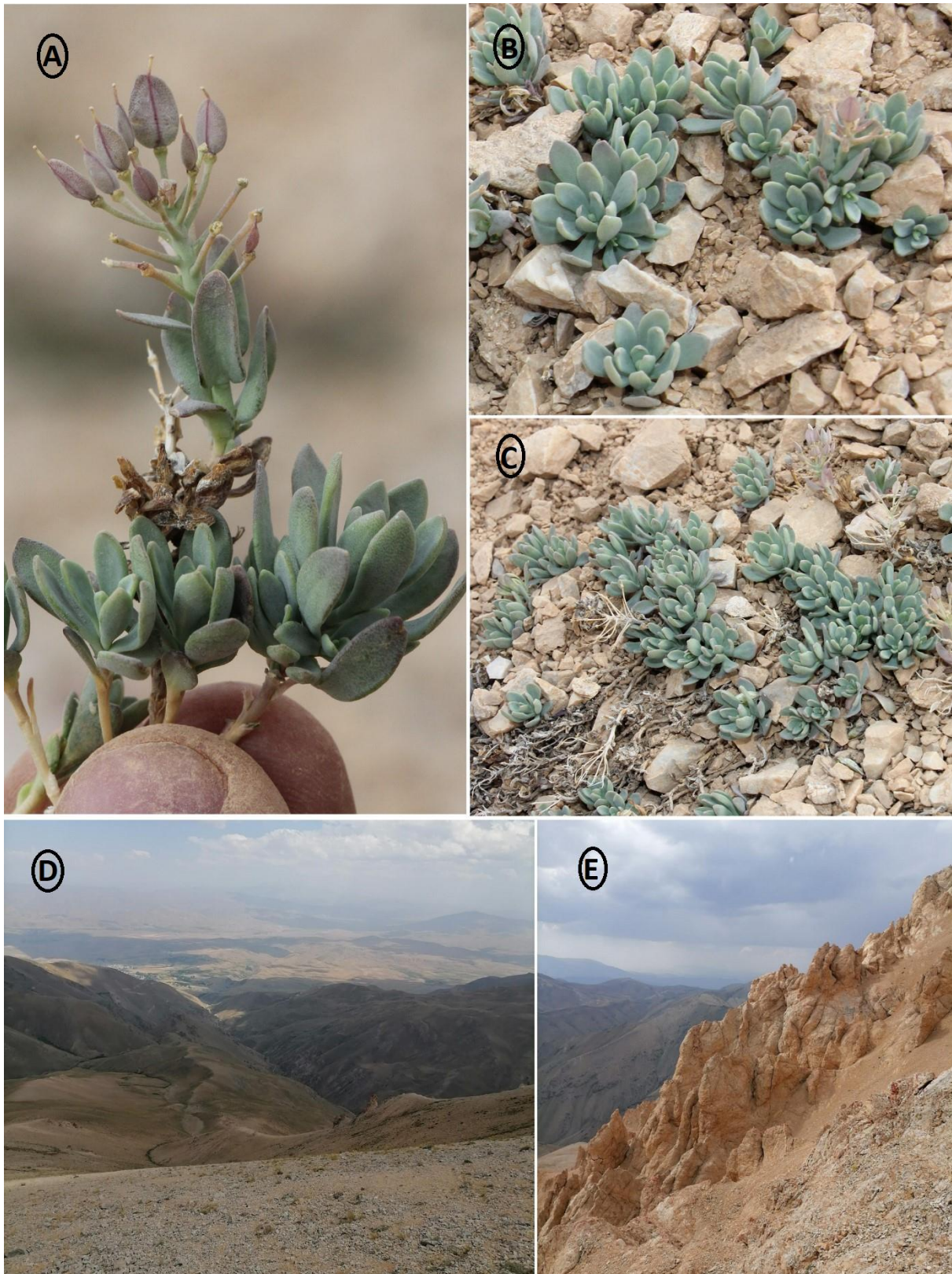
Figure 2. *Noccaea anatolica*: A.-C. habitus, D. habitat and E. Summit of Ispiriz Mountain.
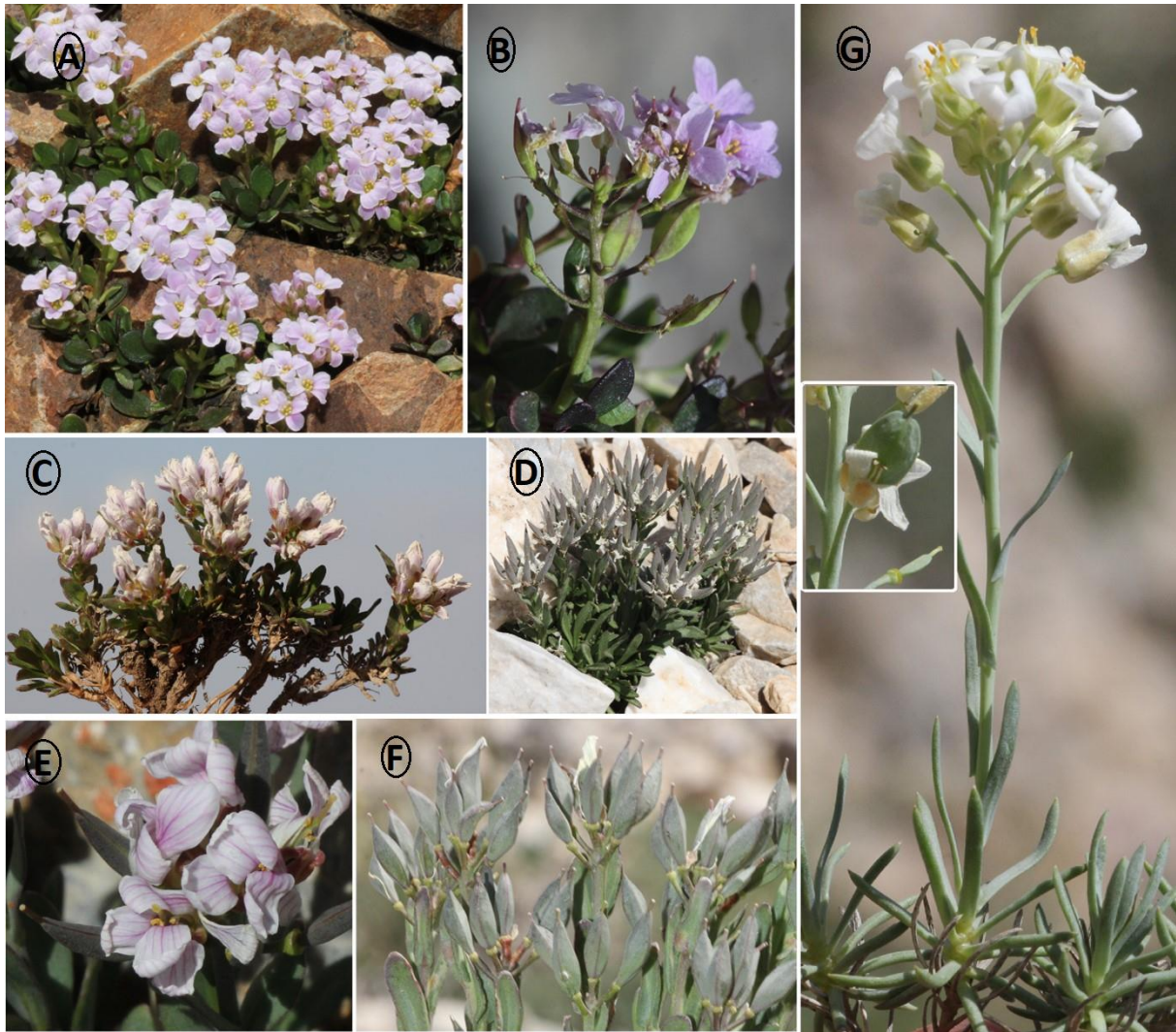
Figure 3. Compared related species in their habitat: A-B. *Noccaea sintenisii*, C-F. *N. valerianoides* and G. *N. kurdica*.
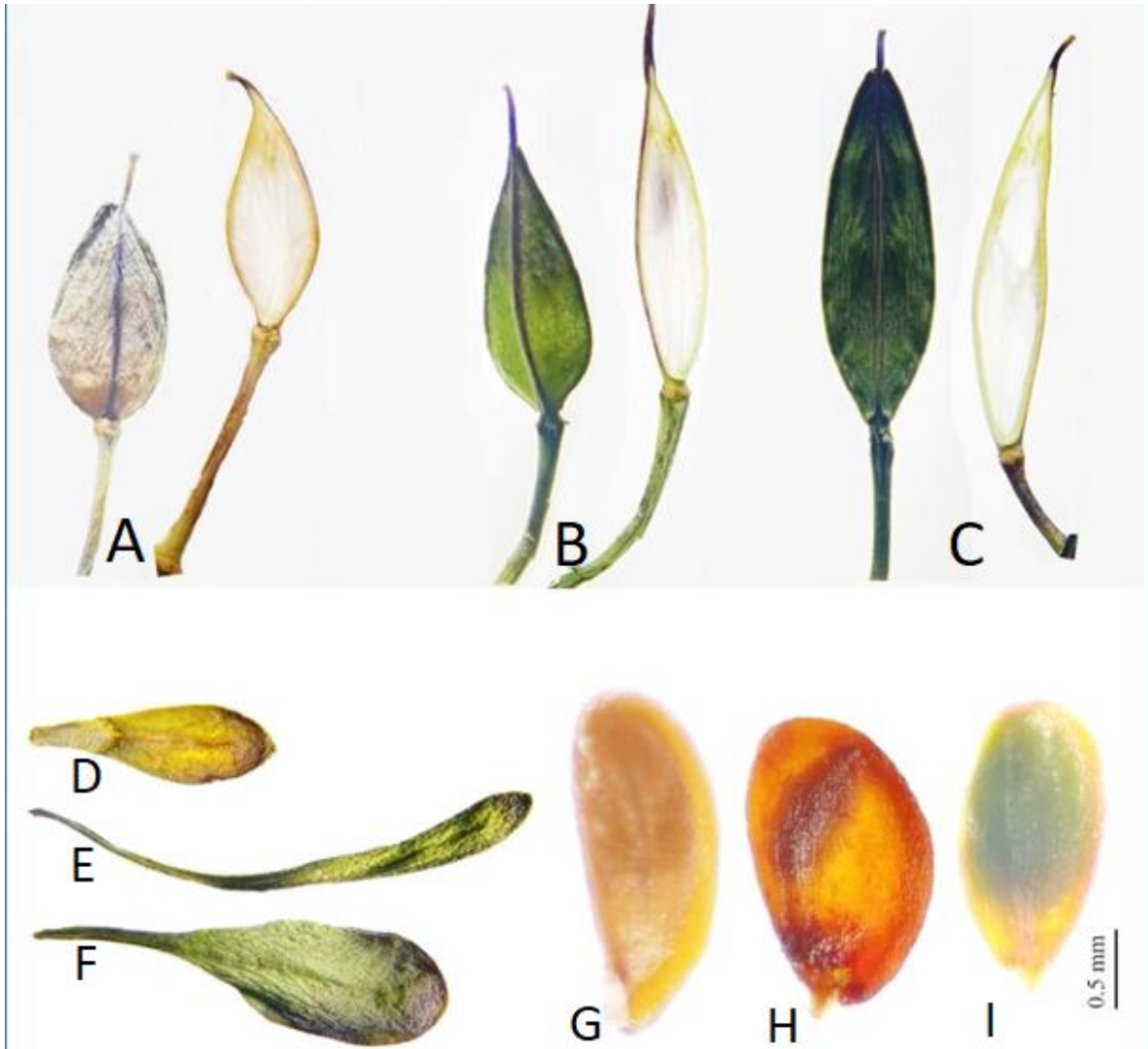
Figure 4. Fruit, seed and basal leaves: **A**. Fruit and septum of *N. anatolica*, **B**. Fruit and septum of *N. sintenisii* and **C**. Fruit and septum of *N. valerianoides*: Basal leaves **D**. *N. anatolica*, **E**. *N. sintenisii*, **F**. *N. valerianoides*; Seeds **G**. *N. anatolica*, **H**. *N. valerianoides*, **I**. *N. sintenisii*.

3.5 Selected Specimens Examined

Noccaea anatolica –TÜRKİYE. Van: Başkale, Southern slopes of Ispiriz Mountain, stony places, 3500 m a.s.l., 13.07.2021, *A. Sefalı, Y. Yapar* and *İ. Demir* 13 (holotype: Bingöl University Herbarium (BIN)).

Noccaea sintenisii –TÜRKİYE. Gümüşhane, Karagöl Mountain, E00376257, B 10 0249982, K000484322; Bayburt: Anzer Mountain, near the summit, stony and mobile slopes, 3100 m of elevation, 10 July 2023, *A. Sefalı, Y. Yapar* and *İ. Demir* 51 (BIN).

Noccaea valerianoides –TÜRKİYE. Van, Artos Dağı, E00059923 (as Vania kurdica (Hedge) F.K. Mey.): Artos Mountain, near the summit, 3250 m of elevation, 03 July 2023, *A. Sefalı, Y. Yapar* and *İ. Demir* 32 (BIN).

Noccaea kurdica –TÜRKİYE. Van, Artos Mountain, near the summit, 3250 m of elevation, 03 July 2023, *A. Sefalı, Y. Yapar* and *İ. Demir* 29 (BIN).

Conflict of Interest

There is no conflict of interest between the authors.

Authors contributions

All authors contributed equally.

Statement of Research and Publication Ethics

The study is complied with research and publication ethics.

REFERENCES

[1]. C. Linnaeus, "Exhibentes plantas rite cognitas, ad genera relatas, cum differentiis specificis, nominibus trivialibus, synonymis selectis, locis natalibus, secundum systema sexuale digestas," in *Species Plantarum* Stockholm, Sweden: Impensis Laurentii Salvii, 1753, pp. 1200.

[2]. C. Moench, "Supplementum ad Methodum Plantas a Staminum situ Describendi," *In Officina Nova Libraria Academiae,* Marburgi Cattorum, Germany: In Officina Nova Libraria Academiae, 1802, pp. 328.

[3]. F.K. Meyer, 'Conspectus der "Thlaspi', *Arten Europas, Afrikas und Vorderasiens. Feddes Repert,* vol. 84, pp. 449–470. . 1753. doi: 10.1002/fedr.19730840503.

[4]. F.K. Meyer, 'Kritische Revision der Thlaspi', *Arten Europas, Afrikas und Vorderasiens, I. Geschichte, Morphologie und Chorologie. Feddes Repert,* vol. 90, 129–154, 1979, doi: 10.1002/fedr.19790900302

[5]. K. Mummenhoff and M. Koch, 'Chloroplast DNA restriction site variation and phylogenetic relationships in the genus Thlaspi sensu lato (Brassicaceae).' *Syst. Bot*., vol. 19, 73–88. 1994, doi: 10.2307/2419713

[6]. K. Zunk, K. Mummenhoff, M. Koch H. Hurka, 'Phylogenetic relationships of Thlaspi s.l. (subtribe Thlaspidinae, Lepidieae) and allied genera based on chloroplast DNA restriction site variation.' *Theor. Appl. Genet*. Vol. 92, 375–381. 1996. doi: 10.1007/BF00223682

[7]. FK. Meyer, 'Kritische Revision der "Thlaspi', *Arten Europas, Afrikas und Vorderasiens. Spezieller Teil. IX. Noccaea Moench. Haussknechtia*, vol.12, 1–343. 2006.

[8]. I.A. Al-Shehbaz, 'A generic and tribal synopsis of the Brassicaceae (Cruciferae)', *Taxon,* vol. 61, 931–954, 2012a.

[9]. I.A. Al-Shehbaz, 'Brassicaceae' in *Flora of Argentina, Vol. 8*. A.M. Anton and F. O. Zuloaga, eds., Buenos Aires, Argentina, 2012b, pp. 273.

[10]. I.A. Al-Shehbaz, and M.F. Watson, 'Cruciferae (Brassicaceae)' in: *Flora of Nepal. Vol. 3*. F. Watson, S. Akiyama, H. Ikeda, C. A. Pendry, K. R. Rajbanadri and K. K. Shrestha, Edinburgh, UK:2011, pp. 108–181

[11]. B. Özüdoğru, K. Özgişi, B. Tarıkahya, A. Ocak, K, Mummenhoff, and I.A. Al-Shehbaz, 'Phylogeny of the Genus Noccaea (Brassicaceae) and a Critical Review of Its Generic Circumscription1, 2.' *Annals of the Missouri Botanical Garden*, vol. 104 no.3, pp. 339-354. 2019.

[12]. IC. Hedge, "Thlaspi," In: *Flora of Turkey and East Aegean Islands, Vol. 1*, PH, Davis Ed. Edinburgh, UK: Edinburgh, 1965, pp. 330-341.

[13]. PH. Davis, RR. Mill and K. Tan. "Thlaspi L." In: *Flora of Turkey and the East Aegean Islands (Suppl. 1), Vol. 10*. PH, Davis, Edinburgh, UK: 1988, Edinburgh pp. 39-47.

[14]. Y. Gemici and E. Leblebici, 'Seven new species for the Flora of Turkey' *Candollea*, vol 50, pp. 41-50, 1995.

[15]. S. Yıldırımlı, 'A reconstruction of the generic status of Syrenopsis Jaub. and Spach (Brassicaceae) endemic to Turkey', *Ot Sistematik Botanik Dergisi*, vol. 7, pp. 1-7, 2000.

[16]. Z. Aytaç, B. Nordt and G. Parolly, 'A new species of Noccaea (Brasicaceae) from South Anatolia, Turkey', *Bot J Linn Soc.*, vol. 150, pp. 409-416. 2006.

[17]. K. Özgişi, A. Ocak and B. Özüdoğru, 'Noccaea birolmutlui, a new crucifer species from southwest Anatolia, Turkey', *Phytotaxa*, vol. 345, pp. 59-67, 2018a.

[18]. B. Atasagun, 'Comparative anatomy and pollen morphology of two endemic Noccaea species (Brassicaceae) and their taxonomic significance', *Notulae Botanicae Horti Agrobotanici Cluj-Napoca*, vol. 50, no. 3, pp.12849-12849, 2022.

[19]. B. Yılmaz Çıtak, 'Contribution to Knowledge on The Anatomy of The Genus Noccaea Moench (Brassicaceae) From Türkiye', *Kahramanmaraş Sütçü İmam Üniversitesi Tarım ve Doğa Dergisi*, vol. 25, no. 1, pp. 85-92, 2022. doı: 10.18016/ksutarimdoga.vi.881805.

[20]. IA. Al-Shehbaz, 'A synopsis of the genus Noccaea (Coluteocarpeae, Brassicaceae)', *Harvard Papers in Botany*, vol. 19, pp. 25-51, 2014.

[21]. B. Mutlu, 'Brassicaceae' In: *Türkiye Bitkileri Listesi (Damarlı Bitkiler)*, A. Güner Nezahat Gökyigit Botanik Bahçesi ve Flora Araştırmaları Derneği Yayını, İstanbul, Turkey, pp. 246- 299, 2012.

[22]. SI. Warwick, A. Francis and IA. Al-Shehbaz, IA. 'Brassicaceae: Species checklist and database on CD-Rom', *Plant Syst Evol.*, vol. 259, pp. 249- 258, 2006.

[23]. K. Özgişi, B. Özüdoğru and A. Ocak, 'Contributions to Turkish Flora: Taxonomic and distributional notes on the poorly known Noccaea (Brassicaceae) species', *Phytotaxa,* vol. 346, no. 3, pp. 247–257, 2018b.

[24]. B.M. Thiers, *The Worlds herbaria 2019. A summary report based on data from index herbarium*. May. 2023. [Online]. http://sweetgum.nybg.org/science/ih

[25]. A. Baytop, *İngilizce-Türkçe botanik kılavuzu*, İstanbul Türkiye: 1988

[26]. *IUCN Standards and Petitions Subcommittee 2019. Guidelines for using the IUCN Red List Categories and Criteria. Ver. 14.* May. 2023. [Online]. www.iucnredlist.org/documents/RedListGuidelines.pdf>.

DETERMINATION OF GAS POTENTIAL AND URBAN SOLID WASTE MANAGEMENT IN ELAZIĞ

Zeki ARGUNHAN[1],* iD , Halit Lutfi YÜCEL[2] iD , Cengiz YILDIZ[2] iD

[1] *Bitlis Eren University, Department of Mechanical Engineering,* Türkiye, *zargunhan@beu.edu.tr* ,
argunhanzeki@hotmail.com
[2] *Firat University, Department of Mechanical Engineering,* Türkiye, *hlyucel@firat.edu.tr,*
cyildiz@firat.edu.tr
* *Corresponding author*

ABSTRACT

Solid wastes make the most important environmental problems caused by human all over the world. In recent years, the amount of solid waste has been increasing in Elazığ day by day with rise in the population and industrialization.

The solid waste managing systems contain the methods such as proper storage, recycling, processing the solid waste by means of biological methods (compost), and disposal with thermal methods (burning, gasification, and pyrolysis). Of these methods, the proper storage is the most common one in Elazığ. By time, using up the oxygen within the wastes stored in the proper fields, the storage gas occurs as a result the decay without oxygen (anaerobic) with the help of anaerobic bacteria proliferate in this environment.

In this study, solid waste disposal methods have been investigated for storage gas by giving Elazığ example.

1   INTRODUCTION

Because of rapidly increasing population and changing living conditions, the solid wastes of which volume increase and content change set a threat to human health and environment. Solid wastes are stored improperly especially in the towns; therefore, the microbial cases effect the occurring leakage water negatively due to the gases and smell coming out of it. Every year, 5,2 million people of them 4 million children die of the diseases emerging as a result of canalization and improperly released solid wastes. The city wastes pollute the air, soil and water in a great deal. Today, an average of 2,0 – 4,0 kg garbage is produced per capita in the world [1].

Since solid wastes are produced as a result of various kinds of human activity, their content, characteristics and amount display differences. Even these values change within themselves according to the development level. But waste production, its density and component rates change in relation with development level, geographical structure, weather conditions and social conditions and from country to country and from city to city [2]-[3].

Although the environment problems were first handled in the USA in 1869, they appeared in the fast changing world agenda in the beginning of the 1970s. And they entered in our country's agenda in 1980s [4].

In order to prevent them to harm environment and human health, it has been found out that solid wastes should be recycled and made use of properly. For this reason, determining proper disposal methods is of great importance.

Stored or thrown in the fertile agriculture fields, solid wastes cause the soil and the underground water and rivers to be polluted with the leakage waters, and air to be polluted because of bad smell and gases. When changing environmental problems are together evaluated according to the cities in our country, it is observed that water pollution with 31 %, wastes with 20% and air pollution with 20 % come in the first three pollutions [5].

Economical solutions are produced for urban solid wastes throughout the world. Hence these wastes are made use. Today many researchers and practitioners have focused on solid waste methods. For this purpose, on one hand technologies for

collecting and disposal of waste are developed; on the other hand, the studies to reduce the amount of waste are in progress.

The technologies of evaluating and disposal applied in solid waste management system can be expressed as follows:

- Recycling

- Proper storage

- Thermal transformation technologies

- Burning

- Gasification

- Pyrolysis

- Biological transformation technologies

    - Aerobic composting

    - Anaerobic composting [6].

After becoming aware of the energy value of wastes, the idea to make use of the energy they contain while disposing is becoming more common. Today, there are several plants producing energy from the urban waste in developed countries. When comes to the technologies used to obtain energy from the urban solid wastes,

- Proper storage

- Burning

- Gasification

- Anaerobic decaying processes. Technologies can be seen in (Figure 1) [7]

In this study, the solid waste volumes in Elazığ, Türkiye have been analysed. While these analyses are being carried out, they have been sorted out according to the type of solid waste; and their amount has been identified. Predicted energy values of the gathered values have been found out with the help of the data obtained after the analyses and with the help of bioenergy equations. Therefore, the energy potential of solid waste volume in this region has been tried to be found out.
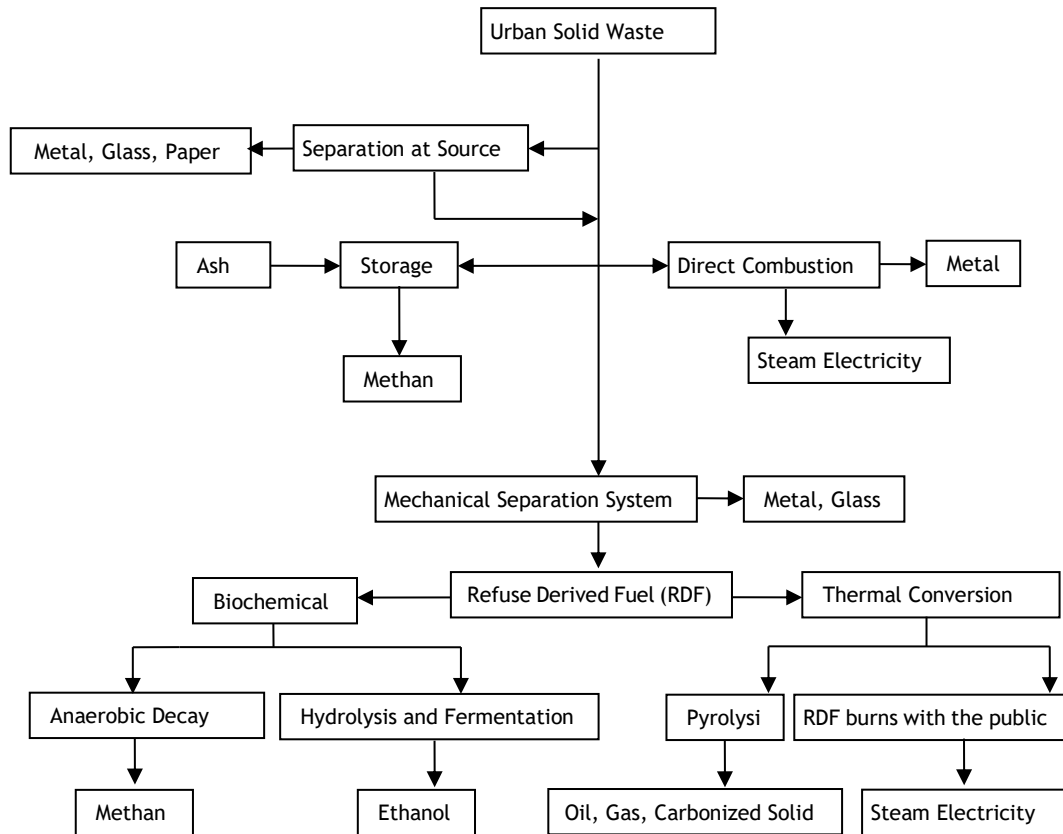
Figure 1. Energy production technologies of urban solid wastes [8].

2 SOLID WASTES

Solid waste is every type of substance and material that do not contain enough liquid to be fluid and become useless as a result of living, social and economic activities of human. The solid wastes can be classified as follows according to their features [9]:

a) Organic waste

b) Inorganic waste

They can be classified as follows according to their sources:

a) Domestic wastes,

b) Industrial wastes,

c) Wastes stemming from the open areas,

d) Agricultural wastes,

e) Wastes stemming from the treatment plants,

f) Special wastes,

g) Dangerous wastes

Urban solid wastes make the biggest part of the solid wastes. The urban solid wastes are of domestic wastes, commercial and institutional wastes, park, garden and bazaar wastes, construction, demolition and excavation wastes, treatment plant wastes and hospital wastes [9].

Table 1. *Urban solid waste sources [6].*

Settlements	Waste produced locations and activities	Solid waste types
Commercial premises	Detached dwellings, low, medium and high apartment buildings and so on.	Food waste, paper, plastic, glass and so on.
Institutions	Shops, restaurants, grocery stores, service stations and so on.	Food waste, paper, plastic, glass metal and hazardous waste
Construction and demolition	Building sites, road construction, restoration and demolition of buildings	Cardboard, food waste, paper, plastic, glass, metal, hazardous waste and special wastes
Urban activities	Parks, gardens, recreational facilities and streets	Waste and special wastes
Treatment plant and incinerator units	Waste water and industrial treatment processes	Treatment plant waste

An average of 60% of the urban solid waste is the waste coming from the houses. In connection with the urbanization ratio, these rates can change [10]. The change according to the area where urban solid wastes occur is given in (Table 2).

Table 2. *Classification of Urban Solid Waste According to Formation Areas [11].*

Sources	Examples
Residential (Single or multi-family waste)	Newspapers, clothing, Disposable products, packaging, PET bottles and cans
Commercial (Wholesale and retail businesses, offices)	Cardboard boxes, wooden materials, office papers, disposable materials
Corporate (Schools, Hospitals, Prisons)	Resting place, cafeterias, classrooms, and medical wastes
Industrial (Packaging, Administrative Affairs)	Paperboard, plastic films, food waste, wood pallets

Generally, by years the solid waste amount that people cause is increasing. Part from these, the waste produced is directly proportional with the population of the cities (U.S). In (Table 3) waste compounds belonging to different countries have been given.

Table 3. Composes of solid wastes for different countries [12].

Component	Amount of Waste Component (%)			
	Türkiye	Western Europe	U.S.	Middle East
Organics	20-90	21,3	22,6	62,3
Paper and cardboard	0,5-15	27,4	45,6	25,3
Plastic	1,5-12	3,1	2,6	5,8
Textile	0,3-5	3,5	4,5	1,4
Glass	0,3-5	9,5	6,2	1,0
Metal	0,3-5	8,5	9,1	2,8
Ash	--	19,8	7,6	--
Other	--	6,9	1,8	1,4

In parallel with rapid urbanization, changes in living conditions and increasing consuming tendencies, a constant increase in the amount of solid waste production for per capita is the matter of question. In (Table 4) the daily amount of domestic solid waste in some countries has been displayed.

Table 4. Daily Amount of Domestic Solid Waste per capita in Some Countries [13].

Country	Amount of Waste (kg / person-day)
Türkiye	0,67
Germany	0,71
U. S.	1,4

Approximately 65 tonnes of waste are produced a day in Türkiye. This amount in our country is very changeable. While it is about 0.25 kg/per person/day in some rural areas, it rises up to 2 -3 kg/per person/day in some settlement places. In (Table 5), the solid waste amounts produced a day for per capita in some countries have been given [14].

Table 5. Amount of solid waste produced a day for per capita in some countries (kg) [14].

Country	Amount of Waste (Kg / person-day)
Developed Countries	
U. S.	**2,17**
England	**1,37**
Middle Income Level Countries	
Mexico	**1,33**
Türkiye	**0,95**
Singapore	**0,87**
Low Income Level Countries	
Indonesia	**0,56**
Pakistan	**0,55**
India	**0,51**

The solid wastes the amounts of which increase each passing day are stored improperly especially in underdeveloped countries and cities, and effect human health negatively due to leakage water, microbial diseases gas and smell outgoing. Therefore, the fact that the solid wastes should be collected effectively and efficiently in the settlement places, and they should be transported, evaluated and made harmless with proper methods are the basic problems that the local governments face.

3 SOLID WASTE MANAGEMENT

As a result of potential risks related to the pollution that solid wastes make up are increasing day by day and the natural sources are gradually decreasing, solid waste management has gained a complex structure. Although a lot of definitions have been made about solid waste management, in general sense, solid waste management is determining, application and improvement of an efficient and economical serving system with the aim that all kinds of solid waste should not give any harm to soil, water and air, and they should not spoil animal and plant kingdom, natural wealth and ecological balance, and they should be collected, carried, stored and purified or disposed in the shortest time under healthy conditions [15]

An efficient solid waste management contains six basic features, such as;

- Generation of waste
- Classification, accumulating, selecting and processing in the source
- Collecting
- Transporting and transfer
- Separating, processing and transformation
- Final disposal

In (Figure 2), integrated solid waste management current diagram has been given.
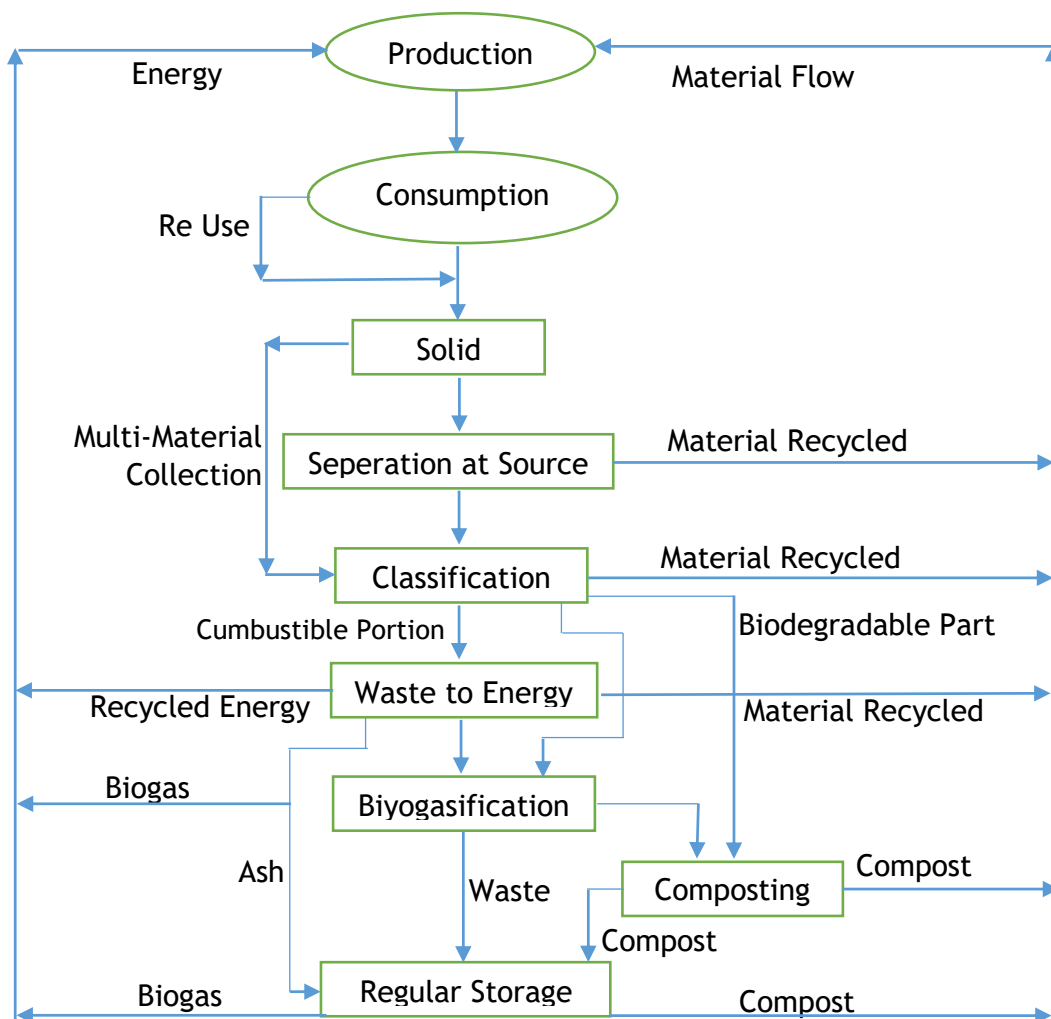
Figure 2. *Integrated solid waste management current diagram [16].*

In the feasibility of a technically efficient solid waste management system, the following parameters should be taken into consideration:

- Determination of the present situation;
- Predictions to the future;
- Accumulation and collecting options:
- Separation, processing, transformation and final disposal [17]

The wastes should be collected and transported by means of efficient methods; after economically recyclable substance groups are taken, the rest should be converted into harmless forms using appropriate methods.

Major solid waste disposal methods used are as follows:

1) Retrieving
2) Proper storage
3) Burning
4) Composting
5) Pyrolysis

The most common methods among these are retrieving, burning, composting and proper storage. In (Table 6), the distribution of solid waste management technologies in various countries can be seen.

Table 6. Distribution of solid waste management technologies percentage in countries [18].

Country	Proper Storage	Incineration	Composting	Recovery
Australia	82	2,5	----	15,5
Canada	80	8	2	10
Germany	46	36	2	16
France	45	42	10	3
Greece	100	---	---	---
Ireland	97	---	---	3
Italy	74	16	7	3
England	88	6	---	6
U. S.	74	16	2	15
Portugal	85	---	15	---
The Netherlands	45	35	5	15
Spain	64	6	17	13

The distribution of waste disposal methods applications in our country is as in the Figure. As can be seen in the figure, the commonly used method in Türkiye is wild storage method with 57.97 %. In (Table 7), the distribution application of waste disposal methods in our country has been given.

Table 7. The distribution of waste disposal methods applications in Türkiye [19].

Disposal Methods	Open Burning	Burial	Pour into the Stream	Uncontrolled Storage	Composting Facility	Proper Storage	Other
(%)	1,37	1,92	0,4	57,97	0,87	33,04	4,44

4   ELAZIĞ PROVINCE SOLID WASTE MANAGEMENT AND STORAGE GAS

With acceleration of migration from rural areas to the urban areas in Türkiye in recent years, Elazığ province has become one of the most populous cities in the East Anatolia Region because of rapid population growth. As in many settlement places of Türkiye, this problem has also reached to serious levels every passing day in Elazığ city centre. Collecting solid wastes, carrying them and disposing them are done efficiently, separating hospital wastes is carried out and they are stored properly.

4.1   Elazığ Population Projection

According to 2009 census, the population of Elazığ city together with provincial towns is 560.000, the city centre population is 375.000. Collecting solid wastes and transporting them are carried out by Elazığ Municipality Sanitation Department. For the resource about Elazığ solid waste collecting, Elazığ Municipality Sanitation Department data were used.

The population of Elazığ was found as 392722 in 2010 due to increase in migration and in population projection this was taken into consideration.

The population growth coefficient is calculated by means following equation:

$$P = \left(\sqrt[a]{\frac{N_y}{N_e}} - 1 \right) 100 \tag{1}$$

P =Population growth coefficient

a =Duration passing between two population census (year)

N_y =New population value of the settlement place

N_e =Ex population value of the settlement place

By making use of Bank of Provinces, population growth coefficient is calculated as P=2.678 %. According to this, the next ten-year projection of Elazığ province has been found as follows.

Population calculation is done by means of following equation:

$$N_y = N_e * \left(1 + \frac{P}{100}\right)^n \tag{2}$$

Ny = New population value of the settlement place

Ne = Ex population value of the settlement place

P = Population growth coefficient

Target duration of the project has been determined as 10 years, and the population changes within 10 years have been calculated taking 2.678 as population growth coefficient (Table 8)

Table 8. Elazığ Population Projection Prediction.

Duration (year)	Year	Population (person)
0	2010	392722
1	2011	403239
2	2012	414037
3	2013	425125
4	2014	436510
5	2015	448200
6	2016	460203
7	2017	472527
8	2018	485181
9	2019	498174
10	2020	511515

4.2   Province Solid Waste Calculation

Following parameters were taken basically in originating solid wastes related to population. Solid waste originating per capita is 1.20 kg/day. Rate of waste pressing in solid waste proper storage field is 0.65 tonnes/m³.

Calculations made taking these parameters into consideration show that there will be 1211800 tons or 1743695 m³ of solid waste during the 10-year period. The calculated solid waste amount is given in (Table 9) and the change in the total waste amount over the years is given in (Figure 3).

Table 9. Amount of Waste for the Coming Years, Depending on the Population.

Duration (years)	Years	Population	The amount of waste per Capita (kg/person-day)	The amount of waste (tons/day)	Total (tons/year)	The amount of waste (m³/year)	Total (m³)
0	2010	392722	1.20	471	171915	264484	264484
1	2011	403239	1.20	483	384210	271223	535707
2	2012	414037	1.20	496	529250	278523	814230
3	2013	425125	1.20	510	710400	286384	1100614
4	2014	436510	1.20	523	901295	293684	1394298
5	2015	448200	1.20	537	1097300	301546	1695844
6	2016	460203	1.20	552	1298780	309969	2005813
7	2017	472527	1.20	567	1505735	318392	2324205
8	2018	485181	1.20	582	1718165	326815	2651020
9	2019	498174	1.20	597	1936070	335238	2986258
10	2020	511515	1.20	613	2159815	344223	3330481
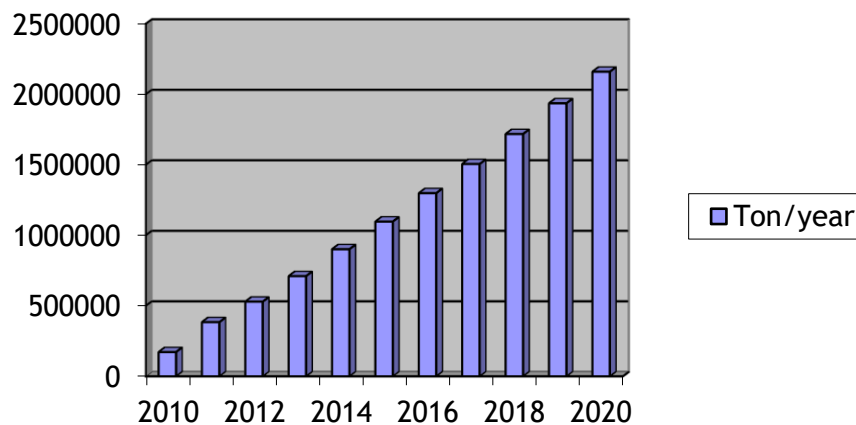
Figure 3. Variation of total waste amounts by years.

4.3   Elazığ Solid Waste Proper Storage Field

The solid waste proper storage field of Elazığ is approximately 31 km far from the city centre of Elazığ. The size of the field allocated is 130 hectares. There is waste cell container in the plant. Due to the necessity that the medical wastes should be controlled, sterilization, proper storage and disposal method are used.

4.4   Elazığ Storage Gas Projection

Generating of gas in the solid waste storage field begins nearly after 2 and 6 months. Normally, it is accepted that there is one year between the dates when the solid waste is started to be stored and gas production starts.

During filling up the solid waste proper storage field, especially after completing the final cover, anaerobic reaction starts because there is no access of air into this layer. As a result of this reaction, the organic substances beak into pieces and gases such as CO_2 (carbon dioxide), H, CO, H_2S (hydrogen sulphur) and CH_4 (methane) occur. In order to dispose these gases, gas collecting chimneys are fixed in the solid waste proper storage field. Via gas collecting wells, the gases which will be collected are burned by means of portable gas burning gadgets.

In order that the gas generating potential of Elazığ solid waste storage plant can be calculated, [20] correlation has been used:

$$Gt = 1{,}868 \times Co \times (0{,}014 \times T + 0{,}28) \times (1 - 10^{-kt}) \qquad (1)$$

Gt: The gas volume generated within t time per tonne (m^3/tonne)

Co: The organic carbon content in 1 tonne of waste (kg/tonne-waste). These values are for domestic wastes. They are between 170 and 220, and changes according to carbon content of the waste

T: Temperature (°C). The Temperature values for solid waste storage fields change between 30°C and 35°C.

k: Reduction fixed value. This value is taken as 0,035 – 0,04 for decaying of the organic substances in solid waste proper storage fields for 10-25 years.

t: Duration (year)

Co: 170 kg/ton-waste

T: 30$°$C

k: is taken as 0,035.

Stored gas projection has been done for the acceptance that the solid waste will be properly stored between the years 2010 and 2020. The calculated gas generating potential is given in (Table 10) and stored gas according to the years is given in (Figure 4).

Table 10. Gas Potential of Waste Storage Area for the Years.

Year	Annual waste ton/year	Total waste ton/year	Total Gas m^3/hour	Gas m^3/year	Total Gas m^3/year
2010	171915	171915	337,7806	2958958	2958958
2011	176295	384210	658,0132	5764196	14198094
2012	181040	529250	962,7738	8433898,49	25182936
2013	186150	710400	1253,977	10984841,5	36167777
2014	190895	901295	1531,956	13419938	49587715
2015	196005	1097300	1798,997	15759215	65346930
2016	201480	1298780	2055,225	18003773	83350703
2017	206955	1505735	2302,72	20171824	103522527
2018	212430	1718165	2541,808	22266241	125788768
2019	217905	1936070	2773,142	24292725	150081493
2020	223745	2159815	2558,422	22411774	172493267
2021			2360,327	20676462	193169729
2022			2177,57	19075513	212245242
2023			2008,964	17598524	229843766

In the solid waste disposal plant of Elazığ, the gas can be released to atmosphere after it has been collected (passive system); or, can be burned after it has been collected under control (active system). Disposing the collected gas by burning so eliminating the potential hazard or preventing the danger as much as possible is very important in terms of environment.

As burning options, central burning unit or portable independent burning units are used. For a central burning unit, installing a gas collecting network from gas

collecting wells to the burning unit and establish interval collectors in specific parts are necessary.

The working principle of the burning unit is based on the principle of collecting gas by means of collectors and collecting wells by creating pressure difference and then burning it.
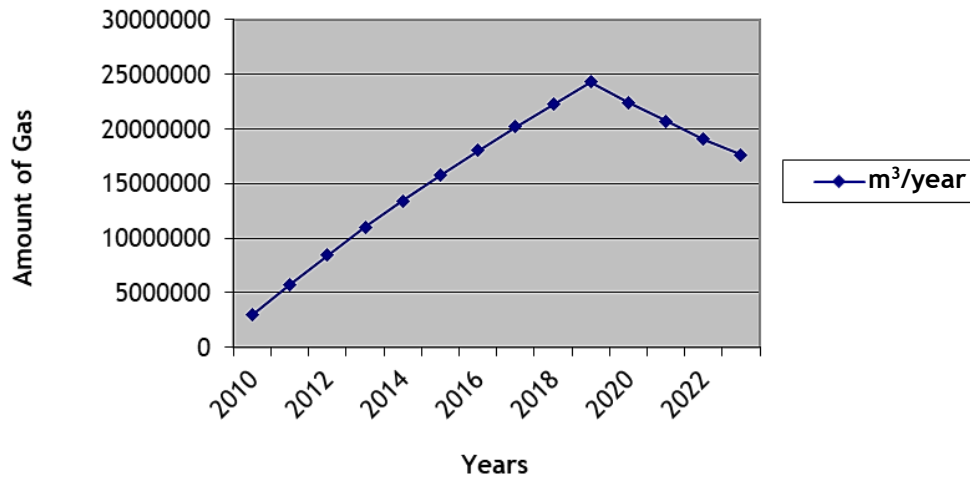
Figure 4. *Change of Storage Gas According to Years.*

5   RESULT

The garbage gas occurring in airless means in the solid waste proper storage fields should certainly be disposed by burning or with the aim of energy production. For this, it is important that an active stored gas system should be established in garbage fields. Every kind of activity towards eliminating the negative effects of stored gas on human health and environment or decreasing its effects is considered in the context of this method.

As seen in the activities in proper storage fields of Elazığ province, it is possible to eliminate the negative effects of storage gas on environment and human health besides making the generated gas economic achievement by utilizing it. Under all these conditions, and as in the example of Elazığ, it has turned out that storage gas management is very important and necessary.

The electric potential of storage gas generated in the proper storage fields has an important potential from the perspective of energy obtaining. Therefore, it

is essential that the local governments search the gas generation in the storage fields and electric production potential and provide contribution to economy.

Taking into account the capacity and emission output of the landfill, contribution to the economy can be made by using the appropriate system (using an internal combustion engine, gas turbine or steam turbine) to generate electricity.

Conflict of Interest

There is no conflict of interest between the authors.

Authors contributions

Halit Lutfi YÜCEL collected the data and evaluated it. Cengiz YILDIZ conceptualized the research. Zeki ARGUNHAN wrote the research article. Finally, Cengiz YILDIZ corrected the mistakes in the article.

Statement of Research and Publication Ethics

The study is complied with research and publication ethics.

REFERENCES

[1] M. Karpuzcu, *Çevre Kirlenmesi ve Kontrolü*, İstanbul, Türkiye: Boğaziçi Üniversitesi Çevre Bilimleri Enstitüs, 1996.

[2] CS. Rao, *Environmental pollution control engineering,* New Delhi, Hindistan: *Wiley*, 1992, pp. 396-414.

[3] M.A. Sufian, and B.K. Bala, *Modelling of electrical energy recovery from urban solid waste system: The case of Dhaka City,* Bangladeş: Renewable Energy, 2006, pp. 1573-1580

[4] H. Ertürk, *Çevre Bilimlerine Giriş*, Bursa, Türkiye: Uludağ Üniversitesi Güçlendirme Vakfı Yayınları, No:10, 1996.

[5] M. Şahin, *Yeni Binyıla Girerken Çevrenin Durumu*, Ankara, Türkiye: Çevre ve İnsan Dergisi, Ekim,Kasım,Aralık 2001.

[6] G.Tchobanoglous, H.Theisen and S.A. Vigil, *Integrated Solid Waste Management: Engineering Principles and Management Issues*, UK: McGrawHill International Editions. 1993.

[7] S. Kumar, "Technology Options For Municipal Solid Waste-To-Energy Project", *TERI Information Monitor on Environmental Science,* volume 5, number 1, pp. 1-11, 2000.

[8] J.V.L. Kiser, and B.K. Burton, "Energy from municipal waste: Picking up where recycling leaves off", *Waste Age*, November 92, 1992.

[9] O. Buenrostro, G. Bocco, and S. Cram, "Classification of Sources of Municipal Solid Wastes in Developing Countries"), *Resources, Conservation and Recycling*, 2001.

[10] A.H. Igoni, M.J. Ayotamuno, S.O.T. Ogaji, and S.D. Probert", Municipal Solid Waste in Port-Harcourt,Nigeria" *Applied Energy*, Volume 84, pp.664-670, 2007.

[11] U.S. *Environmental Protection Agency, Office of Solid Waste Management Programs. Second Report to Congress:* Resource Recovery and Source Reduction (SW-122). 1974.

[12] METU (ODTÜ) *Geoteknik Açıdan Düzenli Katı Atık (Çöp) Depolanması,* Sürekli Eğitim Merkezi, Ankara, Türkiye: 11-12 Nisan 1996.

[13] M. Borat, *Katı Atıkların Yönetimi.* İstanbul Üniversitesi, Mühendislik Fakültesi, Çevre Mühendisliği Bölümü, Türkiye: 1999.

[14] S.O. Benitez, and J.L. Beraud, "The Municipal Solid Waste Cycle in Mexico Final Disposal", *Resources, Conservation and Recyling*, v.39, 2003.

[15] O. Ergun, S. Çoruh, and G. Gökbulut, "Solid Waste Management in The Black Sea Region of Türkiye", *The Kriton Curi Symposiom on Environmental Management in TheMedkerranean Region*, Boğaziçi Üniversitesi, İstanbul, Türkiye. 1998.

[16] Alpan, S. "Katı Atıkların Yönetimi", *T.M.M.O.B., Çevre Mühendisleri Odası, Katı Atık Yönetimi Semineri,* Ankara,Türkiye: Ekim 1998.

[17] A. Demir, B. Özkaya, and F. Avşar, "İstanbul Katı Atık Yönetiminde Kompostlaştırma ve Geri Kazanma", *1. Ulusal Katı Atık Kongresi*, İzmir, Türkiye: 18-21 Nisan 2001.

[18] S. Leao, I. Bishop, and D. Evans, "Assessing the demand of solid waste disposal in Urban Region by urban dinasmc modelling in a GIS environment", *Resources, Conservation and Recycling*, 2001.

[19] Türkiye Statistics Office (TUİK) Haber Bülteni, Sayı:75, Ankara, Türkiye: 30 Nisan 2008.

[20] O.Tabasaran, and G. Rettenberger, *Grundlagen zur Planung von Entgasungsanlagen (Fundamentos Para la Planificación del Equipamiento de Drenaje de Gases de Relleno)* Müllhandbuch Erich Schmidt- Verlag, Berlin, Germany: 1987.

THE INTERACTION BETWEEN ZINC AND CADMIUM IN TERMS OF ANTIOXIDANT AND ANTI-INFLAMMATORY PERSPECTIVES. IS ZINC A NATURAL PROTECTOR?

Fatih Çağlar ÇELİKEZEN[1] (iD)

[1] *Bitlis Eren University, Department of Chemistry, Turkey, celikezen@gmail.com*

ABSTRACT

Cadmium is known as a toxicant for animals and human beings. Despite of its toxic properties it is used in many industrial branches. Thus, people are likely to be exposed to cadmium due to professional and environmental reasons. The underlying mechanisms of cadmium toxication are oxidative stress, oxidative stress-related inflammation and interaction with bio-elements. Many studies have reported a protective role of zinc against cadmium toxication in animals and at cellular levels. Thus, this review focuses on the protective effect of zinc due to its antioxidant and anti-inflammatory effects. In this study, documents analyzing the interaction between Zn and Cd in metabolism were examined.

1 INTRODUCTION

Environmental metal pollution is important because it causes toxic effects in biological systems [1]. Although metals are essential for physiological functions, non-essential metals are harmful to animals and human beings [2,3]. Being one of the non-essential metals, cadmium (Cd) is a highly common metal with high toxicity [4]. Cd is a soft silver-white metal element in group of IIB in periodic table with 112.41 atomic weight. Cd may be present in the pure form or in compounds with oxygen, chlorine and sulfur in the environment [5]. Being a heavy metal, Cd was discovered as an impurity of zinc (Zn) carbonate for the first time. Besides, Cd is a rare element having concentrations of 0.15 mg/kg and $1.1 \times 10{-4}$ mg/L in the earth's crust and seas, respectively [6]. Cd is released into the environment naturally or from industrial, agricultural, and other sources [7].

Cd is used in numerous industrial applications including electroplating, pigments, paint additives, welding, and Ni-Cd batteries [8]. It is stated that Cd may be associated with toxic effects in some tissues and organs including kidneys, liver, lungs, bones, endocrine and reproductive systems [9-11]. Moreover, Cd causes diabetes mellitus [12], cardiovascular diseases [13], and neurodegeneration [14]. It is also identified by International Agency for Research on Cancer (IARC) as a human carcinogen causing development of tumor in the lung, injection site, prostate, and other tissues [15]. In addition, Cd may cause oxidative damage in some tissues that leads to defects in membrane functions [16]. Moreover, heavy metals cause inflammation [17], and thus Cd can induce inflammation in various animals [18,19]. Although human beings are exposed to Cd regularly through foods, there is no identified method for inhibiting or minimizing Cd contamination in foods [20]. However, studies have been still ongoing to reduce the absorption of metals or to reduce Cd toxicity by increasing the antioxidant capacity of metabolism. Remarkably, medical plants and natural antioxidant substances have been found to be beneficial [21]. Furthermore, antioxidant molecules have been suggested to inhibit Cd-induced oxidative damage due to their upregulation features in cellular antioxidant system [22].

Zn, a trace element, has important beneficial functions including cell proliferation, and antioxidant and anti-inflammatory defense and immune system [23,24]. Zn exhibits antioxidant properties because it has a role in cell membrane stabilization, Cu/Zn SOD structure, and metallothionein (MT) induction [25]. Zn treatment may prevent absorption and accumulation of Cd and inhibit adverse actions [26].

The aim of this review is to explain the interactions between Zn and Cd and evaluate possible protective effects of Zn against oxidative damage and inflammation induced by Cd. This study is limited to evaluate the interactions between Zn and Cd in rats.

2   MATERIAL AND METHODS

A systemic review was performed using Science Direct by combining the terms of zinc and cadmium, antioxidant, anti-inflammatory and toxicity terms. The literature review was limited with studies published in English between 2010 and 2023 years. This study focused only on rat-based experimental studies that investigated only Zn supplementation (not in combination with any other metals or agents) as a potential antioxidant/antidote (including MDA, GSH, GPX, SOD, and CAT) and anti-inflammatory (including TNF-α, NF-κB, Interleukin-6, and IL-1ß) effects against Cd-induced oxidative damage. This is because there were only a few in vivo experimental studies except for rat models. At the end of the literature review, approximately 30 studies including experimental studies between 2010–2023 were found. The number of studies on both antioxidant and anti-inflammatory effects is limited. Moreover, according to our knowledge there is no report that shows negative effect of Zn on Cd toxication. Appendix 1 shows the detailed results of the studies used in this work.

3   Cd EXPOSURE

The most important sources of Cd exposure in the community are food and smoking. Seafood, kidney, liver, flaxseed, cocoa powder, wild mushrooms, potatoes, cereals, and vegetables grown on contaminated soil contain high levels of Cd [27]. Tobacco is one of the Cd-accumulating plants and it has been reported that one

cigarette contains approximately 1-2 µg Cd. Besides it has been observed that children are exposed to Cd through cigarette smoke [28, 29]. Furthermore, air is another source of Cd exposure but Cd concentration in the air is low [30].

It has been reported that inhalation of cadmium oxide particles may cause lung and acute pneumonia. In case of occupational or environmental exposure, Cd can damage the lungs and cause obstructive pulmonary disease (COPD), heart failure, and heart attack [31,32]. Moreover, studies provide evidence showing that Cd exposure is positively associated with different liver diseases such as non-alcoholic steatohepatitis, non-alcoholic fatty liver disease, hyperglycemia, necroinflammation, etc. [33,34].

FAO/WHO has reported that the tolerable weekly intake of Cd is 400-500 µg per person or 140-260 µg/day for over 50 years and 2000 mg for life-time [35]. A recent report of FAO/WHO (2010) states that Cd is 0.83 µg/kg body weight per day or 58 µg/day for a 70 kg person [36]. In addition, European Food Safety Authority reported 25 µg/day Cd for a 70 kg person [37,38]. The absorbed Cd amount can change based on its exposure and entry route. Cd is absorbed by the gastrointestinal system at the rate of nearly 3-10% and 50% of inhaled Cd is absorbed [39]. Cd is transferred to other organs including liver, kidney, pancreas, heart, spleen, testicles, lungs and bones via albumin and alpha -2- macroglobulin. Cd binds glutathione (GSH) and metallothionein (MT) and these compounds are slowly secreted from bile or released to blood stream. [40,41]. In general population, Cd blood levels were determined as 3.5–8.9 nM for non-smokers and 12.4–35.5 nM for smokers. But IARC detected Cd blood levels much higher for environmental and occupational exposure (above 89 nM and up to 445 nM) respectively [42]. Blood Cd levels are examined in whole blood generally. The half-life of Cd may be in 3- 4 months to 10 years in blood [43]. In another study, it has been reported that the effect of Cd can last for about 10 years due to its long biological half-life [44].

3.1 Mechanism of Cd Action

In the bloodstream, Cd binds to alpha-2-macroglobulin and albumin, and by this way it is transferred to organs. Cd binds to GSH or MT in the liver. These complexes have significant storage and transport roles because of their long life time. They are slowly secreted into the bile or bloodstream [40,41].

Cd exhibits its toxic effects via the Cd^{+2} ion's physical and chemical properties which are similar to those of Ca and Zn. For this reason, it is possible that Cd replaces Ca and Zn in important physiological processes in which a number of signaling pathways might be incorrectly activated or repressed. And in this case various signaling pathways can be activated or inhibited [45]. Cd has been addressed with some structural and biochemical changes. It causes apoptosis at low doses and necrosis at higher doses in cell cultures [46].

Besides, Cd affects plasma membranes and damages mitochondrial and nuclear membranes and DNA [47,48]. Joseph et al. (2004) have stated that four group mechanisms have an effective role in Cd carcinogenesis including inhibition of DNA damage repair, inhibition of apoptosis, inhibition of aberrant gene expression, and induction of oxidative stress [49]. Furthermore, previous studies have revealed that the mechanisms underlying Cd toxicity are both oxidative stress and inflammation [50,51,52].

3.2 Cd and Inflammation

Inflammation is a protective response of metabolism to injury caused by microorganisms, and physical and chemical agents to prevent tissue damage [53]. Chronic Cd exposure, through the downstream effects of Cd-induced oxidative stress or through various mechanisms, induces systemic levels of inflammation. [54]. Previous reports documented systemic inflammation and oxidative stress as main reasons of some chronic diseases including diabetes mellitus (type 2) and cancer [55,56]. In another study, Kayama et al. [48] revealed that high levels of pro-inflammatory cytokines associated with Cd exposure cause pathological conditions in biologic systems.

NF-κB is a transcription factor of genes including cell survival, inflammation, differentiation and growth [57]. Different studies have revealed that Cd exposure may increase activity of NF-κB in various systems. Go et al. (2012) indicated that low dose Cd treatment caused to increase NF-κB activity in HeLa cells [58]. In a mice study, it was determined that cadmium chloride (CdCl2) led to an important increase in the expression of NF-κB [59]. However, in their study, Souza et al. (2004) reported that the NF-κB activity did not increase after Cd treatment (1.5 or 10 μM CdCl2) of human liver hepatoma HepG2 cells [60].

219

Interleukin-6 (IL-6) is an important pro-inflammatory cytokine that promotes the induction of acute phase proteins [61]. In a previous study, it was determined that Cd treatment increased IL-6 status at doses of 0.5 mg and 1 mg Cd/kg body weight [62]. When an important increase was determined in the levels of IL-6 in M1 fibroblasts and type 2 epithelial cell cultures, there was no increase in alveolar macrophages [61].

Tumor-necrosis factor (TNF) is a sufficient mediator which reflects systemic or local inflammation [63]. Lag et al. [61] stated that Cd caused an important increase in the TNF-α release (from 3 to 10 μM) in rat alveolar macrophages after exposure for 20 hours. Freitas and Fernandez [64] showed that Cd treatment induced the release of TNF-α in THP-1 human monocytic leukemia cells. However, in their study, Cormet-Boyaka et al. [65] revealed that Cd administration did not increase the levels of TNF-α in human SAEC and Calu-3 cells.

IL-1ß and TNF-α are important players in the onset of inflammatory processes as well as regulation and expression of the other chemokines and cytokines [61]. Cormet-Boyaka et al. (2012) reported that Cd treatment did not change IL-1ß status in human SAEC and Calu-3 cell lines [65].

3.3 Cd and Oxidative Stress

Cd may cause oxidative stress via different pathways. It shows high affinity to sulfhydryl (SH) groups and thus it reduces glutathione (GSH), catalase (CAT), superoxide dismutase (SOD), and glutathione peroxidase (Gpx) activities of the tissues [66,67]. Besides, the intracellular release of Cd affects the structure of the cellular membrane via lipid peroxidation (LPO) [68]. There is more evidence that support Cd induced oxidative stress and increased LPO [69], decreasing of GSH [70], and activity of some stress response genes [71]. Many studies have reported that Cd increases LPO and causes an increase in malondialdehyde (MDA) levels, which is the most important biomarker of LPO [72]. In a recent study, Taşdemir et al. (2020) reported that MDA levels statistically significantly increased in rats exposed to Cd [73]. Athmounia et al. [74] stated that MDA levels showed an important increase in liver tissue of CdCl2-induced group compared to the control. In another study, Ahmada et al. [75]. reported that Cd caused decreasing of CAT activity in the liver,

kidneys, and red blood cells. Moreover, Cd-induced oxidative stress has a major role in inhibiting DNA damage repair mechanisms and inducing apoptosis [76].

3.4 Zinc (Zn)

Zn is one of the most abundant metals and an essential trace element. It has an important role in maintaining physiological and cellular functions of body. It is absorbed from small bowel and stored in liver and kidney. It binds to metalloproteins in intracellular conditions. It has a key role for many enzymes and supports the immunity of the body [77-79]. Zn deficiency causes failure of immunity and growth, hypogonadism, diarrhea and alopecia, impaired taste and smell, dermatitis and respiratory tract infections [79]. However, the increased amount of Zn in the cell has a neurotoxic effect [80].

Intracellular Zn binds to proteins in cellular physiology. Between 30 and 40 per cent of cellular zinc is found in the nucleus, 50 per cent in the cytosol and organelles, and the remainder is associated with the membranes. Moreover, it has many roles in phosphorylation/ dephosphorylation cascades and in the signaling system [81,82]. Zn homeostasis is provided via zinc transporters (ZnT). Totally 25 zinc transporters have been identified as 10 zinc exporters (ZnT) and 15 zinc importers (Zip). ZnT proteins exports intracellular Zn through organelles or across the membrane. Zn is transported across plasma membrane only via ZnT-1. The other ZnT transporters provide Zn sequestration into zincosomes [83,84]. Zip proteins allow Zn to enter the cell and release Zn from the zincosomes [83]. Zip proteins are divided into four groups: I, II, gufA, and LIV-1 subfamilies of Zip transporters. In addition, both ZnT and Zip proteins need energy and their production is regulated based on Zn status [85].

Zn has a role in the structure of enzymes as a cofactor and metabolic pathways. For instance, it is required for phosphatases, glutamate dehydrogenase or SOD and many other enzymes [86]. Valle and Auld [87] reported that approximately 200 enzymes were related with Zn. It may inhibit some enzymes including caspase-3 and protein tyrosine phosphatase [88], NAD+-dependent isocitrate dehydrogenase, succinate dehydrogenase, α-ketoglutarate dehydrogenase, aconitase, and cytochrome C oxidase [89]. These findings are supported by the data showing that

treatment of 30 mol/L Zn causes inhibition of the GSH and the increase of oxidized glutathione (GSSG) in liver cells [90,91].

Zn is a trace element which has an antioxidant capacity to neutralize free radical generation [92]. Zn shows an antioxidant ability with different properties as shown in Figure 1. Zn2+ inhibits reactive oxygen species (ROS) and supports a cellular membrane stability [93]. Besides, it acts as an antagonist of Cd, prevents Cd toxicity and supports the antioxidant system [94]. Zn may have different antioxidant features. It keeps intracellular levels of GSH by preventing oxidation of sulfhydryl groups [95]. It also reduces oxidant promoting enzymes such as iNOS and supports activities of antioxidant enzymes (CAT, SOD) [96].

SODs are metalloenzymes and four SOD types have been identified; Cu-Zn SOD, Mn SOD, Fe SOD, and Ni SOD. The most important type is Cu-Zn SOD due to importance of its physiological and therapeutic properties in eukaryotic cells [97]. In addition, Zn induces synthesis of MT, an important scavenger of free radicals [98] and regulates metabolism of other antioxidant vitamins such as vitamin E and vitamin C [99-101]. Zn can also inhibit ROS production through competition with Fe2+ and Cu+ ions which have prooxidative action [102].

On the other hand, MT is a metal-binding protein rich in cysteine [103]. It has antioxidant features and it is induced via Zn [92,104,105]. It has been reported that MT neutralizes hydroxyl radicals and inhibits oxidative stress [106]. MTs are also thought to have an efficient role in the homeostasis of cellular Zn metabolism [107]. Zn and Cd are good inducers of MT transcription and protein synthesis. Cd toxicity can be improved by Zn through the induction of MTs [108,109].
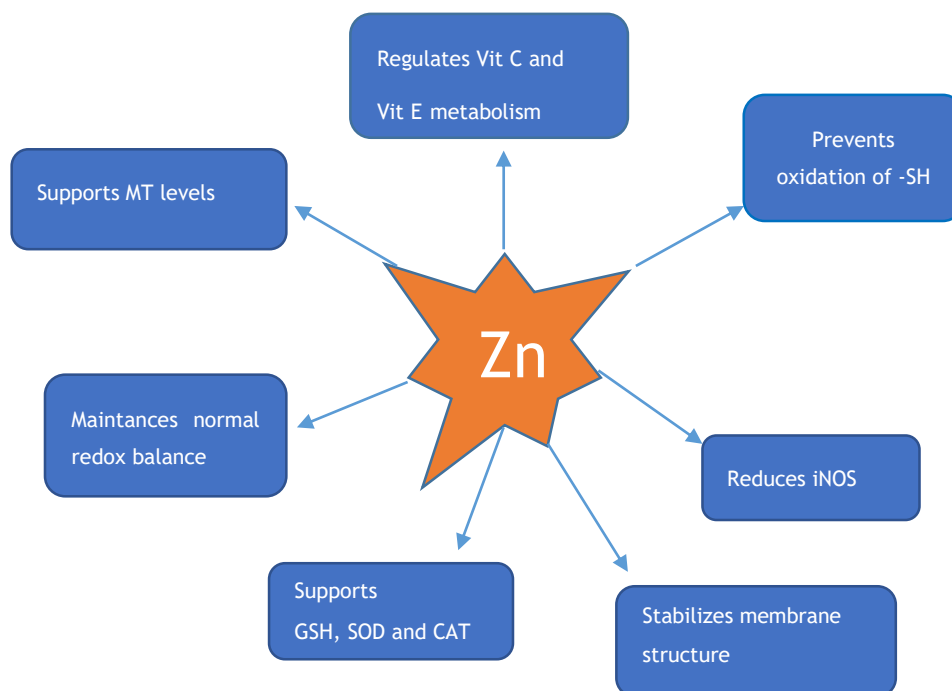
Figure 1. *The summary of antioxidant properties of Zn.*

3.5 Preventive Effects of Zn Against Cd Toxicity

The preventive effect of Zn against Cd toxicity is known for many years. Zn has an ability to strongly reverse Cd intoxication in different organisms [110,111]. According to reports, Zn limits the gastrointestinal tract absorption of Cd and its accumulation, hence preventing its detrimental effects. [112]. Moreover, its preventive effect against Cd toxicity may be related to maintenance of redox balance in the cell [113].

Sidorczuk et al. [114] observed a decrease of 29% in LPO levels in 5 mg Cd/L + 30 mg Zn/L treated group only compared to Cd (5 mg Cd/L)-treated group in serum of rats. Accordingly, the detected decrease became 46% when Cd concentration increased to higher levels. In this study, the researchers showed increasing levels of GPx in serum, liver, and kidney samples only after Zn administration compared to Cd-treated groups.

Another study, Messaoudi et al. [115], determined that Zn administration decreased Cd- induced testicular MT-1 and MT-2 gene expression and an increasing antioxidant status in rats. Zn binds and detoxifies Cd by inducing MT synthesis. It also

reduces oxidative stress induced by Cd with its antioxidant properties [116]. In their study, Messaoudi et al. [117] stated that administration of Zn supported GSH, GSHPx (or GPX) and CAT levels of rat erythrocytes. Jemai et al. [118] revealed that pre-treatment with Zn played a preventive role against Cd intoxication and caused an important increase in GSH levels of rats.

Jihen et al. [119] revealed that Zn treatment may reverse Cd-induced oxidative stress in kidney of rats. Another study by the same group [120] reported that Zn has an indirect ameliorative effect in the liver of Cd-induced rats. In their study, they administrated 200 mg/L Cd of CdCl2 and 500 mg Zn of ZnCl2 to the subject animals. At the end of the study, they detected an increased CuZn SOD activity and GSH levels. Brzóska and Rogalska [121] evaluated GSH levels, GPX, SOD, and CAT activities of bones in Cd-induced rats. In their study, they administrated Cd (as CdCl2·2½H2O) of 5 or 50 mg for 6 months and Zn (as ZnCl2) of 30 and 60 mg for 6 months. At the end of the study, they did not notice any change in antioxidant parameters. Ebaid et al. [122] stated that Zn showed ameliorative effects on MDA status in Cd-treated rats. Moreover, they reported a positive effect of Zn on CAT, SOD, and GSH levels in the same study. Mimouna et al. [123] observed lower SOD activities after Zn treatment in rat fetal brain tissue compared to the Cd-induced groups. In addition, they found that MT levels of Cd+Zn induced group showed a decrease when compared to Cd-induced group.

Bashandy et al. [124] concluded that Zn administration showed a positive effect on Cd-induced oxidative stress, sex hormones, spermatogenesis, and inflammatory biomarkers. In the study, they administrated CdCl2 and ZnCl2 at dose level of 2.2 mg/kg. According to the study results, Cd exhibited significant increases in the level of testicular MDA, TNF-α and hydroperoxide of blood. And Zn treatment mitigated the toxic effect of Cd. Rogalska et al. [125] indicated that 30 mg Zn/L and 60 mg Zn/L treatment decreased TNF-α levels according to the Cd-induced group of rats.

Cd is an environmental pollutant that causes widespread oxidative stress and inflammation in metabolism, and its exposure leads to impairment of the innate immune system. Cd causes oxidative stress by triggering free radical production during metabolism. Free radicals have been reported to cause many diseases such as

diabetes mellitus, neurodegenerative diseases, DNA damage and cancer. Studies have shown that substances with antioxidant activity can counteract the oxidative stress-induced toxic effects of Cd. Strengthening antioxidant defense mechanisms may be a good option to counteract the harmful effects of free radicals. Because Zn is involved in the activity of many enzymes including antioxidant enzymes, and induces MT synthesis, it is a good option to strengthen the antioxidant defense system. Considering the side effects of synthetic antioxidants, the use of natural antioxidants will undoubtedly be more beneficial. Therefore, Zn may be an important candidate for the prevention and/or reversal of Cd-induced damage.

4 CONCLUSION

Zn is a well-known natural antioxidant agent against Cd toxicity for many years. The preventive effect of Zn is manifested via the antioxidant and anti-inflammatory properties based on the used dose. Besides, oxidative stress is one of basic reasons of Cd toxication. It has been revealed that Zn may reverse Cd toxicity by supporting GSH, SOD, CAT, and MT levels and regulating Vit E and Vit C status. In addition, it stabilizes membrane structure, prevents LPO, and supports redox balance. However, zinc is not used as a detoxifying agent in clinical trails, yet. Zinc may be a good candidate for detoxifying Cd, but there is a need for further studies to be conducted at cellular levels, in animals, and in human beings. In addition, although an abundance of data available more research is required to fully understand the mechanisms underlying zinc's protection against Cd toxicity. Investigators may find new avenues to pursue in this field.

Statement of Research and Publication Ethics

The study is complied with research and publication ethics.

REFERENCES

[1] P.C. Nagajyoti, K.D. Lee, and T.V.M. Sreekanth, "Heavy metals, occurrence and toxicity for plants: a review," Environ. Chem. Lett., vol.8, pp. 199–216, 2010.

[2] S. Banik, K.C. Das, M.S. Islam, and M. Salimullah, "Recent advancements and challenges in microbial bioremediation of heavy metals contamination," JSM Biotechnol. Bioeng., vol.2, no. 1,1035, 2014.

[3] A.T. Jan, M. Azam, K. Siddiqui, A. Ali, I. Choi, and Q.M.R. Haq, "Heavy metals and human health: mechanistic insight into toxicity and counter defense system and antioxidants," Int. J. Mol. Sci., vol.16, pp. 29592–29630, 2015.

[4] S. Honey, R. Neetu, B.M. Blessy, "The characteristics, toxicity and e_ects of cadmium," Int. J. Nanosci.,vol.3, pp. 1–9, 2015.

[5] Agency for Toxic Substances and Disease Registry (ATSDR) (1998) U.S. Public Health Service. Toxicological Profile for Cadmium. Atlanta, GA

[6] W.M. Hayes, CRC Handbook of Chemistry and Physics. CRC Press, Boca Raton, 2016

[7] H. Zhang, and M. Reynolds, "Cadmium exposure in living organisms: a short review," Sci. Total. Environ., vol.678, pp. 761–767, 2019.

[8] G.G. Schwartz, and I.M. Reis, "Is cadmium a cause of human pancreatic cancer?," Cancer Epidemiol. Biomark. Prev., vol. 9, pp.139–145, 2000.

[9] G. Bjørklund, G. Crisponi, V.M. Nurchi, R. Cappai, A. Buha Djordjevic, J. Aaseth (2019) "A review on coordination properties of thiolcontaining chelating agents towards mercury, cadmium, and lead," Molecules, vol. 24, no. 18, https://doi.org/10.3390/molecules24183247.

[10] A. Buha, V. Matovic, B. Antonijevic, Z. Bulat, M. Curcic, E.A. Renieri, A.M. Tsatsakis, A. Schweitzer, and D. Wallace, "Overview of cadmium thyroid disrupting effects and mechanisms," Int. J. Mol. Sci., vol. 17;19, no. 5, 1501 https://doi.org/10.3390/ijms19051501.

[11] S. Sarkar, P. Yadav, R. Trivedi, A.K. Bansal, and D. Bhatnager, "Cadmium-induced lipid peroxidation and the status antioxidant system in rat tissues," J. Trace Elem. Med. Biol., vol. 9, pp. 144–149, 1995.

[12] A.A. Tinkov, T. Filippini, O.P. Ajsuvakova, J. Aaseth, Y.G. Gluhcheva, J.M. Ivanova, G. Bjørklund, M.G. Skalnaya, E.R. Gatiatulina, E.V. Popova, O.N. Nemereshina, M. Vinceti, and A.V. Skalny, "The role of cadmium in obesity and diabetes," Sci. Total Environ., vol. 601, pp. 741-755, 2017.

[13] M. Tellez-Plaza, A. Navas-Acien, K.L Caldwell, A. Menke, P. Muntner, and E. Guallar, "Reduction in cadmium exposure in the United States population 1988-2008: the contribution of declining smoking rates," Environ. Health Perspect., vol.120, no.2, pp. 204-209, 2012.

[14] J.Y. Min, and K.B. Min, "Blood cadmium levels and Alzheimer's disease mortality risk in older US adults," Environ. Health-Glob., vol.5, no:1, pp. 69, 2016.

[15] M.P. Waalkes, "Cadmium carcinogenesis," Mutat. Res., vol. 533, pp. 107–120, 2003.

[16] A.N. Sarkar, G.E. Ravindran, and V.I. Krishnamurthy, "A brief review on the effect of cadmium toxicity: from cellular to organ level," Int. J. Bio. Technol. Res., vol.3, pp.17–36, 2013.

[17] S.C. Gupta, A. Sharma, M. Mishra, R.K. Mishra, and D.K. Chowdhur, "Heat shock proteins in toxicology: How close and how far," Life Sci., vol. 86, pp. 377–384, 2010.

[18] J. Demenesku, I. Mirkov, M. Ninkov, A.P. Aleksandrov, L. Zolotarevski, D. Kataranovski, and M. Kataranovski, "Acute cadmium administration to rats exerts both immunosuppressive and proinflammatory effects in spleen," Toxicology, pp. 96-108, 2014.

[19] Z. Zhao, J.S. Hyun, H. Satsu, S. Kakuta, and M. Shimizu, "Oral exposure to cadmium chloride triggers an acute inflammatory response in the intestines of mice, initiated by the over-expression of tissue macrophage inflammatory protein-2 mRNA," Toxicol. Lett., vol.164, pp. 144–154, 2006.

[20] A. Winiarska-Mieczan, "Protective effect of tea against lead and cadmium-induced oxidative stress-a review," Biometals, vol. 31,no. 6. pp. 909–926, 2018.

[21] R.S. Almeer, G.I. AlBasher, S. Alarifi, S.Alkahtani, D.Ali, and A.E. Abdel Moneim, "Royal jelly attenuates cadmium-induced nephrotoxicity in male mice," Sci. Rep., vol.9, no.1, pp. 5825, 2019.

[22] E.M. Al Olayan, A.S. Aloufi, O.D. Al Amri, O.H. El-Habit, A.E. "Abdel Moneim Protocatechuic acid mitigates cadmium-induced neurotoxicity in rats: Role of oxidative stress, inflammation and apoptosis," Sci. Total Env., vol.723, 137969, 2020.

[23] R. Marchan, C. Cadenas, and H.M. Bolt, "Zinc as a multipurpose trace element," Arch. Toxicol., vol. 86, pp.519-520, 2012.

[24] M. Stefanidou, C. Maravelias, A. Dona, and C. Spiliopoulou " Zinc: a multipurpose trace element," Arch. Toxicol., vol.80, pp.1-9, 2006.

[25] P.I. Oteiza, V.N. Adonaylo, and C.L. Keen, "Cadmium-induced testes oxidative damage in rats can be influenced by dietary zinc intake," Toxicology, vol. 137, pp.13–22, 1999.

[26] M. Brzoska, and J. Moniuszko-Jakoniuk, "Interactions between cadmium and zinc in the organism," Food Chem. Toxicol., vol. 39, pp. 967–980, 2000.

[27] I.M. Olsson, I. Bensryd, T. Lundh, H. Ottosson, S. Skerfving, and A. Oskarsson " Cadmium in blood and urine–impact of sex, age, dietary intake, iron status, and former smoking–association of renal effects," Environ. Health Perspect., vol. 110, pp. 1185–1190, 2002.

[28] S. Willers, L. Gerhardsson, and T. Lundh, "Environmental tobacco smoke (ETS) exposure in children with asthma relation between lead and cadmium, and cotinine concentrations in urine," Respir. Med., vol. 99, pp. 1521–1527, 2005.

[29] M. Arora, J. Weuve, J. Schwartz, and R.O. Wright, "Association of environmental cadmium exposure with pediatric dental caries," Environ. Health Perspect., vol.116, pp. 821–825, 2008.

[30] M. Vahter, M. Berglund, S. Slorach, L. Friberg, M. Sarić, X.Q. Zheng, and M. Fujita, " Methods for integrated exposure monitoring of lead and cadmium," Environ. Res., vol. 56, pp.78–89, 1991.

[31] H.H. Rahman, D. Niemann, and S.H. Munson-McGee, "Association between environmental toxic metals, arsenic and polycyclic aromatic hydrocarbons and chronic obstructive pulmonary disease in the US adult population," Environ. Sci. Pollut. Res. Int., vol. 29, no. 36, pp. 54507-54517, 2022.

[32] S. Ma, J. Zhang, C. Xu, M. Da, Y. Xu, Y. Chen, and X. Mo, "Increased serum levels of cadmium are associated with an elevated risk of cardiovascular disease in adults," Environ. Sci. Pollut. Res. Int., vol. 29, no. 2, pp. 1836-1844, 2022.

[33] P.Rosales-Cruz, M. Domínguez-Pérez, E. Reyes-Zárate, O. Bello-Monroy, C. Enriquez Cortina, R. Miranda-Labra, L.Bucio, L. E. Gomez-Quiroz, E.Rojaz-Del Castillo, M. C. Gutierrez-Ruiz, and V. Souza-Arroyo, " Cadmium exposure

exacerbates hyperlipidemia in cholesterol overloaded hepatocytes via autophagy dysregulation, "Toxicology, 398-399, pp. 41-51,2018.

[34]Y.Zhu,Y.Zhao,X.X.Chai,J.Zhou,M.J.Shi,Y.Zhao,Y.Tian,X.M.Wang,T.X.Ying,Q.Feng,J.Sheng,and C.Luo, "Chronic exposure to low-dose cadmium facilitated nonalcoholic steatohepatitis in mice by suppressing fatty acid desaturation," Ecotoxicol. Environ. Saf., vol.15, 233, 113306, 2022

[35] FAO/WHO (1993) Evaluation of Certain Food Additives and Contaminants: Forty-first Report of the Joint FAO/WHO Expert Committee on Food Additives. WHO Technical Report Series No. 837. WHO, Geneva.

[36] FAO/WHO (2010) Seventy-third Meeting, Geneva, 8e17 June 2010. Summary and Conclusions. JECFA/73/SC. Food and Agriculture Organization of the United Nations; World Health Organization, Geneva, Switzerland.

[37] EFSA, "Statement on tolerable weekly intake for cadmium," EFSA J., vol.9, 1975 (pp. 1-19), 2011.

[38] EFSA, "Cadmium dietary exposure in the European population," EFSA J., vol.10, 2551(pp. 1-36), 2012.

[39] A.E. Sahmoun, L.D. Case, S.A. Jackson, and G.G. Schwartz, "Cadmium and prostate cancer: a critical epidemiologic analysis," Cancer Investig. vol.23, pp. 256–263, 2005.

[40] K. Martinez-Flores, V. Souza Arroyo, L. Bucio Ortiz, L.E. Gomez-Quiroz, M.C. Gutierrez-Ruiz, "Cadmio: efectos sobre la salud. Respuesta celular y molecular," Acta Toxicol. Argent., vol. 21, no.1, pp. 33–49, 2013.

[41] A.L. Koons, and V. Rajasurya, "Cadmium Toxicity," Stat Pearls. Stat Pearls Publishing, Treasure Island (FL), pp. 2018–2019, 2018.

[42] International Agency for Research on Cancer (IARC). "Cadmium and cadmium compounds. In: Arsenic, metals, fibres and dusts. A review of human carcinogens," IARC Monographs 100C, IARC, Lyon, pp 121–145, 2012.

[43] L. Järup, A. Rogenfelt, C.G. Elinder, K. Nogawa, and T. Kjellström, "Biological half-time of cadmium in the blood of workers after cessation of exposure," Scand. J Work Environ. Health, vol.9, pp.327–331, 1983.

[44] L. Jarup, and A. Akesson, "Current status of cadmium as an environmental health problem," Toxicol. Appl. Pharmacol., vol. 238, pp. 201–208, 2009.

[45] E.R. Siu, D.D. Mruk, C.S. Porto, C.Y. Cheng, "Cadmium-induced tes- ticular injury," Toxicol. Appl. Pharmacol., vol. 238, pp. 240–249, 2009.

[46] D.M. Templeton, and Y. Liu, "Multiple roles of cadmium in cell death and survival," Chem. Biol. Interact., vol.188, pp. 267–275, 2010.

[47] C. Fasanyaodewumi, L.M. Latinwo, C.O. Ikediobi, L. Giliard, G. Sponholtz, J. Nwoga, F. Stino, N. Hamilton, and G.V. Erdos, "The genotox- icity and cytotoxicity of dermally-administered cadmium: effects of dermal cadmium administration," Int. J. Mol. Med., vol. 1, pp. 1001–1006, 1998.

[48] S. Klimova, and E. Misurova, "Effects of cadmium and ionizing radiation on histones in rat testes," Acta Vet. Brno., vol. 73, pp. 483–489, 2004.

[49] P. Joseph, "Mechanisms of cadmium carcinogenesis," Tox. and App. Pharm., vol. 238, pp. 272–279, 2009.

[50] S.H. Gavett, and G. Oberdörster, "Cadmium chloride and cadmium metallothionein-induced pulmonary injury and recruitment of polymorphonuclear leukocytes," Exp. Lung Res., vol. 20, pp. 517-37, 1994.

[51] F. Kayama, T. Yoshida, M.R. Elwell, and M.I. Luster, "Cadmium-induced renal damage and proinflammatory cytokines: possible role of IL-6 in tubular

epithelial cell regeneration," Toxicol. Appl. Pharmacol., vol. 134, pp. 26-34, 1995.

[52] F. Kayama, T. Yoshida, M.R. Elwell and M.I. Luster, "Role of tumor necrosis factor-alpha in cadmium-induced hepatotoxicity," Toxicol. Appl. Pharmacol., vol. 131, pp. 224-234, 1995.

[53] U.N. Das, 2011. Inflammation. In: Das UN (ed) Molecular Basis of Health and Disease. Springer Science+Business Media BV, London, pp 15–100.

[54] M. Knoflach, B. Messner, Y.H. Shen, S. Frotschnig, G. Liu, K. Pfaller, X. Wang, B. Matosevic, J. Willeit, S. Kiechl, G, Laufer, and D. Bernhard, "Non-toxic cadmium concentrations induce vascular inflammation and promote atherosclerosis," Circ. J., vol. 75, pp. 2491–2495, 2011.

[55] K.E. Wellen, and G.S. Hotamisligil, "Inflammation, stress, and diabetes," J Cli. Inv., vol. 5, pp. 1111-1119, 2005.

[56] L.M. Coussens, and Z. Werb," Inflammation and cancer," Nature, vol. 420, pp. 860–867, 2002.

[57] M. Valko, H. Morris, and M.T.D. Cronin, " Metals, toxicity and oxidative stress," Curr. Med. Chem., vol.12, pp. 1161–1208, 2005.

[58] Y.M. Go, M. Orr, and D.P. Jones, "Increased nuclear thioredoxin-1 potentiates cadmium-induced cytotoxicity," Toxicol. Sci., vol.131, no.1, pp. 84-94, 2012.

[59] J. Lee, and K.T. Lim, "Preventive effect of phytoglycoprotein (27 kDa) on inflammatory factors at liver injury in cadmium chloride-exposed ICR mice," J. Cell Biochem., vol 112, pp. 694–703, 2011.

[60] V. Souza, C. Escobar Md Mdel, L. Gómez-Quiroz, L. Bucio, E. Hernández, E.C. Cossio, and M.C. Gutiérrez-Ruiz, "Acute cadmium exposure enhances AP-1 DNA binding and induces cytokines expression and heat shock protein 70 in HepG2 cells," Toxicology, vol.197, pp. 213–228, 2004.

[61] M. Lag, D. Rodionov, J. Ovrevik, O. Bakke, P.E. Schwarze, and M. Refsnes, "Cadmium-induced inflammatory responses in cells relevant for lung toxicity: Expression and release of cytokines in fibroblasts, epithelial cells and macrophages," Toxicol. Lett., vol. 193, pp. 252–260, 2010.

[62] Kataranovski M, Mirkov I, Belij S, Nikolic M, Zolotarevski L, Ciric D, and Kataranovski D " Lungs: remote inflammatory target of systemic cadmium administration in rats," Environ. Toxicol. Pharmacol., vol. 28, pp. 225–231, 2009.

[63] K.J. Tracey, "The inflammatory reflex," Nature, vol. 420, pp.853–859, 2002.

[64] M. Freitas, and E. Fernandes, " Zinc, cadmium and nickel increase the activation of NF-κB and the release of cytokines from THP-1 monocytic cells," Metallomics, vol. 3, pp.1238–1243, 2011.

[65] E. Cormet-Boyaka, K. Jolivette, A. Bonnegarde-Bernard, J. Rennolds, F. Hassan, P Mehta, S. Tridandapani, J. Webster-Marketon, and P.N. Boyaka, "An NF-κB-independent and Erk1/2-dependent mechanism controls CXCL8/IL-8 responses of airway epithelial cells to cadmium," Toxicol. Sci., vol. 125, pp. 418–429, 2012.

[66] A. Cuypers, M. Plusquin, T. Remans, M. Jozefczak, E. Keunen, H. Gielen, K. Opdenakker, A.R. Nair, E. Munters, T.J. Artois, T. Nawrot, J. Vangronsveld, and K. Smeets, " Cadmium stress: an oxidative challenge," Biometals, vol. 23, pp. 927–940, 2010.

[67] J. Ivanova, Y. Gluhcheva, D. Tsanova, A. Piskova, R. Djaleva, S. Mokresheva, D. Kamenova, and M. Mitewa, "On the effect of chelating agents and antioxidants

on Cd induced organ toxicity An overview," Eur. J. Chem., vol.4, pp. 74–84, 2013.

[68] A.S. El-Sharaky, A.A. Newairy, M.M. Badreldeen, S.M. Eweda, and S.A. Sheweita, "Protective role of selenium against renal toxicity induced by cadmium in rats," Toxicology, vol. 235, pp.185–193, 2007.

[69] M. Jurczuk, M.M. Brzoska, J. Moniuszko-Jakoniuk, M. Galazyn-Sidorczuk, and E. Kulikowska- Karpinska, "Antioxidant enzymes activity and lipid peroxidation in liver and kidney of rats exposed to cadmium and ethanol," Food Chem. Toxicol. vol. 42, pp. 429–438, 2004.

[70] D. Nigam, G.S. Shukla, and A.K. Agarwal, "Glutathione depletion and oxidative damage in mitochondria following exposure to cadmium in rat liver and kidney," Toxicol. Lett., vol. 106, pp.151–157, 1999.

[71] V.L. Badisa, L.M. Latinwo, C.O. Odewumi, C.O. Ikediobi, R.B. Badisa, A. Brooks-Walter, A.T. Lambert, and J. Nwoga, "Cytotoxicity and stress gene microarray analysis in cadmium-exposed CRL-1439 normal rat liver cells," Int. J. Mol. Med., vol. 22, pp. 213–219, 2008.

[72] S. Nemmiche, D. Chabane-Sari, P. Guiraud, "Role of alpha-tocopherol in cadmiuminduced oxidative stress in Wistar rat's blood, liver and brain," Chem. Biol. Interact., vol.170, no. 3, pp. 221–230, 2007.

[73] M. Taşdemir, F.Ç. Çelikezen, G. Oto, and F. Özbey, "The effects of pretreatment with lithium metaborate dihydrate on lipid peroxidation and Ca, Fe, Mg, and K levels in serum of wistar albino male rats exposed to Cd," Env. Sci. and Poll. Res., vol. 27, pp. 7702–7711, 2020.

[74] K. Athmounia, D. Belhaja, A. El Feki, and H. Ayadi, "Optimization, antioxidant properties and GC–MS analysis of Periploca angustifolia polysaccharides and chelation therapy on cadmium-induced toxicity in human HepG2 cells line and rat liver," Int. J. Biol. Macromol., vol.108, pp. 853–862, 2018.

[75] M. Ahmada, G.M. Abu Taweel, and S. Hidayathulla, "Nano-composites chitosan-curcumin synergistically inhibits the oxidative stress induced by toxic metal cadmium," Int. J. Biol. Macromol., vol. 108, pp. 591–597, 2018.

[76] J. Xie, Z.A. Shaikh, "Cadmium-induced apoptosis in rat kidney epithelial cells involves decrease in nuclear factor-kappa B activity," Toxicol. Sci., vol. 91, pp. 299–308, 2006.

[77] M. Hettiarachchi, C. Liyanage, R. Wickremasinghe, D.C. Hilmers, and S.A. Abrams, "The efficacy of micronutrient supplementation in reducing the prevalence of anaemia and deficiencies of zinc and iron among adolescents in Sri Lanka," Eur. J. Clin. Nutr., vol. 62, pp. 856–65, 2008.

[78] I.J. Griffin, S.C. Kim, P.D. Hicks, L.K. Liang, and S.A. Abrams, "Zinc metabolism in adolescents with Crohn's disease," Pediatr. Res., vol. 56, pp. 235–239, 2004.

[79] S.A. Abrams, "Assessing mineral metabolism in children using stable isotopes," Pediatr. Blood Can., vol. 50, pp. 438–41, 2008.

[80] S.L. Sensi, and J.M. Jeng, "Rethinking the excitotoxic ionic milieu: the emerging role of Zn(2+) in ischemic neuronal injury," Curr. Mol. Med. vol. 4, pp. 87–111, 2004.

[81] I. Korichneva, B. Hoyos, R. Chua, E. Levi, and U. Hammerling, "Zinc release from protein kinase C as the common event during activation by lipid second messenger or reactive oxygen," J. Biol. Chem., vol. 277, pp. 44327–44331, 2002.

[82] I. Korichneva, "Zinc dynamics in the myocardial redox signaling network," Antioxid Redox Signal., vol. 8, pp. 1707–1721, 2006.

[83] R.D. Palmiter, and S.D. Findley, "Cloning and functional characterization of a mammalian zinc transporter that confers resistance to zinc," EMBO J., vol. 14, pp. 639–649, 1995.

[84] S.L. Sensi, D. Ton-That, and J.H. Weiss, "Mitochondrial sequestration and Ca(2+)-dependent release of cytosolic Zn(2+) loads in cortical neurons," Neurobiol. Dis., vol. 10, pp. 100–108, 2002.

[85] S.R. Powell, L. Aiuto, D. Hall, and A.J. Tortolani, "Zinc supplementation enhances the effectiveness of St. Thomas' Hospital No. 2 cardioplegic solution in an in vitro model of hypothermic cardiac arrest," J. Thorac. Cardiovasc. Surg., vol. 110, pp.1642–1648, 1995.

[86] A.S. Prasad, "Zinc is an antioxidant and anti-inflammatory agent: its role in human health," Front. Nutr., vol. 1, pp. 1-14, 2014.

[87] B.L. Vallee, and D.S. Auld, "Zinc coordination, function, and structure of zinc enzymes and other proteins," Biochemistry, vol. 29, pp. 5647–5659, 1990.

[88] F. Chimienti, M. Seve, S. Richard, J. Mathieu, and A. Favier, "Role of cellular zinc in programmed cell death: temporal relationship between zinc depletion, activation of caspases, and cleavage of Sp family transcription factors," Biochem. Pharmacol., vol. 62, pp. 51–62, 2001.

[89] J. Lemire, R. Mailloux, and V.D. Appanna, "Zinc toxicity alters mitochondrial metabolism and leads to decrease ATP production in hepatocytes," J. Appl. Toxicol., vol. 28, pp. 175–182, 2008.

[90] M.O. Parat, M.J. Richard, J.C. Beani, and A. Favier, "Involvement of zinc in intracellular oxidant/antioxidant balance," Bio. Trace Elem. Res., vol. 60, pp.187–204, 1997.

[91] A. Meister, M.E. Anderson, "Glutathione," Annu Rev. Biochem., vol. 52, pp. 711–760, 1983.

[92] S.R. Powell, "Antioxidant properties of zinc," J. Nutr., vol. 130, pp.1447–1454, 2000.

[93] M. Bicer, M. Günay, A.K. Baltacı, K. Uney, R. Mogulkoc, and M. Akil, "Effect of zinc supplementation on lipid peroxidation and lactate levels in rats with diabetes induced by streptozotocin and subjected to acute swimming exercise," Bratisl. Lek. Listy., vol.113, pp.199–205, 2012.

[94] M. Dżugan, M.W. Lis, M. Droba, and J.W. Niedziółka, "Protective effect of zinc on cadmium embryotoxicity and antioxidant status of blood plasma in newly hatched chicks," Environ. Lett., vol. 47, pp. 1288–1293, 2012.

[95] F.T. Celino, S. Yamaguchi, C. Miura, T. Ohta, Y. Tozawa, T. Iwai, T. Miura "Tolerance of spermatogonia to oxidative stress is due to high levels of Zn and Cu/Zn superoxide dismutase," PLoS One, vol. 6, no.2, e16938, 2011.

[96] B. Bao, A. Ahmad, A. Azmi, Y. Li, A. Prasad, and F.H. Sarkar, "The biological significance of zinc in inflammation and aging. In: Rahman I, Bagchi D (eds). Inflammation, advancing age and nutrition. Academic Press, San Diego, pp 15-27, 2014.

[97] Y. Sheng, I.A. Abreu, D.E. Cabelli, M.J. Maroney, A.F. Miller, M. Teixeira, and J.S. Valentine, "Superoxide dismutases and superoxide reductases," Chem. Rev., vol.114, pp. 3854–3918, 2014.

[98] Z.E. Suntres, and E.M. Lui, "Biochemical mechanism of metallothionein –carbon tetrachloride interaction in vitro," Biochem. Pharmacol., vol. 39, no.5, pp. 833-840, 1990.

[99] M. Cabre, J. Camps, N. Ferre, J.L. Paternain, and J. Joven, "The antioxidant and hepatoprotective effects of zinc are related to hepatic cytochrome P450

depression and metallothionein induction in rats with experimental cirrhosis," Int. J. Vitam. Nutr. Res., vol. 71, pp. 229-236, 2001.

[100] H.T. Abul, T.C. Mathew, F. Abul, H. Al-Sayer, and H.M. Dashti, "Antioxidant enzyme level in the testes of cirrhotic rats," Nutr., vol.18, pp. 56-59, 2002.

[101] A. Kojima-Yuasa, T. Ohkita, K. Yukami, H. Ichikawa, N. Takami, T. Nakatani, D.O. Kennedy, S. Nishiguchi, and I. Matsui-Yuasa, "Involvement of intracellular glutathione in zinc deficiency induced activation of hepatic stellate cells," Chem. Biol. Interact., vol. 146, pp. 89-99, 2003.

[102] K. Jomova and M. Valko, "Advances in metal-induced oxidative stress and human disease," Toxicology, vol. 283, pp. 65–87, 2011.

[103] P. Coyle, J.C. Philcox, L.C. Carey, and A.M. Rofe, "Metallothionein: the multipurpose protein," Cell. Mol. Life Sci., vol.59, pp. 627–647, 2002.

[104] G.K. Andrews, "Regulation of metallothionein gene expression by oxidative stress and metal ions," Biochem. Pharmacol., vol.59, pp. 95–104, 2000.

[105] R.J. Cousins, and L.M. Lee-Ambrose, "Nuclear zinc uptake and interactions andmetallothionein gene expression are influenced by dietary zinc in rats," J. Nutr., vol. 122, pp. 56–64, 1992.

[106] S. Bodiga, and M.N. Krishnapillai, "Concurrent repletion of iron and zinc reduces intestinal oxidative damage in iron- and zinc-deficient rats," World J. Gastroenterol, vol. 13, pp. 5707–5717, 2007.

[107] S.R. Davis, and R.J. Cousins, "Metallothionein expression in animals: a physiological perspective on function," J. Nutr., vol.130, pp. 1085–1088, 2000.

[108] C.D. Klaassen, J. Liu, and S. Choudhuri, "Metallothionein: an intracellular protein to protect against Cadmium Toxicity," Annu Rev. Pharmacol. Toxicol., vol.39, pp. 267-294, 1999.

[109] M.P. Waalkes, "Cadmium carcinogenesis," Mutat. Res., vol. 533, pp. 107–120, 2003.

[110] A.M. Sandbichler, and M. Hockner, "Cadmium protection strategiesea hidden trade-off," Int. J. Mol. Sci., vol.17, no.1, pp. 139, 2016.

[111] N. Babaknejad, A.A. Moshtaghie, H. Nayeri, M. Hani, S. Bahrami, " Protective role of zinc and magnesium against cadmium nephrotoxicity in male wistar rats," Biol. Trace. Elem. Res. vol.174, no.1, pp.112-120, 2016.

[112] L. Said, M. Banni, A. Kerkeni, K. Said, and I. Messaoudi, " Influence of combined treatment with zinc and selenium on cadmium induced testicular pathophysiology in rat," Food Chem. Toxicol., vol. 48, no. 10, pp. 2759-2765, 2010.

[113] V. Souza, C. Escobar Mdel, L. Bucio, E. Hernandez, and M.C. Gutierrez-Ruiz, "Zinc pretreatment prevents hepatic stellate cells from cadmium-produced oxidative damage," Cell Biol. Toxicol., vol. 20, pp. 241–251, 2004.

[114] M.G. Sidorczuk, M.M. Brzóska, J. Rogalska, A. Roszczenko, and M. Jurczuk, "Effect of zinc supplementation on glutathione peroxidase activity and selenium concentration in the serum, liver and kidney of rats chronically exposed to cadmium," J. Trace Elem.Med. Bio., vol. 26, pp. 46– 52, 2012.

[115] I. Messaoudi, M. Banni, L. Saïd, K. Saïd, and A. Kerkeni, "Evaluation of involvement of testicular metallothionein gene expression in the protective effect of zinc against cadmium-induced testicular pathophysiology in rat," Reprod. Toxicol., vol.29, pp. 339–345, 2010.

[116] Md.M. Rahman, K.F. Binte Hossain, S. Banik, Md.T. Sikder, M. Akter, S.E. Corpus Bondad, Md.S. Rahaman, T. Hosokawa, T. Saito, and M. Kurasaki, "Selenium

and zinc protections against metal-(loids)-induced toxicity and disease manifestations: A review," Ecotox. and Env. Safety, vol. 168,pp. 146–163, 2019.

[117] I. Messaoudia, F. Hammoudab, J. Ji El Heni, T. Baati, K. Said, and A. Kerkeni, "Reversal of cadmium-induced oxidative stress in rat erythrocytes by selenium, zinc or their combination," Exp. Tox. Path., vol. 62, pp. 281–288, 2010.

[118] H. Jemai, H.A. Lachkar, I. Messaoudi, and A. Kerkeni, "Effects of zinc pre-treatment on blood glutathione, serum zinc and kidney histological organisation in male rats exposed to cadmium," J Trace Elem. Med. Bio., vol. 24, pp. 277–282, 2010.

[119] E.H. Jihen, H. Fatima, A. Nouha, T. Baati, M. Imed, and K. Abdelhamid, "Cadmium retention increase: A probable key mechanism of the protective effect of zinc on cadmium-induced toxicity in the kidney," Toxicol. Lett., vol. 196, pp. 104–109, 2010.

[120] E.H. Jihen, S. Sonia, H. Fatima, M.S. Tahar, and K. Abdelhamid, "Interrelationships between cadmium, zinc and antioxidants in the liver of the rat exposed orally to relatively high doses of cadmium and zinc," Ecotoxic and Env. Safety, vol. 74, pp. 2099–2104, 2011.

[121] M.M. Brzóska, and J. Rogalska, "Protective effect of zinc supplementation against cadmium-induced oxidative stress and the RANK/RANKL/OPG system imbalance in the bone tissue of rats," Tox. App. Pharm., vol. 272, no. 208–220, 2013.

[122] H. Ebaid, I. Hassan, S. Bashandy, N.A. Taha, A. Mahmood, S. Alomar, I. Alhazza, A. Mashaly, and A. Rady, "Zinc improves the immune function and the proliferation of lymphocytes in cadmium-treated rats. Experimental immunology," Centr. Eur. J. Immunol., vol. 39, no. 4, pp. 441-448, 2014.

[123] S.B. Mimouna, S. Boughammoura, M. Chemek, Z. Haouas, M. Banni, I. Messaoudi, "Disruption of the zinc metabolism in rat foetal brain after prenatal exposure to cadmium," Chem. Bio. Int., vol. 286, pp. 88–95, 2018.

[124] S.A.M. Bashandy, E.A.A. Omara, H. Ebaid, M.M. Amin, and M.S. Soliman, "Role of zinc as an antioxidant and anti-inflammatory to relieve cadmium oxidative stress induced testicular damage in rats," Asian Pac. J. Trop Biomed., vol. 6, no.12, pp.1056–1064, 2016.

[125] J. Rogalska, B.P. Marcinkiewicz, and M.M. Brzoska, "Protective effect of zinc against cadmium hepatotoxicity depends on this bioelement intake and level of cadmium exposure: A study in a rat model," Chem. Bio. Interac., vol. 193, pp. 191–203, 2011.

APPENDIX

Appendix 1. Details of the studies evaluating Zn effects on Cd induced toxicity in rat models. This table shows that changing of MDA, GSH, GPx, SOD, CAT and TNF-a levels after Zn treatment (Zn+Cd) according to the only Cd induced groups of the studies. Statistical importance of the alterations reflected also. (**Note:** ↑ means increasing; ↓means decreasing; ● means no changing)

Sample	Cd Source /Dose/ Administration type/ Duration time	Zn Source/Dose/Administration type / Duration time	MDA	GSH	GPx	SOD	CAT	TNF-α	Reference
Testis	CdCl2, 200 ppm, drinking water, 5 weeks	ZnCl2, 500 ppm, drinking water, 5 weeks	↓ p< 0.01	-	-	↑ p< 0.01	↓	-	[115]
Erythrocyte	CdCl2, 200 ppm, drinking water, 35 days	ZnCl2, 500 ppm, drinking water, 35 days, 5 weeks	-	↑	↑ p< 0.05	↓ p< 0.01	↑ p<0.0001	-	[117]
Kidney	CdCl2, 200ppm, drinking water, 35 days	ZnCl2, 500 ppm, drinking water, 35 days	-	↑ p<0.0001	↑ p<0.0001	↑ p<0.0001	-	-	[119]
Liver	CdCl2 200 mg, within drinking water 35 days	ZnCl2, 500 mg, drinking water. 35 days		↑ p<0.0001	↑ p<0.0001	↑ CuZn SOD p<0.0001 ↓ MnSOD			[120]
Liver	CdCl2, (5 and 50 mg/l), within drinking water, 6 months	ZnCl2 30 or 60 mg Zn/l, drinking water, 6 months						↓ p<0.0001 ↓ p< 0.05	[125]
Testis	CdCl2, 2.2mg/kg, subcutaneously,8 weeks	ZnCl2, 2.2mg/kg, subcutaneously, 8 weeks.	-	↑ p< 0.01	-	↑ p< 0.01	↑ p< 0.01	↓ p< 0.01	[124]
Blood	CdCl2, 2.2 mg/kg, subcutaneously, 60 days	ZnCl2, 2.2 mg/kg, subcutaneously, 60 days	↓ p< 0.05	↑ p< 0.05	-	↑ p< 0.05	↑ p< 0.05	-	[122]
Bone	CdCl2·2½H2O 5 or 50 mg, drinking water 6 months,	ZnCl2, 30 and 60 mg, drinking water 6 months	-	●	●	●	●	-	[121]
Brain	CdCl2, 50 mg/L, drinking water, during gestation	ZnCl2, 60 mg/L, drinking water, during gestation				↓ p < 0.05			[123]
Serum	5 or 50 mg Cd/L (as CdCl2 2 ½ H2O), drinking water, 6 months	ZnCl2, 30 mg Zn/L, drinking water, 6 months	↓		↑ P < 0.01				[114]
Liver					↑ p< 0.05				
Kidney					↑ p< 0.05				